

**UNVEILING ENZYMATIC MECHANISMS WITH MALONYL-
THIOESTER ISOSTERES**

by

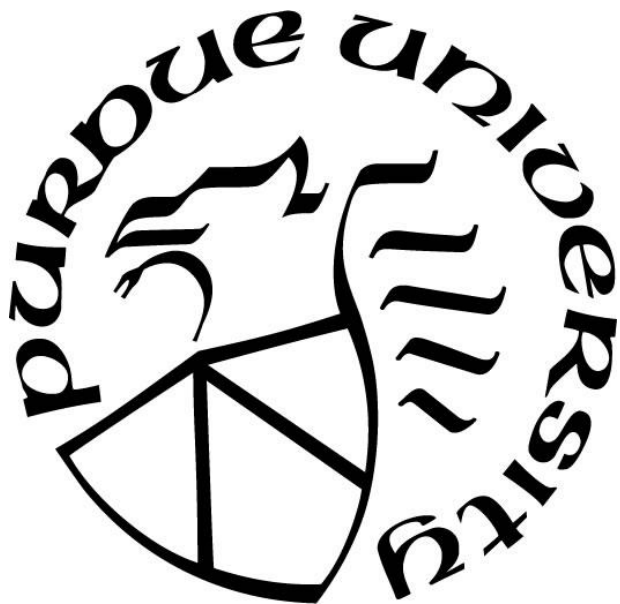
Lee Stunkard

A Dissertation

Submitted to the Faculty of Purdue University

In Partial Fulfillment of the Requirements for the degree of

Doctor of Philosophy



Department of Biochemistry

West Lafayette, Indiana

December 2019

**THE PURDUE UNIVERSITY GRADUATE SCHOOL
STATEMENT OF COMMITTEE APPROVAL**

Dr. Jeremy R. Lohman, Chair

School of Biochemistry

Dr. Barbara L. Golden

School of Biochemistry

Dr. Clinton C.S. Chapple

School of Biochemistry

Dr. Kevin V. Solomon

School of Agricultural & Biological Engineering

Approved by:

Dr. Andrew D. Mesecar

This dissertation is dedicated to my wife, Michelle, and son, William, who encouraged me to pursue my passion and to my parents, Scott and Veronica, who supported me along the way.

ACKNOWLEDGMENTS

This work was possible through the financial support of the Purdue University Biochemistry Department, the Bird Stair Graduate Research Fellowship, the Purdue Research Foundation Research Grant, and the Bilsland Dissertation Fellowship.

Each member of my Thesis Committee provided extensive professional and research guidance. They all offered mentoring and support for scientific research and life in general. I would like to thank Dr. Jeremy Lohman, the chair of my committee, for his time and effort in mentoring me to think like an experienced biochemist. I want to thank all of the colleagues I had the privilege of working with in my time in the Lohman lab.

I wish to thank my parents for supporting and loving me through my every pursuit. Most notably, I would like to thank my loving wife, Michelle, and my newborn son, William, for their everlasting support and encouragement.

TABLE OF CONTENTS

LIST OF TABLES	8
LIST OF FIGURES	9
LIST OF SCHEMES.....	11
LIST OF ABBREVIATIONS.....	12
ABSTRACT.....	13
CHAPTER 1. UNVEILING ENZYMATIC MALONYL-THIOESTER DECARBOXYLATION WITH MALONYL-THIOESTER ISOSTERS	14
1.1 Natural products are a successful source for drug discovery.....	14
1.2 Polyketide synthases are a good source for new drugs with engineering potential.....	14
1.3 The ketosynthase produces the carbon-carbon bonds in PKS and FAS	16
1.4 Malonyl-thioesters are reactive at the thioester carbonyl and carboxylate.....	19
1.5 Synthesized malonyl-thioester analogs altered at the thioester carbonyl	21
1.6 New malonyl-thioester analogs will preserve the thioester carbonyl and alter the carboxylate.....	22
1.7 References.....	24
CHAPTER 2. SULFONATE/NITRO BEARING METHYLMALONYL-THIOESTER ISOSTERES APPLIED TO METHYLMALONYL-COA DECARBOXYLASE STRUCTURE- FUNCTION STUDIES	27
2.1 Abstract.....	27
2.2 Malonyl-thioester analogs do not orient the altered thioester carbonyls in the oxyanion hole	28
2.3 Synthesis of carboxylate isosteres to perform structure-function studies with MMCD...	29
2.4 Methylmalonyl-CoA active site positioning promotes decarboxylase mechanism	31
2.5 Alternative active site orientations lead to hydrolysis	32
2.6 Inhibition of MMCD with methylmalonyl-CoA analogs	33
2.7 Malonyl-CoA analogs provide an avenue to test β -ketoacyl synthase mechanism	33
2.8 References.....	34

CHAPTER 3. CO-CRYSTAL STRUCTURES OF METHYLMALONYL-COA EPIMERASE CONTRADICT GENERAL ACID-BASE CATALYSIS, PROVIDE SUBSTRATE SPECIFICITY INSIGHTS	36
3.1 Abstract	36
3.2 Methylmalonyl-CoA epimerase was proposed to undergo acid/base catalysis	37
3.3 Structures of MMCE with methylmalonyl-CoA and nitro analog and mutant assays suggest acid/base catalysis is not the catalytic mechanism	38
3.4 Other possible mechanisms for MMCE epimerization.....	41
3.5 Proposed experiments to test directional or mixed epimerase activity.....	42
3.6 Experiments to test substrate engineering potential.....	42
3.7 Conclusions.....	42
3.8 References.....	43
CHAPTER 4. SYNTHESIS OF MALONYL-THIOESTER ANALOGS WITH SULFONATE CARBOXYLATE ISOSTERES AND ACTIVITY WITH FATTY ACID SYNTHASE KETOSYNTHASE.....	46
4.1 Abstract.....	46
4.2 Malonyl-thioester reactivity has led to limited structure-function studies	47
4.3 Synthesis of malonyl-thioester analogs overcomes substrate reactivity.....	48
4.4 Stability and inhibition assays of malonyl-thioester analogs with FabH.....	50
4.5 Synthesis of malonyl-ACP analogs	51
4.6 Conclusions.....	51
4.7 Appendix A. Stability and inhibition assays of malonyl-thioester analogs with FabH....	52
4.8 Appendix B. Experimental synthesis procedures	56
4.9 Appendix C. NMR characterization.	65
4.10 References	108
CHAPTER 5. CONCLUDING REMARKS.....	109
5.1 Malonyl-thioester isosteres limit enzyme reactivity allowing for structure-function studies	109
5.2 Methylmalonyl-CoA analog studies with MMCD yield proposed decarboxylation mechanism	109
5.3 Studies with LnmK reveal substrate geometry leading to proposed mechanism	110

5.4	Expanding malonyl-thioester analog toolbox to study ketosynthases	113
5.4.1	Malonyl-thioester analogs inhibit KasIII revealing potential structure-function applications	113
5.4.2	Preliminary structure-function studies with CHS II from <i>Medicago sativa</i>	114
5.4.3	Future goals for type I KS enzymes	116
5.5	Excitement of new malonyl-thioester analogs and their ability to perform structure function studies on enzymes not previously possible	116
5.6	References.....	117

LIST OF TABLES

Table 3.1 MMCE WT and mutant epimerization assays.	40
Table 4.1 FabH inhibition constants for malonyl-thioester analogs.	55

LIST OF FIGURES

- Figure 1.1 Domain architecture of fatty acid synthase and polyketide synthase. A) Mammalian type I FAS is one complex made up of catalytic domains to form a dimer. B) Fungal type I FAS is one complex made up of catalytic domains to form a dodecamer. C) Bacterial and plant type II FAS are made up of independent enzymes. D) Modular type I PKS is one complex made up of catalytic domains with the minimum domains to form a module including the KS, AT, and ACP. E) Trans-acyltransferase modular type I PKS is one complex made up of catalytic domains with the exception of the AT which exists as an independent enzyme acting in trans to the PKS enzyme. Type II PKS are comprised of independent enzymes. F) Type III PKS are similar to type II where enzymes are independent, but type III are ACP independent. 15
- Figure 1.2 Ketosynthases perform an acyl transfer reactions resulting in an acyl-KS intermediate. A malonyl-thioester undergoes a Claisen condensation to form a carbon-carbon bond and produce an acetoacetyl-ACP/CoA product. 17
- Figure 1.3 Co-crystal structure of CHS in complex with malonyl-CoA (PDB 1CML). A) A $2F_o - F_c$ electron density map set to an RMSD value of 1.0 showing disconnected electron density for the bound malonyl-CoA at the adenosine, pantetheine, alpha carbon, and carboxylate moieties. B) Malonyl-CoA in complex with CHS revealing malonyl-CoA (MLC) not bound near the active site residues Cys164, His303, and Asn336. C) The proposed model for how malonyl-CoA is positioned in the active site of CHS with the thioester carbonyl stabilized by His303 and Asn336. 18
- Figure 1.4 Reactivity of malonyl-CoA at the thioester carbonyl and carboxylate. A) Acyl transfer or hydrolysis takes place when a nucleophile attacks the thioester carbonyl forming a tetrahedral intermediate that collapses to form the product. B) Decarboxylation occurs when the carbon-carbon bond between the C_{α} - $C_{\text{carboxylate}}$ breaks resulting in an enolate intermediate which needs to be stabilized and protonated to form the product. 20
- Figure 1.5 Malonyl-thioester analogs altered at the thioester carbonyl. A) 2-carboxypropyl-S-CoA (black sticks) in complex with MMCD (PDB 1EF9) revealing the thioether carbon oriented towards solvent. B) The oxetane analog (black sticks) in complex with DpsC (PDB 5WGC) revealing the oxetane moiety oriented towards solvent. 22
- Figure 1.6 Malonyl-thioester analogs preserving the thioester carbonyl or altering it to an ester or amide and altering the carboxylate to a sulfonate or nitro group. 23
- Figure 2.1 Our methylmalonyl-CoA analogs **4–9** compared to the previously used thioether (**2**) and oxetane (**3**). Phosphopantetheine moiety is abbreviated ppant. 28
- Figure 2.2 MMCD-isostere binding interactions. (A) Overlay of MMCD chain A with **4**-black, **5**-gray and **6**-white. Green dashes indicate oxyanion hole. Both C-1 stereoisomers of **4–6** modeled. Surface of active site residues is shown for **4** bound, notice His66-imidazole contacts solvent and active site surfaces. Hydrogens (diminutive ball-sticks) predicted based on geometry. (B) Overlay of MMCD chain A with **7**-black and **9**-white. Red dashes illustrate intramolecular hydrogen bond of **9**. (C) Overlay of **4** and **7** structures, demonstrating similar carboxylate isostere orientations, suggesting methylmalonyl-carboxylate interacts with Pro133. Yellow dashes indicate potential hydrogen bond. 30

Figure 2.3 Flattened schematics for the binding of isosteres to MMCD and proposed catalytic mechanism. (A) Generalized binding of the isosteres, with the color of the R-groups matching the structures in Figure 2.2. (B) Proposed (2 <i>R/S</i>)-methylmalonyl-CoA binding modes for MMCD and the following decarboxylase mechanism invoking rotation of His66 side chain into the active site.	31
Figure 3.1 Possible catalytic mechanisms. A) Substrate binding B) General acid-base catalysis. C) Enolization via 1,3-H shift with metal displacement and solvent tautomerization. D) Decarboxylation/re-carboxylation. E) Metal hydroxide displacement with concomitant enolate formation.....	37
Figure 3.2 Overlay of apo-ScMMCE structure (green), methylmalonyl-CoA bound in ScMMCE (yellow), and nitropropionyl-S-CoA bound in ScMMCE (blue) with the pink sphere modeled as nickel.....	38
Figure 3.3 NMR analysis of (2 <i>RS</i>)-methylmalonyl-CoA conversion to propionyl-CoA via MMCE and PccB.	41
Figure 4.1 A) Carbon-carbon bond forming activity of FabH. B) FabH C→Q mutant decarboxylation activity. C) Possible inhibition of FabH by stable malonyl-thioester analogs. Squiggly line represents phosphopantetheine.....	47
Figure 4.2 Stability assays of sulfonate-bearing analogs with FabH. Red is 1 hour without enzyme, orange is 24 hours without enzyme, green is 1 hour with enzyme, and blue is 24 hours with enzyme. A) 37 with FabH wt B) 38 with FabH wt C) 39 with FabH wt D) 37 with FabH C→Q E) 38 with FabH C→Q F) 39 with FabH C→Q.....	54
Figure 5.1 Nitro-bearing substrate analogs reveal substrate binding mode and active site amino acid residues Phe65, Phe223, and Asn216.....	111
Figure 5.2 Model of LnmK decarboxylation: Phe223 amide stabilizes enolate, carboxylate interacts with Asn216 and Asn216. Tyr62 is the nucleophile for self-acyl-transfer.	112
Figure 5.3 CHS II (cyan sticks) with carboxy-carba(dethia)-CoA bound (black sticks) overlaid with an acyl-S-KS (FabH, PDB 1HNH) intermediate to monitor a Claisen condensation-like conformation. The white sticks are theoretical carboxylate positions.....	115

LIST OF SCHEMES

Scheme 2.1 Synthetic Scheme for Methylmalonyl-CoA Analogs.....	29
Scheme 4.1 Synthesis of sulfonate-bearing and nitro-bearing malonyl-thioester analogs.	48
Scheme 4.2 Chemoenzymatic synthesis of ppant, CoA and ACP containing malonyl-thioester analogs	49

LIST OF ABBREVIATIONS

ACN – acetonitrile	MAT - Malonyl CoA/acetyl-CoA-acyl carrier protein transacylase
ACP – acyl carrier protein	MCD – malonyl-CoA decarboxylase
ATP – adenosine triphosphate	MMCD – methylmalonyl-CoA decarboxylase
CHS – Chalcone synthase II	MMCE – methylmalonyl-CoA epimerase
CF – chloroform	N.I. – not isolated
CoA – Coenzyme A	<i>P. shermanii</i> - <i>Propionibacterium shermanii</i>
DCM – dichloromethane	Pant – pantetheine
DH – β -hydroxyacyl dehydratase	Ppant - phosphopantetheine
DMF – dimethylformamide	PDB – protein databank
DMP- 2,2-dimethoxypropane	PKS – polyketide synthase
<i>E. coli</i> - <i>Escherichia coli</i>	pTsOH – p-toluenesulfonic acid
ECF – ethylchloroformate	<i>R. palustris</i> - <i>Rhodopseudomonas palustris</i>
EtOAc – ethyl acetate	Rms – root-mean-square
EtOH – ethanol	<i>S. coelicolor</i> - <i>Streptomyces coelicolor</i>
ER – enoyl-reductase	SLP – SCP2-thiolase-like protein
FabH or KasIII - 3-oxoacyl-[acyl-carrier-protein] synthase 3	TE – thioesterase
FAS – fatty acid synthase	TEA – trimethylamine
GNAT - GCN5-related N-acetyltransferase	TFA – trifluoroacetic acid
KR – β -ketoacyl reductase	
KS – ketosynthase	
<i>M. sativa</i> – <i>Medicago sativa</i>	

ABSTRACT

Malonyl-thioesters are reactive at the thioester carbonyl and the carboxylate moieties, as seen in acyl transfer or hydrolysis and decarboxylation. Enzymes use these reactive centers to perform different enzyme chemistry throughout metabolism. This enzyme chemistry coupled with the inherent reactivity of malonyl-thioesters makes structure-function studies difficult. When malonyl-thioesters are used for structure-function studies, it usually results in a hydrolyzed or decarboxylated product. There are examples, however, where this is overcome, many of which are discussed throughout this thesis. To overcome the inherent reactivity of malonyl-thioesters and enzymes, analogs have been synthesized to perform structure-function studies. Initial studies focused on altering the thioester carbonyl to limit hydrolysis and decarboxylation; however, these studies revealed the importance of retaining the thioester carbonyl to be positioned in the oxyanion hole. My thesis work focused on the synthesis, characterization, and use in structure-function studies of malonyl-thioester analogs that either preserve the thioester carbonyl or alter it to an ester or amide, and alter the carboxylate to a sulfonate or nitro group. After synthesizing the methylmalonyl-CoA analogs, we performed structure-function studies with methylmalonyl-CoA decarboxylase. This case study revealed the potential of these analogs to both inhibit decarboxylase activity and their use in structure-function studies to gain mechanistic insights. This successful study prompted us to continue these structure-function studies in enzymes with different chemistries such as an epimerase or bi-functional acyltransferase/decarboxylase. The widespread use of these methylmalonyl-CoA analogs also motivated us to add more malonyl-thioester analogs to our toolbox. I have preliminary data that these malonyl-thioester analogs inhibit β -keto-acyl-synthase III, an enzyme involved in fatty acid production in *E. coli*. This inhibition gives us confidence that these analogs will be useful in structure-function studies that will reveal answers to long standing mechanism and protein-protein interaction questions in the polyketide and fatty acid synthase field.

CHAPTER 1. UNVEILING ENZYMATIC MALONYL-THIOESTER DECARBOXYLATION WITH MALONYL-THIOESTER ISOSTERS

1.1 Natural products are a successful source for drug discovery

Almost two-thirds of drugs or drug leads come from natural products, natural product derivatives, or synthetic variations of a natural product¹. Natural product derivatives have commonly been shown to enhance the efficacy of a natural product's drug efficacy or limit side reactivity. One of the most popular examples is the discovery of the antibiotic erythromycin which had antibacterial activity but also had severe side effects such as liver disease, muscle weakness, blurred vision, and hearing loss. The synthetic derivatization of erythromycin to azithromycin made azithromycin one of the most popular antibiotics to date².

1.2 Polyketide synthases are a good source for new drugs with engineering potential

Polyketide synthases (PKS) are an enzyme class that produces diverse chemical compounds many of which have made it into the clinic³. Some of the most popular drugs made by polyketide synthases are the antibiotics tetracycline and erythromycin, the statin lovastatin, and the anticancer drug epothilone. PKS have various types of architectures categorized into two main types, multimodular mega-enzymes (type I) or independent enzymes (type II), Figure 1.1. The common enzymes to PKS and fatty acid synthases (FAS) are the acyltransferase (AT) that loads malonyl-thioester substrates onto the acyl carrier protein (ACP), which moves the substrate and growing natural product through all catalytic domains and the ketosynthase (KS) which forms carbon-carbon bonds between the growing polyketide and a malonyl-thioester substrate. The resulting β -keto is reduced to various levels by ketoreductase (KR), dehydratase (DH), or enoyl reductase (ER), and can be altered by other specialized domains unique to PKS. The order of enzymes performing these specific reactions follows the same order as the PKS genes, referred to as a collinear relationship, make it possible to predict the natural product of a PKS through its genetic code.

The collinear genetic architecture of PKS reveals potential for genetic engineering. Domain deletion to alter the natural product is possible with reasonable engineered product production; however, when a domain/enzyme is attempted to be added or replaced with a homolog from a

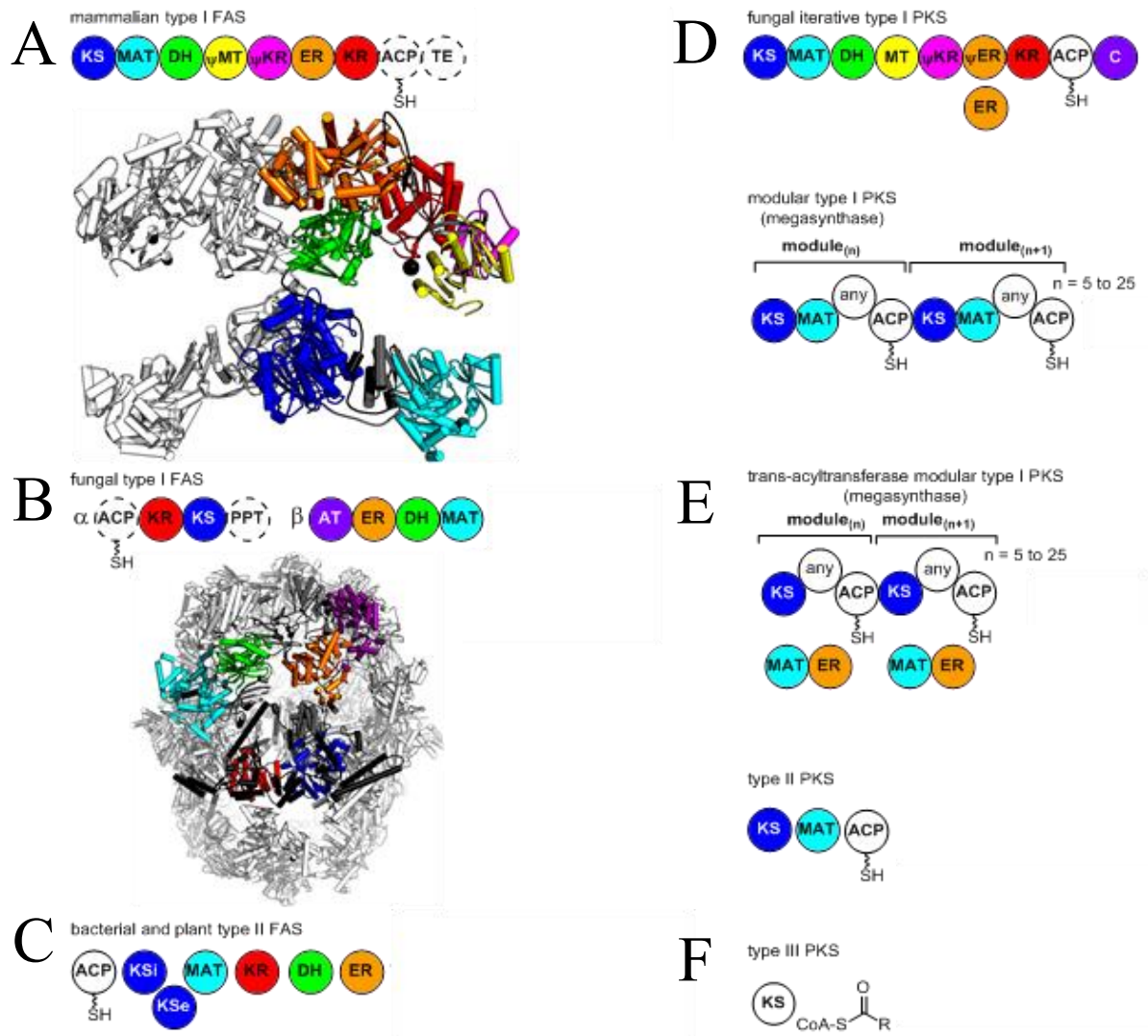


Figure 1.1 Domain architecture of fatty acid synthase and polyketide synthase. A) Mammalian type I FAS is one complex made up of catalytic domains to form a dimer. B) Fungal type I FAS is one complex made up of catalytic domains to form a dodecamer. C) Bacterial and plant type II FAS are made up of independent enzymes. D) Modular type I PKS is one complex made up of catalytic domains with the minimum domains to form a module including the KS, AT, and ACP. E) Trans-acyltransferase modular type I PKS is one complex made up of catalytic domains with the exception of the AT which exists as an independent enzyme acting in trans to the PKS enzyme. Type II PKS are comprised of independent enzymes. F) Type III PKS are similar to type II where enzymes are independent, but type III are ACP independent.

different PKS the production of the desired engineered product drops to below one percent yields⁴⁻⁸. The success in these engineering attempts provided the preliminary possibility of engineering PKS. To increase the yields of the engineered natural product, we need a better understanding of

the new protein-protein interactions that are introduced into the engineered PKS. Another possibility is that the new protein-protein interactions do not allow for proper substrate positioning within the enzyme to promote chemistry.

Attempts to study the differences between different PKS protein-protein interactions have yielded conflicting results. These studies commonly consist of tethering enzymes for structural studies through chemical crosslinking, most commonly through the active site residues, which has the greater potential of producing artifactual protein-protein interactions⁹⁻¹². Crosslinking these enzymes results in an inherent bias of the protein-protein interactions that are captured and since the active site residues are being used for the crosslinking we are unable to determine which catalytic state was captured, if a catalytic state was captured at all. Therefore, the field lacks the tools to perform protein-protein interaction structural studies that can mimic the substrate, intermediate, or product bound state to capture potential conformational states.

Some PKS and FAS have similar domain/enzyme genetic architecture, Figure 1.1. Therefore, performing protein-protein interaction studies on the domains/enzymes in PKS or FAS will yield important conclusions for one another. FAS contain many of the same domains discussed above with the only difference being that all of the β -keto reducing domains are present (KR, DH, ER). Since FAS have different overall structural topologies in mammalian, fungal, and bacterial, studying the protein-protein interactions could lead to noticeable differences between FAS in different organisms. Knowledge of these differences could be used to develop drugs against a specific organisms' FAS which would greatly help the drug development against FAS for diseases such as cancer or weight loss.

1.3 The ketosynthase produces the carbon-carbon bonds in PKS and FAS

The domain/enzyme responsible within PKS and FAS for forming the carbon-carbon bond is the KS. KS perform an acyl transfer reaction followed by a decarboxylative Claisen condensation reaction, Figure 1.2. The acyl transfer substrate comes from a loading acyl substrate or an upstream module acyl intermediate. The active site cysteine of the KS is the nucleophile for the acyl-ACP or acyl-CoA which results in an acyl-KS intermediate and free ACP or CoA. This

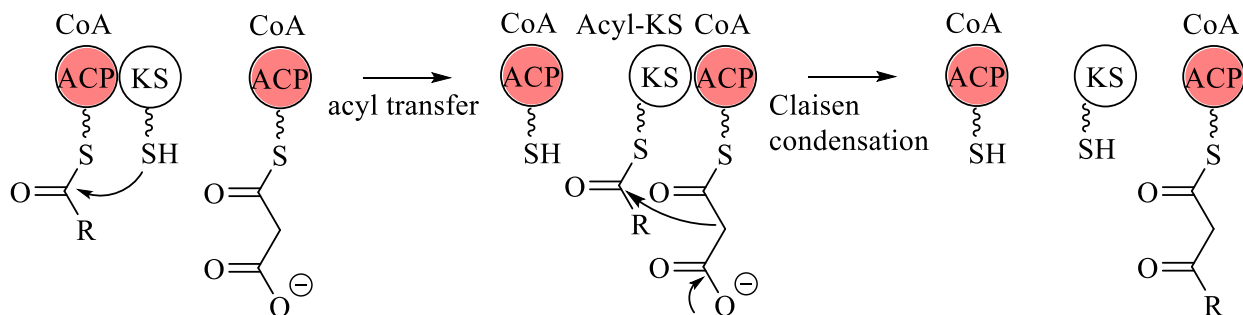


Figure 1.2 Ketosynthases perform an acyl transfer reactions resulting in an acyl-KS intermediate. A malonyl-thioester undergoes a Claisen condensation to form a carbon-carbon bond and produce an acetoacetyl-ACP/CoA product.

acyl-KS intermediate accepts a malonyl-CoA or malonyl-ACP (generally referred to as malonyl-thioester) which is decarboxylated to yield an enolate. The enolate intermediate reacts with the acyl-KS intermediate producing a β -ketoacyl-ACP or -CoA. The complex reaction taking place within the KS most likely requires the substrates and acyl-KS intermediates to be properly positioned in the active site. If that positioning is altered due to different protein-protein interactions, as is seen in engineered PKS, it is likely that the reaction would not take place.

A remaining question in the PKS/FAS field is how protein-protein interactions lead to malonyl-thioester binding in the KS active site to allow for decarboxylative Claisen condensation. Attempts to study KS-ACP interaction have relied on the crosslinking of the KS active site cysteine and pantetheine arm of the ACP⁹⁻¹². These studies reveal some protein-protein interactions; however, the protein-protein interactions relevant to malonyl-thioester active site positioning is unknown because of the absence of the substrate. Simpler studies look at KS that use coenzyme A (CoA) tethered substrates (type III PKS) instead of ACP tethered substrates. When structure-function studies are performed with KS and malonyl-CoA they result in poor residual density for the active site malonyl moiety. This can be seen with chalcone synthase II co-crystallized with malonyl-CoA leading to missing density for the malonyl moiety (PDB 1CML), Figure 1.3A¹³.

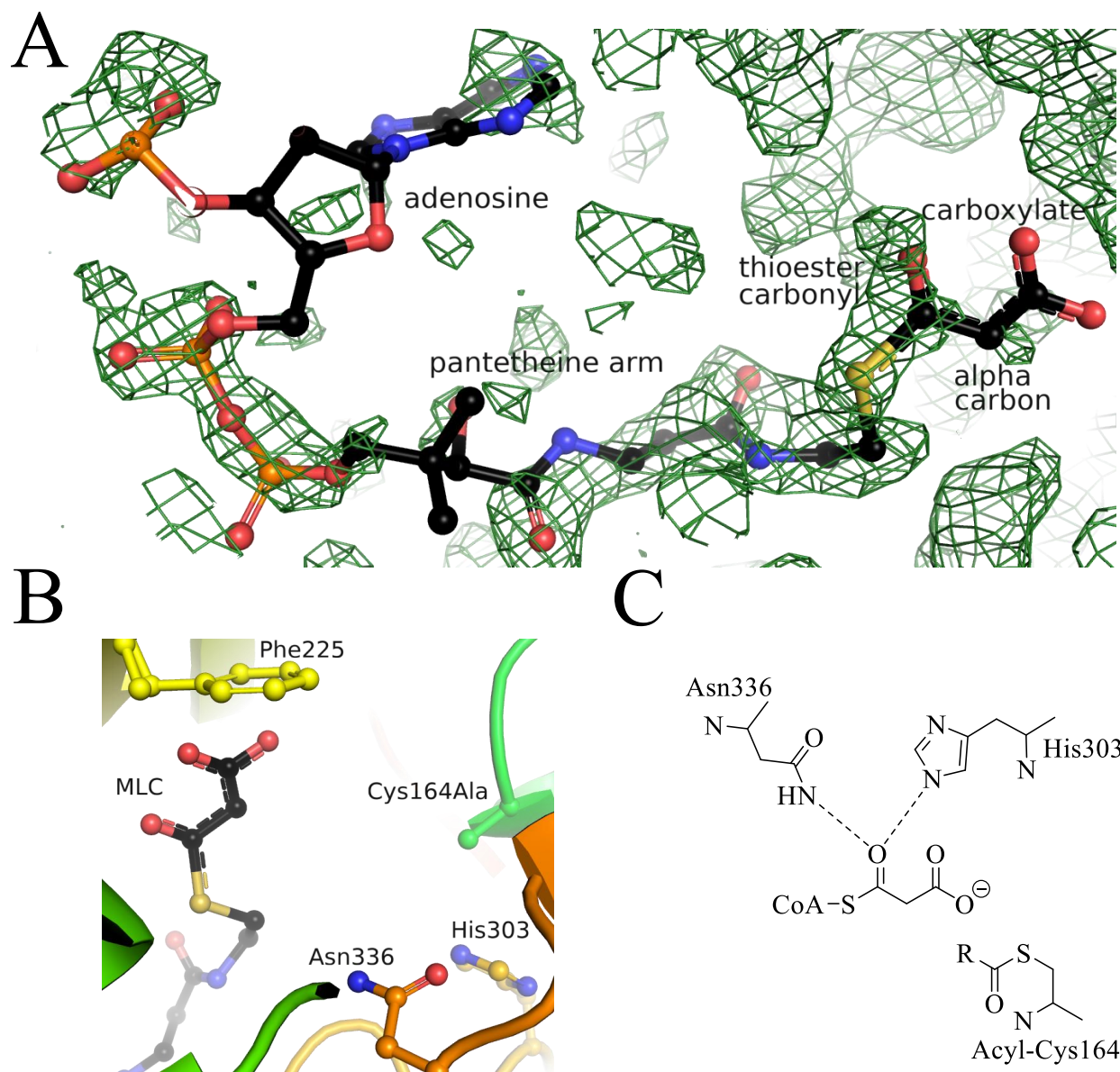


Figure 1.3 Co-crystal structure of CHS in complex with malonyl-CoA (PDB 1CML). A) A 2Fo-Fc electron density map set to an RMSD value of 1.0 showing disconnected electron density for the bound malonyl-CoA at the adenosine, pantetheine, alpha carbon, and carboxylate moieties. B) Malonyl-CoA in complex with CHS revealing malonyl-CoA (MLC) not bound near the active site residues Cys164, His303, and Asn336. C) The proposed model for how malonyl-CoA is positioned in the active site of CHS with the thioester carbonyl stabilized by His303 and Asn336.

This missing density led to a CHS structure with malonyl-CoA not bound near the active site residues, Figure 1.3B, as predicted by the authors and their enzymology data, Figure 1.3C¹³⁻¹⁶. The missing electron density in the active site is likely due to the inherent reactivity of malonyl-

thioesters, Figure 1.4¹⁷⁻¹⁹. This missing density phenomena is seen repeatedly for enzymes such as the KS-MAT didomain in mouse FAS (PDB 5MY0), malonyl-CoA decarboxylase (PDB 2REF, 2YGW, 4F0X, 4KSA, 4KSF, 4KS9, and 5AB7), LnmK (PDB 4HZO and 4HZP), β -ketoacyl-acyl carrier protein synthase III (PDB 1HNJ), and stilbene synthase (PDB 1XET)²⁰⁻²⁶. These results in various enzymes suggest that malonyl-CoA is too reactive of a molecule for structure-function studies, establishing a need for malonyl-thioester analogs.

1.4 Malonyl-thioesters are reactive at the thioester carbonyl and carboxylate

Malonyl-thioesters are reactive molecules at the thioester carbonyl and the beta-carboxylate performing energetically favorable acyl transfer and decarboxylation, respectively, Figure 1.4. The thioester carbonyl is an easy target for a nucleophilic attack due to the carbonyl's electrophilic characteristic, Figure 1.4A. Hydrolysis of the thioester bond releases 31.4 kJ/mol of energy making it a high energy bond¹⁷. The exact amount of energy released on decarboxylation is unknown, especially the decarboxylation in a Claisen condensation which is seen in fatty acid metabolism. The energy necessary to produce carbon-carbon (C-C) bonds through two acyl-CoA molecules is $\Delta G^\circ = +12$ kJ/mol¹⁸. However fatty acid metabolism uses a malonyl-thioester substrate which is made through an ATP-dependent carboxylation and has an energy of $\Delta G^\circ = -37$ kJ/mol for ATP hydrolysis¹⁹. Therefore, the decarboxylative Claisen condensation of malonyl-thioesters must have an energy larger than what is required for C-C bond formation which is less than or equal to 25 kJ/mol ($\Delta G^\circ = 12$ kJ/mol - 37 kJ/mol = -25 kJ/mol). The high free energy for each of these reactions explain why hydrolysis and decarboxylation are “nearly” irreversible. The favorable and irreversible characteristics of malonyl-thioesters to hydrolyze and decarboxylate can explain why many of the structure-function studies attempted with different malonyl-thioesters resulted in hydrolyzed or decarboxylated active site density.

Malonyl-thioester

reactivity is harnessed by many different enzyme classes within cells. Malonyl-CoA can be made by carboxylases, carboxytransferases and ligases. Acyltransferases and hydrolases can react with the thioester carbonyl of malonyl-CoAs and decarboxylases can react to break the C_{α} - $C_{\text{carboxylate}}$ bond. If substituents exist off of the C_{α} , they can be epimerized through epimerases. A combination of these reactions can be used by more complicated enzymes, such as KS mentioned above.

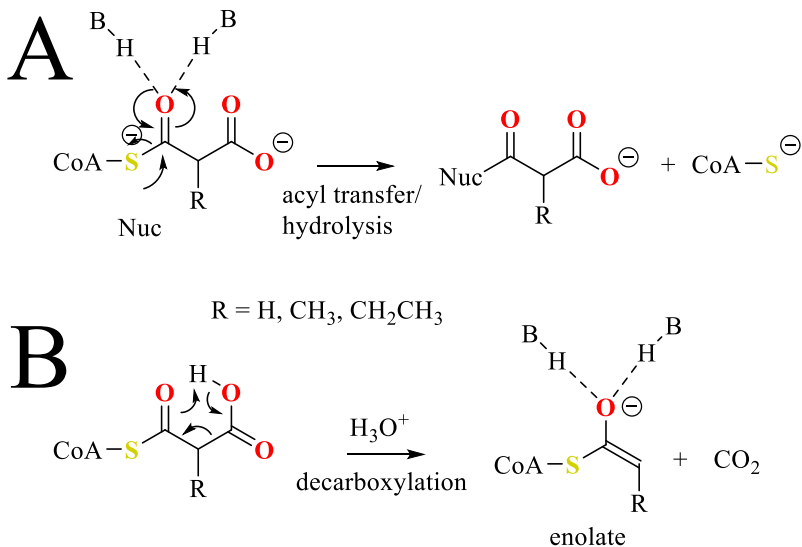


Figure 1.4 Reactivity of malonyl-CoA at the thioester carbonyl and carboxylate. A) Acyl transfer or hydrolysis takes place when a nucleophile attacks the thioester carbonyl forming a tetrahedral intermediate that collapses to form the product. B) Decarboxylation occurs when the carbon-carbon bond between the C_{α} - $C_{\text{carboxylate}}$ breaks resulting in an enolate intermediate which needs to be stabilized and protonated to form the product.

Since so many different enzymes use or produce malonyl-thioesters, how do enzymes stabilize a reactive molecule to perform a specific chemistry and prevent side reactions? To answer this question structure-function studies and follow-up enzymology is needed. Many of the enzymes mentioned above are thoroughly characterized in terms of kinetic mechanism and stereochemical control. However, there are almost no enzyme structures with malonyl-thioesters bound leaving most structure-function studies incomplete²⁰⁻³⁶. The lack of structure-function studies with malonyl-thioesters is not due to a lack of effort as many attempts have been made with carboxylases, decarboxylases, acyltransferases, epimerases, and ketosynthases²⁰⁻²⁶. Rather, as seen in the CHS example mentioned above, Figure 1.3, many of the structure-function studies performed on these enzymes resulted in hydrolysis or decarboxylation of the malonyl-thioester. Therefore, in order to perform structure-function studies on enzymes that use malonyl-thioesters as a substrate or product, malonyl-thioester analogs need to be synthesized to overcome the inherent reactivity of the molecule with enzymes.

1.5 Synthesized malonyl-thioester analogs altered at the thioester carbonyl

Malonyl-thioester analogs altered at the thioester carbonyl have been synthesized for structure-function studies. The first example of a malonyl-thioester substrate analog was 2-carboxypropyl-*S*-CoA, Figure 1.5A. This compound mimics methylmalonyl-CoA with the thioester carbonyl replaced with a methylene thioether bond, which is completely stable to hydrolysis and decarboxylation. 2-carboxypropyl-*S*-CoA has been solved in complex with methylmalonyl-CoA mutase (PDB 7REQ) and methylmalonyl-CoA decarboxylase (PDB 1EF9). A superimposition of methylmalonyl-CoA mutase structures with either 2-carboxypropyl-*S*-CoA or methylmalonyl-CoA bound, reveals the analog mimics the substrate. However, 2-carboxypropyl-*S*-CoA in complex with methylmalonyl-CoA decarboxylase (MMCD) reveals the carboxylate moiety binds in the proposed oxyanion hole rather than in a catalytically relevant orientation. In order for methylmalonyl-CoA to decarboxylate, the thioester carbonyl needs to be stabilized in the oxyanion hole. Therefore, 2-carboxypropyl-*S*-CoA does not mimic methylmalonyl-CoA in MMCD, as such the authors predicted the substrate position through MMCD's structural homology with a substrate bound structure of 4-chlorobenzoyl-CoA dehalogenase. Another example of a malonyl-thioester substrate analog was malonyl-*S*-phosphopantetheine with an oxetane moiety in place of the thioester carbonyl (oxetane analog), Figure 1.5B. The oxetane moiety mimics the thioester carbonyl by having the oxygen in a similar position and limits hydrolysis and decarboxylation. The oxetane analog was solved in complex with DpsC (PDB 5WGC), Figure 1.5B. Within the active site of DpsC, the oxetane analog was positioned with the oxetane oxygen oriented towards solvent. In order to perform acyl transfer or ACP priming, it requires the stabilization of an enolate intermediate, and based on the orientation of oxetane analog in the structure with DpsC, the enolate intermediate would need to be stabilized by only water molecules which is unlikely. The 2-carboxypropyl-*S*-CoA and oxetane analogs with the altered thioester carbonyl oriented towards solvent suggests that both of these analogs are not suitable to mimic malonyl-thioesters within enzymes that use an oxyanion hole to stabilize an enolate or tetrahedral intermediate.

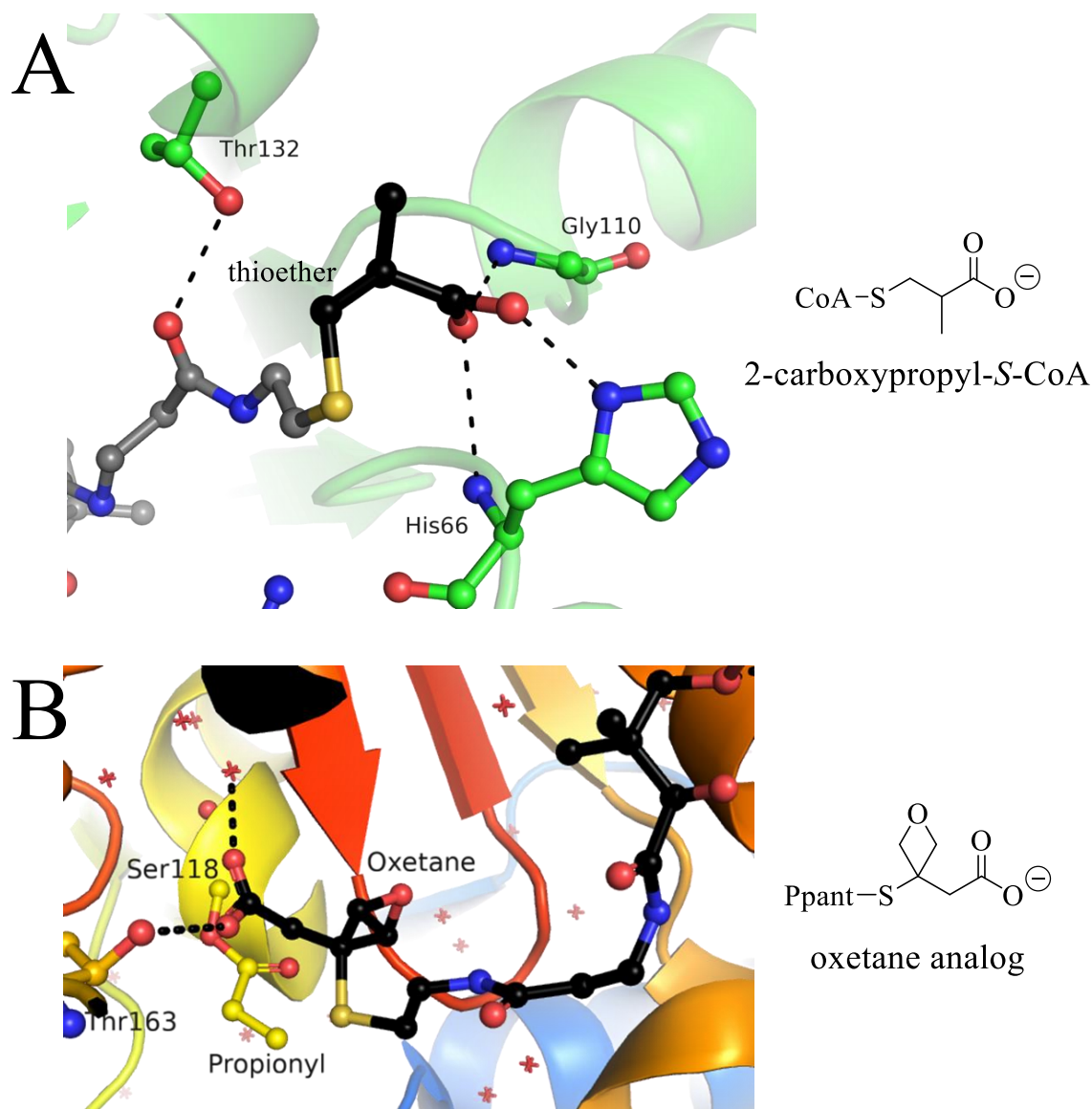


Figure 1.5 Malonyl-thioester analogs altered at the thioester carbonyl. A) 2-carboxypropyl-S-CoA (black sticks) in complex with MMCD (PDB 1EF9) revealing the thioether carbon oriented towards solvent. B) The oxetane analog (black sticks) in complex with DpsC (PDB 5WGC) revealing the oxetane moiety oriented towards solvent.

1.6 New malonyl-thioester analogs will preserve the thioester carbonyl and alter the carboxylate

Since the 2-carboxypropyl-S-CoA and oxetane analogs exemplified the importance of the thioester carbonyl, the compounds that will be discussed in this thesis preserved the thioester carbonyl or retained it as an ester or amide and altered the carboxylate to sulfonate and nitro groups, Figure 1.6. The panel of thioester, ester, and amide carbonyl compounds is to help limit

hydrolysis while the sulfonate and nitro moieties will limit breaking the C α -N or C α -S bond. Since capture the KS-ACP protein-protein interactions and active site positioning entails multiple proteins and substrates, we began testing our malonyl-thioester analogs against simpler enzymes. The first structure-function study we

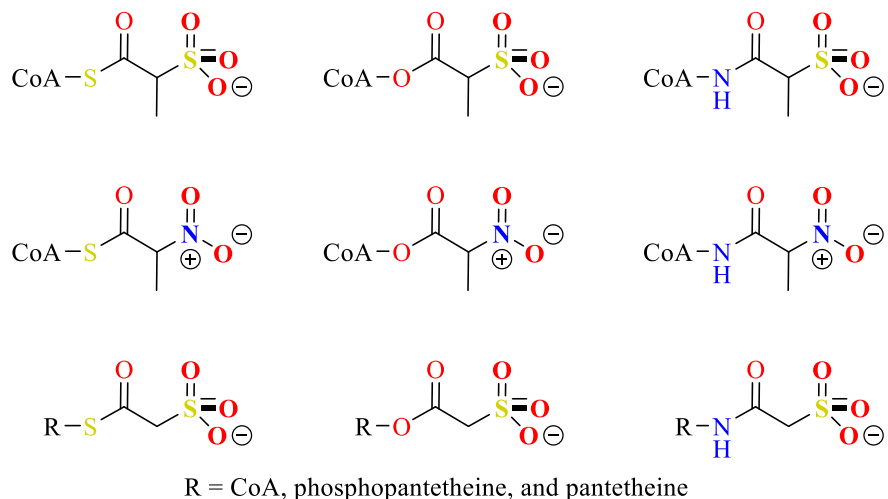


Figure 1.6 Malonyl-thioester analogs preserving the thioester carbonyl or altering it to an ester or amide and altering the carboxylate to a sulfonate or nitro group.

used our sulfonate and nitro bearing analogs in was with MMCD, which allowed us to directly compare these new compounds to 2-carboxypropyl-S-CoA in the same enzyme, discussed in chapter 2. After seeing the stability of our sulfonate and nitro bearing compounds in MMCD we performed structure-function studies with LnmK, a bifunctional acyltransferase-decarboxylase, discussed in chapter 5. Since the nitro bearing compounds appeared as a planar nitronate in both studies, we used it as a transition state analog in a structure-function study with methylmalonyl-CoA epimerase, discussed in chapter 3. After testing panel of malonyl-thioester analogs against many different enzyme chemistries, we began inhibition studies with β -ketoacylsynthase III from *Escherichia coli*, discussed in chapter 4. All of our studies with the panel of malonyl-thioester analogs gives us confidence to start performing structure-function studies with ketosynthases to capture the multiple substrate positions as well as the KS-ACP protein-protein interactions.

1.7 References

1. Newman, D. J.; Cragg, G. M., Natural Products as Sources of New Drugs from 1981 to 2014, *Journal of natural products* **2016**, *79* (3), 629-61.
2. Jelic, D.; Antolovic, R., From Erythromycin to Azithromycin and New Potential Ribosome-Binding Antimicrobials. *Antibiotics* **2016**, *5* (3).
3. Cummings, M.; Breitling, R.; Takano, E., Steps towards the synthetic biology of polyketide biosynthesis. *FEMS Microbiology Letters* **2014**, *351* (2), 116-25.
4. Marsden, A. F.; Caffrey, P.; Aparicio, J. F.; Loughran, M. S.; Staunton, J.; Leadlay, P. F., Stereospecific acyl transfers on the erythromycin-producing polyketide synthase. *Science* **1994**, *263* (5145), 378-80.
5. Pfeifer, B. A.; Admiraal, S. J.; Gramajo, H.; Cane, D. E.; Khosla, C., Biosynthesis of complex polyketides in a metabolically engineered strain of *E. coli*. *Science* **2001**, *291* (5509), 1790-2.
6. McDaniel, R.; Ebert-Khosla, S.; Fu, H.; Hopwood, D. A.; Khosla, C., Engineered biosynthesis of novel polyketides: influence of a downstream enzyme on the catalytic specificity of a minimal aromatic polyketide synthase. *Proceedings of the National Academy of Sciences of the United States of America* **1994**, *91* (24), 11542-6.
7. McDaniel, R.; Kao, C. M.; Hwang, S. J.; Khosla, C., Engineered intermodular and intramodular polyketide synthase fusions. *Chemistry & biology* **1997**, *4* (9), 667-74.
8. McDaniel, R.; Thamchaipenet, A.; Gustafsson, C.; Fu, H.; Betlach, M.; Betlach, M.; Ashley, G., Multiple genetic modifications of the erythromycin polyketide synthase to produce a library of novel “unnatural” natural products. *Proceedings of the National Academy of Sciences of the United States of America* **1999**, *96*, 1846-1851.
9. Bruegger, J.; Haushalter, R. W.; Vagstad, A. L.; Shakya, G.; Mih, N.; Townsend, C. A.; Burkart, M. D.; Tsai, S. C., Probing the selectivity and protein-protein interactions of a nonreducing fungal polyketide synthase using mechanism-based crosslinkers. *Chemistry & biology* **2013**, *20* (9), 1135-46.
10. Barajas, J. F.; Finzel, K.; Valentic, T. R.; Shakya, G.; Gamarra, N.; Martinez, D.; Meier, J. L.; Vagstad, A. L.; Newman, A. G.; Townsend, C. A.; Burkart, M. D.; Tsai, S. C., Structural and Biochemical Analysis of Protein-Protein Interactions Between the Acyl-Carrier Protein and Product Template Domain. *Angewandte Chemie* **2016**, *55* (42), 13005-13009.
11. Miyanaga, A.; Ouchi, R.; Ishikawa, F.; Goto, E.; Tanabe, G.; Kudo, F.; Eguchi, T., Structural Basis of Protein-Protein Interactions between a trans-Acting Acyltransferase and Acyl Carrier Protein in Polyketide Disorazole Biosynthesis. *Journal of the American Chemical Society* **2018**, *140* (25), 7970-7978.
12. Chen, A.; Re, R. N.; Burkart, M. D., Type II fatty acid and polyketide synthases: deciphering protein-protein and protein-substrate interactions. *Natural product reports* **2018**, *35* (10), 1029-1045.
13. Ferrer, J. L.; Jez, J. M.; Bowman, M. E.; Dixon, R. A.; Noel, J. P., Structure of chalcone synthase and the molecular basis of plant polyketide biosynthesis. *Nature Structural & Molecular Biology* **1999**, *6* (8), 775-84.
14. Jez, J. M.; Ferrer, J. L.; Bowman, M. E.; Dixon, R. A.; Noel, J. P., Dissection of malonyl-coenzyme A decarboxylation from polyketide formation in the reaction mechanism of a plant polyketide synthase. *Biochemistry* **2000**, *39* (5), 890-902.

15. Jez, J. M.; Bowman, M. E.; Noel, J. P., Structure-guided programming of polyketide chain-length determination in chalcone synthase. *Biochemistry* **2001**, *40* (49), 14829-38.
16. Jez, J. M.; Bowman, M. E.; Noel, J. P., Expanding the biosynthetic repertoire of plant type III polyketide synthases by altering starter molecule specificity. *Proceedings of the National Academy of Sciences of the United States of America* **2002**, *99* (8), 5319-24.
17. Berg, J., M.; Tymoczko, J., L.; Stryer, L., *Biochemistry*. New York: *W H Freeman* **2002**, 5.
18. Weber, A. L., Origin of fatty acid synthesis: thermodynamics and kinetics of reaction pathways. *Journal of Molecular Evolution* **1991**, *32*, 93-100.
19. Bergman, C.; Kashiwaya, Y.; Veech, R. L., The effect of pH and free Mg²⁺ on ATP linked enzymes and the calculation of Gibbs free energy of ATP hydrolysis. *The journal of physical chemistry. B* **2010**, *114* (49), 16137-46.
20. Rittner, A.; Paithankar, K. S.; Huu, K. V.; Grininger, M., Characterization of the Polyspecific Transferase of Murine Type I Fatty Acid Synthase (FAS) and Implications for Polyketide Synthase (PKS) Engineering. *ACS chemical biology* **2018**, *13* (3), 723-732.
21. Gu, L., T. W. G., Wang, B., Gerwick, W. H., Hakansson, K., Smith, J. L., and Sherman, D. H., GNAT-Like Strategy for Polyketide Chain Initiation. *Science* **2007**, *318*, 970-974.
22. Froese, D. S.; Forouhar, F.; Tran, T. H.; Vollmar, M.; Kim, Y. S.; Lew, S.; Neely, H.; Seetharaman, J.; Shen, Y.; Xiao, R.; Acton, T. B.; Everett, J. K.; Cannone, G.; Puranik, S.; Savitsky, P.; Krojer, T.; Pilka, E. S.; Kiyani, W.; Lee, W. H.; Marsden, B. D.; von Delft, F.; Allerston, C. K.; Spagnolo, L.; Gileadi, O.; Montelione, G. T.; Oppermann, U.; Yue, W. W.; Tong, L., Crystal structures of malonyl-coenzyme A decarboxylase provide insights into its catalytic mechanism and disease-causing mutations. *Structure* **2013**, *21* (7), 1182-92.
23. Aparicio, D.; Perez-Luque, R.; Carpena, X.; Diaz, M.; Ferrer, J. C.; Loewen, P. C.; Fita, I., Structural asymmetry and disulfide bridges among subunits modulate the activity of human malonyl-CoA decarboxylase. *The Journal of biological chemistry* **2013**, *288* (17), 11907-19.
24. Harijan, R. K.; Mazet, M.; Kiema, T. R.; Bouyssou, G.; Alexson, S. E.; Bergmann, U.; Moreau, P.; Michels, P. A.; Bringaud, F.; Wierenga, R. K., The SCP2-thiolase-like protein (SLP) of *Trypanosoma brucei* is an enzyme involved in lipid metabolism. *Proteins* **2016**, *84* (8), 1075-96.
25. Lohman, J. R.; Bingman, C. A.; Phillips, G. N., Jr.; Shen, B., Structure of the bifunctional acyltransferase/decarboxylase LnmK from the leinamycin biosynthetic pathway revealing novel activity for a double-hot-dog fold. *Biochemistry* **2013**, *52* (5), 902-11.
26. Qiu, X.; Janson, C. A.; Smith, W. W.; Head, M.; Lonsdale, J.; Konstantinidis, A. K., Refined structures of beta-ketoacyl-acyl carrier protein synthase III. *Journal of molecular biology* **2001**, *307* (1), 341-56.
27. Sacksteder, K. A.; Morrell, J. C.; Wanders, R. J. A.; Matalon, R.; Gould, S. J., MCD encodes peroxisomal and cytoplasmic forms of malonyl-CoA decarboxylase and is mutated in malonyl-CoA decarboxylase deficiency. *Journal of Biological Chemistry* **1999**, *274* (35), 24461-24468.
28. Hayaishi, O., Enzymatic decarboxylation of malonic acid. *The Journal of biological chemistry* **1955**, *215* (1), 125-36.
29. Wolfe, J. B.; Rittenberg, S. C., Malonate decarboxylation by *pseudomonas fluorescens*. *Journal of Biological Chemistry* **1954**, *209*, 885-892.

30. Hatch, M. D.; Stumpf, P. K., Fat metabolism in Higher Plants. XVII. Metabolism of Malonic Acid and Its α -Substituted Derivatives in Plants. *Plant Physiology* **1962**, *37* (2), 121-126.
31. F., L., Fatty acid synthesis from malonyl coa. *Methods in enzymology* **1962**, *5*, 443-451.
32. Liu, T.; Huang, Y.; Shen, B., Bifunctional Acyltransferase/Decarboxylase LnmK as the Missing Link for beta-Alkylation in Polyketide Biosynthesis. *Journal of the American Chemical Society* **2009**, *131* (20), 6900-+.
33. Tsay, J. T.; Oh, W.; Larsont, T. J.; Jackowski, S.; Rock, C. O., Isolation and Characterization of the 8-Ketoacyl-acyl Carrier Protein Synthase I11 Gene (fubH) from Escherichia coli K-12. *The Journal of biological chemistry* **1992**, *267* (10), 6807-6814.
34. Heath, R. J.; Rock, C. O., Inhibition of beta-ketoacyl-acyl carrier protein synthase III (FabH) by acyl-acyl carrier protein in Escherichia coli. *The Journal of biological chemistry* **1996**, *271* (18), 10996-1000.
35. Huang, W.; Jia, J.; Edwards, P.; Dehesh, K.; Schneider, G.; Lindqvist, Y., Crystal structure of beta-ketoacyl-acyl carrier protein synthase II from E.coli reveals the molecular architecture of condensing enzymes. *The EMBO Journal* **1998**, *17* (5), 1183-91.
36. Qiu, X.; Janson, C. A.; Konstantinidis, A. K.; Nwagwu, S.; Silverman, C.; Smith, W. W.; Khandekar, S.; Lonsdale, J.; Abdel-Meguid, S. S., Crystal structure of beta-ketoacyl-acyl carrier protein synthase III. *The Journal of biological chemistry* **1999**, *274* (51), 36465–36471.

CHAPTER 2. SULFONATE/NITRO BEARING METHYLMALONYL-THIOESTER ISOSTERES APPLIED TO METHYLMALONYL-COA DECARBOXYLASE STRUCTURE-FUNCTION STUDIES

Reprinted with permission from *J. Am. Chem. Soc.* 2019, 141, 13, 5121-5124. Copyright 2019 American Chemical Society.

Contributions: Jeremy R. Lohman and Lee M Stunkard designed experiments, interpreted the resulting data and wrote the manuscript. Lee M Stunkard carried out the vast majority of experiments. Austin D. Dixon and Tyler J. Huth assisted with data collection.

Citation: <https://doi.org/10.1021/jacs.9b00650>

Note: Literature references and chemical numbers within schemes are unique within this chapter.

2.1 Abstract

Malonyl-thioesters are reactive centers of malonyl-CoA and malonyl-S-acyl carrier protein, essential to fatty acid, polyketide and various specialized metabolite biosynthesis. Enzymes that create or use malonyl thioesters spontaneously hydrolyze or decarboxylate reactants on the crystallographic time frame preventing determination of structure–function relationships. To address this problem, we have synthesized a panel of methylmalonyl-CoA analogs with the carboxylate represented by a sulfonate or nitro and the thioester retained or represented by an ester or amide. Structures of *Escherichia coli* methylmalonyl-CoA decarboxylase in complex with our analogs affords insight into substrate binding and the catalytic mechanism. Counterintuitively, the negatively charged sulfonate and nitronate functional groups of our analogs bind in an active site hydrophobic pocket. Upon decarboxylation the enolate intermediate is protonated by a histidine preventing CO₂-enolate recombination, yielding propionyl-CoA. Activity assays support a histidine catalytic acid and reveal the enzyme displays significant hydrolysis activity. Our structures also provide insight into this hydrolysis activity. Our analogs inhibit decarboxylation/hydrolysis activity with low micromolar K_i values. This study sets precedents for using malonyl-CoA analogs with carboxylate isosteres to study the complicated structure–function relationships of acyl-CoA carboxylases, trans-carboxytransferases, malonyltransferases and β-ketoacylsynthases.

2.2 Malonyl-thioester analogs do not orient the altered thioester carbonyls in the oxyanion hole

Hydrolysis and decarboxylation reactions of malonyl-CoA and 2-substituted analogs like methylmalonyl-CoA (**1**) are spontaneous and essentially irreversible¹. While uncatalyzed hydrolysis and decarboxylation reactions are slow, enzymes activating the malonyl-thioester increase rates of nonproductive side reactions. This reactivity prohibits determination of structures with

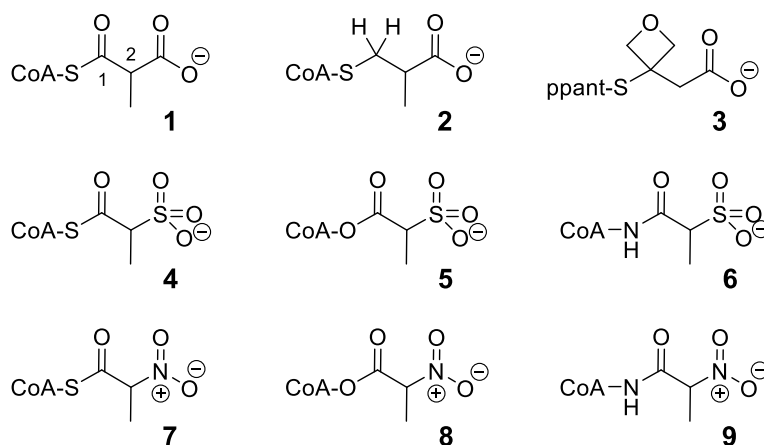
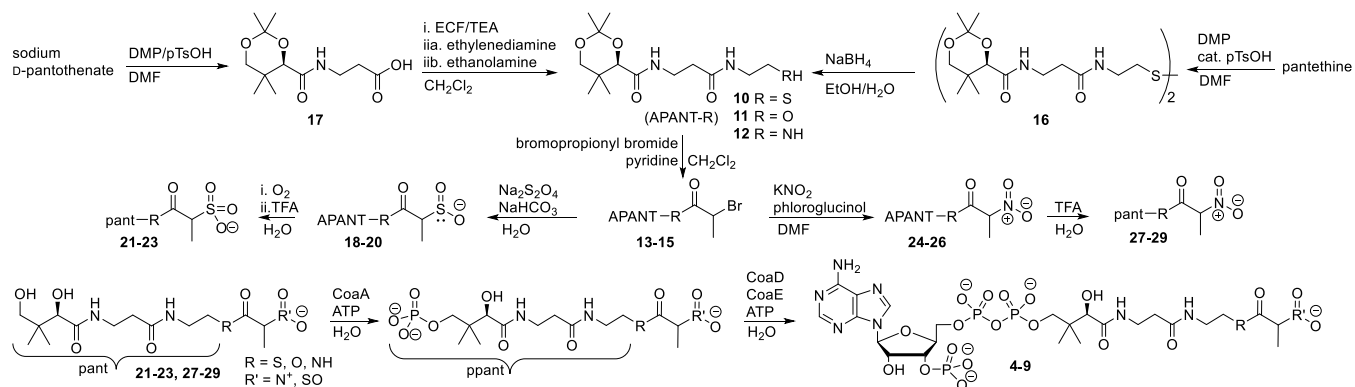


Figure 2.1 Our methylmalonyl-CoA analogs **4–9** compared to the previously used thioether (**2**) and oxetane (**3**). Phosphopantetheine moiety is abbreviated ppant.

malonyl-thioesters bound to enzymes in many biosynthetic pathways of interest to metabolic engineers or drug designers. Structures of these enzymes in complex with malonyl-CoAs or malonyl-thioesters are necessary for understanding the molecular interactions governing catalysis for inhibitor design or enzyme engineering. We synthesized methylmalonyl-thioester isosteres with the carboxylate changed to a sulfonate or nitro to overcome the reactivity problem. Application of our analogs to study *Escherichia coli* methylmalonyl-CoA decarboxylase (YgfG, MMCD) structure–function relationships provides a proof-of-principle. Previously synthesized malonyl-CoA analogs found in crystal structures can bind in noncatalytic orientations. The first malonyl-CoA analog found in a crystal structure is 2-carboxypropyl-CoA (**2**) a thioether analog of **1**, Figure 2.1.

Alteration of the thioester to a thioether makes the analog stable to hydrolysis/decarboxylation. The thioether **2** binds in a catalytically relevant orientation in the structure of *Propionibacterium shermanii* methylmalonyl-CoA mutase (PDB 7REQ)². However, **2** binds in the active site of MMCD inconsistent with any reasonable catalytic mechanism (PDB 1EF9)³. Recently, a malonyl-S-phosphopantetheine analog bearing an oxetane (**3**) was reported in the active site of DpsC (PDB 5WGC), a polyketide synthase enzyme using a malonyl-S-acyl carrier



Scheme 2.1 Synthetic Scheme for Methylmalonyl-CoA Analogs

protein substrate⁴. However, the oxetane oxygen was oriented toward solvent, obscuring the role of the thioester-carbonyl in catalysis. Both **2** and **3** are altered at the thioester-carbonyl, which is necessary for stabilizing the enolate formed upon decarboxylation of malonyl-thioesters and transfer of the malonyl-group to nucleophiles. Alternative malonyl-thioester isosteres that retain the thioester-carbonyl require changing the carboxylate to eliminate decarboxylation, inspiring us to generate the analogs **4-9**, Figure 2.1.

2.3 Synthesis of carboxylate isosteres to perform structure-function studies with MMCD

While carboxylate isosteres are widely used in medicinal chemistry, literature concerning β -keto carboxylate isosteres for mechanistic enzymology is thin⁵. Most isosteres are too bulky or have improper pK_a values for mechanistic probes⁶⁻⁷. Sulfonates/sulfonates/phosphinates/phosphonates are negatively charged at physiological pH similar to carboxylates, but are not planar. Nitro isosteres of carboxylates are common when attached to a benzene ring. However, alkyl-nitro and especially β -keto nitro groups are relatively uncommon. In solution, alkyl nitro groups are in equilibrium with the nitronate form, which carries a charge on the oxygen atoms, mimicking a carboxylate⁸. Since most carboxylate isosteres are suboptimal for mechanistic studies, comparison of multiple helps to reveal trends for modeling the natural substrate. With carboxylate isosteres in mind and awareness of thioester lability, we synthesized **4-9** outlined in Scheme 2.1, details/characterization provided in Supporting Information. Our strategy was to produce acetonyl protected pantetheine (**10**), oxypantetheine (**11**) and aminopantetheine (**12**), followed by alkylation of all three with 2-bromopropionyl bromide to yield **13-15**. This required generation and reduction of acetonyl protected pantetheine

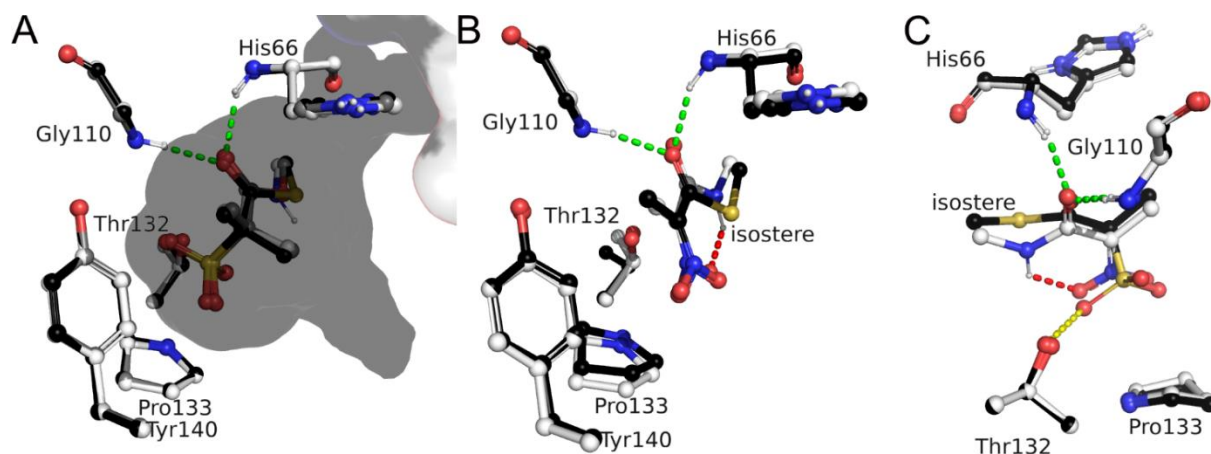


Figure 2.2 MMCD-isostere binding interactions. (A) Overlay of MMCD chain A with **4**-black, **5**-gray and **6**-white. Green dashes indicate oxyanion hole. Both C-1 stereoisomers of **4**–**6** modeled. Surface of active site residues is shown for **4** bound, notice His66-imidazole contacts solvent and active site surfaces. Hydrogens (diminutive ball–sticks) predicted based on geometry. (B) Overlay of MMCD chain A with **7**-black and **9**-white. Red dashes illustrate intramolecular hydrogen bond of **9**. (C) Overlay of **4** and **7** structures, demonstrating similar carboxylate isostere orientations, suggesting methylmalonyl-carboxylate interacts with Pro133. Yellow dashes indicate potential hydrogen bond.

(**16**), and coupling ethylenediamine/ethanolamine to protected pantothenic acid (**17**) via ethylchloroformate. Treatment of the bromides **13**–**15** with dithionite leads to sulfinates, **18**–**20**, confirmed by LC/MS. Upon purification sulfinates oxidize to sulfonates **21**–**23**. Treatment of **13**–**15** with excess sodium nitrite and phloroglucinol in DMF yields β -keto nitro intermediates **24**–**26**, inspired by previous literature⁹. Finally, **21**–**23** and **27**–**29** were generated through TFA catalyzed deprotection and converted to CoAs (**4**–**9**) chemoenzymatically.

To provide proof-of-principle that our analogs are useful for structure–function studies we examined MMCD-analog complexes via X-ray crystallography. Co-crystallization of almost native MMCD (single S2A mutation) with **4**–**9** yielded structures with active site density for the analogs (Figure S1), which provides insight into methylmalonylmoiety:active-site interactions prior to decarboxylation. Our structures were determined at 1.70–1.80 Å resolution, see Table S1 for crystallographic details. Each unit-cell contains a hexamer providing six independent determinations of analog binding orientation, Figure S1. The methylmalonyl-thioester isosteres of analogs **4**–**6** bind almost identically with clear density in every active site, Figure 2.2A and S1. Interestingly, nitro analogs **7**–**9** mostly bind in the nitronate form, Figure 2.2B/C and S1. Analog **9** has a hydrogen bond between a nitro oxygen amide hydrogen, which may contribute to its clear

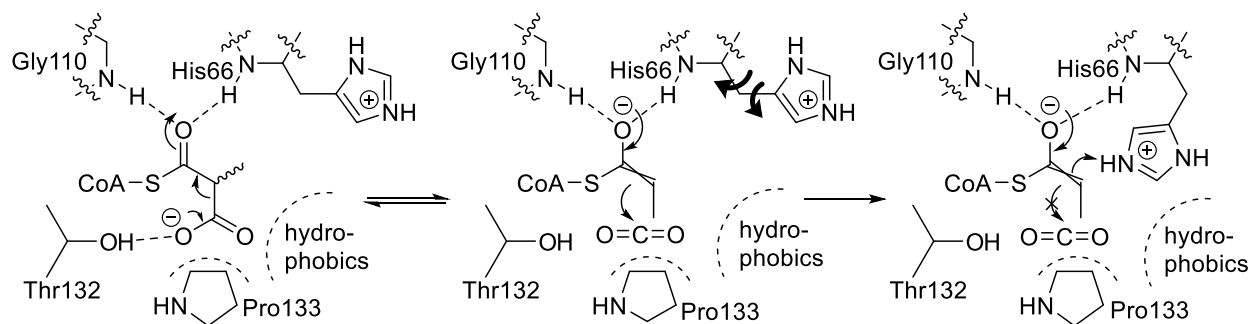


Figure 2.3 Flattened schematics for the binding of isosteres to MMCD and proposed catalytic mechanism. (A) Generalized binding of the isosteres, with the color of the R-groups matching the structures in Figure 2.2. (B) Proposed (2*R/S*)-methylmalonyl-CoA binding modes for MMCD and the following decarboxylase mechanism invoking rotation of His66 side chain into the active site.

active site density compared to **7** and **8**, Figure 2.2B/C and S1. Residual density for **7/8** in many active sites is explained by conformational heterogeneity or isostere degradation via hydrolysis, reduction to oxime, or Nef reaction. Reduction/ hydrolysis reactions are supported by a pyruvate oxime found in crystal contacts of MMCD structures with **7/8**, Figure S2. Presence of NiSO₄ may have catalyzed degradation. Nevertheless, these results support use of **4–6** and **9** with hydrolysis prone enzymes.

2.4 Methylmalonyl-CoA active site positioning promotes decarboxylase mechanism

The key thioester-carbonyl retained in our isosteres sits in an oxyanion hole formed by His66 and Gly110, which supports a previous prediction between methylmalonyl-thioester carbonyl and oxyanion hole, Figure 2.2³. However, previous prediction of a hydrogen bond between methylmalonyl-carboxylate and Tyr140-hydroxyl, is not supported. The closest contact for the nitro and sulfonate moieties of our analogs is with Pro133, Figure 2.2. The carboxylate binding pocket is almost completely hydrophobic, formed from Ile68, Leu71, Leu79, Leu85, Gly109, Met131, Leu136, Val138, and Tyr140. A single polar contact with the carboxylate isosteres is Thr132, Figure 2.2C. The observation that both nitro and sulfonate groups bind near Pro133 in the hydrophobic pocket strongly suggests the natural carboxylate binds in a similar location, Figure 2.2C.

We predict Thr132 temporarily interacts with the methylmalonyl carboxylate on path to the hydrophobic pocket and Pro133, Figure 2.3. Thioester-carbonyl oxyanion hole interaction

stabilizes the enolate resulting from decarboxylation, leaving neutral CO₂ bound in the hydrophobic pocket. To prevent reversion (addition of CO₂ back to the enolate)¹⁰, protonated His66 side chain rotates into the active site and protonates the enolate opposite of the CO₂, yielding product propionyl-CoA. His66 is found in a proton donating conformation in the structure with thioether 2, Figure S3A. In the majority of our structures His66-imidazole is protonated and interacts with Asp83-carboxylate and Asp67-peptide ketone. In a few cases, His66 is neutral and interacts with the Asp67-amide hydrogen rather than ketone, Figure S3B. Further evidence for His66 in enolate protonation comes from activity assays.

Kinetic characterization of MMCD was originally performed using a coupled assay with transcarboxylase generating (2*S*)-methylmalonyl-CoA at pH 7.2 and 37 °C that was not optimized, with reported K_m 13.6 μM, *k*_{cat} 1.6 s⁻¹ and *k*_{cat}/K_m 0.12 μM⁻¹ s⁻¹¹¹. We used direct HPLC detection of substrate transformation from commercial (2*RS*)-methylmalonyl-CoA, details presented in the Supporting Information and Figure S4 and S5. A lower limit for *k*_{cat}/K_m in our system is 0.17 μM⁻¹ s⁻¹ at pH 6.5 and 25 °C. A pH rate profile reveals maximum decarboxylation activity below pH 6.0, with a pK_a of 7.4 consistent with protonated His66 acting as a catalytic acid, Figure S6. Hydrolysis of **1** is fastest at pH 6.8, rates decrease at higher and lower pHs with two titratable groups of pK_a 5.3 and 8.5. CoA is generated from **1** rather than from propionyl-CoA, as CoA does not increase after **1** is depleted.

In vivo, MMCD decarboxylates (2*R*)-methylmalonyl-CoA produced by methylmalonyl-CoA mutase from succinyl-CoA¹¹. *In vitro* MMCD accepts both methylmalonyl-CoA epimers present in commercially available material. MMCD binds both C-2 epimers of **4–6** based on residual electron density for the methyl group, Figure S1 and Figure 2.2. His66 is expected to be able to protonate the enolate resulting from either enantiomer, which is consistent with (2*R/S*)-methylmalonyl-CoA decomposition fitting reasonably well to a single exponential decay, Figure S5. In addition, spontaneous epimerization is slower than catalysis under our experimental conditions, with a half-life of 87 h at pH 7.1 and 38 h at pH 5.0¹². The single exponential fit also suggests hydrolysis and decarboxylation happen on the same time scale.

2.5 Alternative active site orientations lead to hydrolysis

Analogs **7** and **8** have methylmalonyl isosteres that can bind in alternative orientations, leaving a water molecule in the oxyanion hole, Figure S3C. This oxyanion hole water can be

activated for thioester attack by His66 in two ways, Figure S7A/B. Direct deprotonation of water leads to protonated His66 that interacts with the thioester stabilizing hydrolysis, Figure S7A. Alternatively, the malonyl-thioester carbonyl rearranges into the oxyanion hole, displacing water into the hydrophobic pocket interacting with His66. Deprotonation of water promotes hydrolysis through reaction with the activated thioester, Figure S7B.

The water rearrangement hypothesis could lead to decarboxylation through bicarbonate formation as outlined in Figure S7C^{10, 13}. It remains unknown whether MMCD directly generates CO₂ or bicarbonate. However, a carboxylate hydration route is disfavored, because none of our structures with **4–6** has His66 interacting with the sulfonate group, which is an ideal carboxylate hydration intermediate mimic.

2.6 Inhibition of MMCD with methylmalonyl-CoA analogs

Initial attempts using isothermal titration calorimetry to determine MMCD-analog binding affinity suggested MMCD could not be saturated at high analog concentrations. Examination of electron density surrounding the active site revealed a second coenzyme A binding site in approximately half of monomers, typically chains C/E/F, Figure S8. CoA in this allosteric site alters the conformation of Trp108, which directly interacts with methylmalonyl-CoA in the catalytic site. We determined inhibition constants for our analogs to compare relative affinities, Figure S9¹⁴. These assays gave K_i values of 7.5 ± 1.1 , 3.8 ± 1.6 , 7.1 ± 1.7 , 10.8 ± 2.3 , 20.6 ± 2.7 and 19.8 ± 1.4 μM for **4–9**, respectively. The sulfonate isosteres bind tighter than the nitro isosteres in general. This can be explained by the planarity of the nitronate not being complementary to the hydrophobic pocket compared to the sulfonate.

2.7 Malonyl-CoA analogs provide an avenue to test β -ketoacyl synthase mechanism

A long-standing question in β -ketoacyl synthase catalysis is how the malonyl-thioester binds in the active site leading to decarboxylation and carbon–carbon bond formation¹⁵. In one model, the carboxylate binds against a hydrophobic residue, which can act as a driving force for decarboxylation. However, carboxylate desolvation poses an energy barrier, leading to skepticism for the hydrophobic interaction model. In a second model, the carboxylate binds to a conserved histidine side chain, which poses no desolvation problem. In a third model, histidine activates a

water to generate bicarbonate as the leaving group. The environment surrounding the nitro and sulfonyl groups is surprisingly hydrophobic in MMCD. Thus, while there is no sequence or structural homology between MMCD and β -ketoacyl synthases, our study lends credence to the hydrophobic-carboxylate interaction model. While more experiments are required to establish the MMCD catalytic model presented here, this study exemplifies the potential our analogs have for providing new insight into the mechanism of well-studied and complicated enzymes.

2.8 References

1. Kulkarni, R. A.; Worth, A. J.; Zengeya, T. T.; Shrimp, J. H.; Garlick, J. M.; Roberts, A. M.; Montgomery, D. C.; Sourbier, C.; Gibbs, B. K.; Mesaros, C.; Tsai, Y. C.; Das, S.; Chan, K. C.; Zhou, M.; Andresson, T.; Weissman, A. M.; Linehan, W. M.; Blair, I. A.; Snyder, N. W.; Meier, J. L., Discovering Targets of Non-enzymatic Acylation by Thioester Reactivity Profiling. *Cell Chemical Biology* **2017**, *24* (2), 231-242.
2. Mancia, F.; Smith, G. A.; Evans, P. R., Crystal structure of substrate complexes of methylmalonyl-CoA mutase. *Biochemistry* **1999**, *38* (25), 7999-8005.
3. Benning, M. M.; Haller, T.; Gerlt, J. A.; Holden, H. M., New reactions in the crotonase superfamily: structure of methylmalonyl CoA decarboxylase from Escherichia coli. *Biochemistry* **2000**, *39* (16), 4630-9.
4. Ellis, B. D.; Milligan, J. C.; White, A. R.; Duong, V.; Altman, P. X.; Mohammed, L. Y.; Crump, M. P.; Crosby, J.; Luo, R.; Vanderwal, C. D.; Tsai, S. C., An Oxetane-Based Polyketide Surrogate To Probe Substrate Binding in a Polyketide Synthase. *Journal of the American Chemical Society* **2018**, *140* (15), 4961-4964.
5. Kluger, R.; Nakaoka, K., Inhibition of acetoacetate decarboxylase by ketophosphonates. Structural and dynamic probes of the active site. *Biochemistry* **1974**, *13* (5), 910-4.
6. Ballatore, C.; Huryn, D. M.; Smith, A. B., 3rd, Carboxylic acid (bio)isosteres in drug design. *ChemMedChem* **2013**, *8* (3), 385-95.
7. Lassalas, P.; Gay, B.; Lasfargeas, C.; James, M. J.; Tran, V.; Vijayendran, K. G.; Brunden, K. R.; Kozlowski, M. C.; Thomas, C. J.; Smith, A. B., 3rd; Huryn, D. M.; Ballatore, C., Structure Property Relationships of Carboxylic Acid Isosteres. *Journal of medicinal chemistry* **2016**, *59* (7), 3183-203.
8. Nielsen, A. T., Nitronic acids and esters. In *Nitrones, Nitronates and Nitroxides* **1989**, Patai, S., Rappoport, Z., Eds.; John Wiley & Sons Ltd.: New York, 1-138.
9. Kornblum, N.; Blackwood, R. K.; Powers, J. W., A new synthesis of α -Nitroesters. *Journal of the American Chemical Society* **1957**, *79* (10), 2507-2509.
10. Kluger, R., Decarboxylation, CO₂ and the reversion problem. *Accounts of chemical research* **2015**, *48* (11), 2843-9.
11. Haller, T.; Buckel, T.; Retey, J.; Gerlt, J. A., Discovering new enzymes and metabolic pathways: conversion of succinate to propionate by Escherichia coli. *Biochemistry* **2000**, *39* (16), 4622-9.
12. Fuller, J. Q.; Leadlay, P. F., Proton transfer in methylmalonyl-CoA epimerase from *Propionibacterium shermanii*. The reaction of (2R)-methylmalonyl-CoA in tritiated water. *Biochemical Journal* **1983**, *213* (3), 643-50.

13. Witkowski, A.; Joshi, A. K.; Smith, S., Mechanism of the beta-ketoacyl synthase reaction catalyzed by the animal fatty acid synthase. *Biochemistry* **2002**, *41* (35), 10877-87.
14. Lu, J.; Dong, Y.; Ng, E. C.; Siehl, D. L., Novel form of the Michaelis-Menten equation that enables accurate estimation of $(k_{cat}/K_M) \cdot K_I$ with just two rate measurements; utility in directed evolution. *Protein engineering, design & selection : PEDS* **2017**, *30* (5), 395-399.
15. Heath, R. J.; Rock, C. O., The Claisen condensation in biology. *Natural product reports* **2002**, *19* (5), 581-596.

CHAPTER 3. CO-CRYSTAL STRUCTURES OF METHYLMALONYL-COA EPIMERASE CONTRADICT GENERAL ACID-BASE CATALYSIS, PROVIDE SUBSTRATE SPECIFICITY INSIGHTS

A version of this chapter will be submitted for review.

Contributions: Jeremy R Lohman and Lee M Stunkard designed experiments, interpreted the resulting data and wrote the manuscript. Lee M Stunkard carried out the vast majority of experiments. Aaron B. Benjamin synthesized carboxy-carba(dethia)-CoA and assisted in protein preparation. James B. Bower and Tyler J. Huth assisted with sample preparation.

Note: Literature references are unique within this chapter.

3.1 Abstract

There is much interest in generating 2-substituted malonyl-CoAs for incorporation into polyketide biosynthetic pathways. One promising route is the use of malonyl-CoA synthetases. However, malonyl-CoA synthetases like *Streptomyces coelicolor* MatB, generate 2-substituted malonyl-CoAs with the 2*R*- configuration, while polyketide synthase malonyltransferase enzymes typically accept 2*S*- substrates. Methylmalonyl-CoA epimerase swaps the 2*R*- and 2*S*- configuration and has some demonstrated substrate promiscuity. In order to further understand the relationships between the catalytic mechanism, substrate promiscuity and structure, we solved structures with the substrate and a putative transition state analog bound. The original mechanism proposed was the use of general acid-base catalysis similar to the mechanism of proline racemase, based on the exchange of the α -carbon proton with solvent. However, tritium kinetic isotope effects were inconclusive leading to the hypothesis of a “protected base” in catalysis. Our structures reveal that there are no acids or bases near the α -carbon protons to deprotonate or protonate the α -carbon. Using NMR we confirmed that the α -carbon proton is catalytically exchanged with solvent. Therefore, we propose MMCE catalyzes enolization of the thioester as the mechanism, whereby the thioester ketone acts as the “protected base”. This mechanism is more compatible with various 2-substitutions other than carbon over a possible decarboxylation-carboxylation mechanism, which could also explain catalysis with a lack of acids/bases within reach of the α -carbon hydrogen.

3.2 Methylmalonyl-CoA epimerase was proposed to undergo acid/base catalysis

Methylmalonyl-CoA epimerase (MMCE) is central to linking TCA cycle intermediates with other pathways in various organisms. Typically, MMCEs are found with methylmalonyl-CoA mutases where they reversibly convert (2*S*)-methylmalonyl-CoA to (2*R*)-methylmalonyl-CoA and finally to succinyl-CoA. Deficiencies in this pathway can lead to severe acidosis and damage the central nervous system¹. MMCE is also

a promising biotechnology tool for the generation of polyketide synthase substrates. Previously, *Streptomyces coelicolor* MMCE

(ScMMCE) was used to enhance yields of 6-deoxyerythronolide B in *Escherichia coli*²⁻³. Recently, the pikromycin PKS was engineered to incorporate altered α -carbon substituent malonyl-substrates⁴. The malonyl-substrates were chemoenzymatically synthesized using malonyl-CoA synthetase, MatB. MatB has been altered many times to accept larger α -carbon substituents⁵⁻⁹. However, MatB stereo specifically produces the (2*R*)-malonyl epimer and MatB homologs used in pikromycin analog biosynthesis are also expected to generate the (2*R*)-epimer¹⁰. These (2*R*)-epimers aren't suitable PKS substrates as the acyltransferase within PKS is stereo-specific for (2*S*)-malonyl-thioesters². Efficient incorporation of these larger α -carbon substituents is possible if they undergo epimerization to produce the 2*S*-configuration. Therefore, we were interested in performing structure-function studies of MMCE to determine if the mechanism may play a role in substrate specificity.

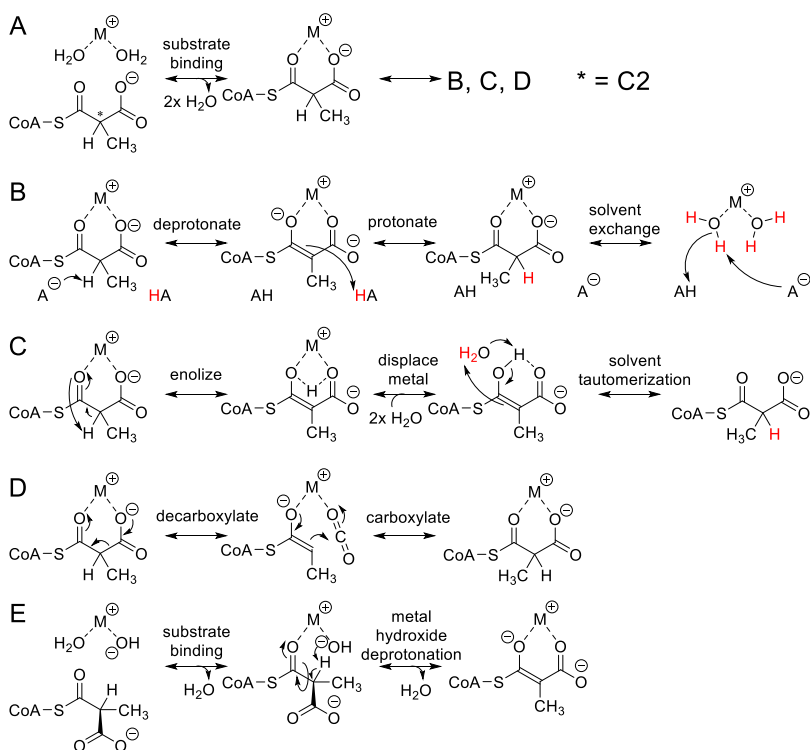


Figure 3.1 Possible catalytic mechanisms. A) Substrate binding B) General acid-base catalysis. C) Enolization via 1,3-H shift with metal displacement and solvent tautomerization. D) Decarboxylation/re-carboxylation. E) Metal hydroxide displacement with concomitant enolate formation.

The most studied MMCE enzyme is from *Propionibacterium shermanii* (*P. shermanii*)¹¹. MMCE is part of the vicinal oxygen chelate superfamily¹²⁻¹⁴. In tritium kinetic isotope effect and NMR studies, it was found that the C2 hydrogen was exchanged with solvent¹⁵⁻¹⁶. This piece of data supported an acid-base catalytic mechanism similar to other vicinal oxygen chelate superfamily enzymes¹⁷⁻²¹, Figure 3.1. More detailed analysis revealed that the kinetic isotope effect was not explained alone by an enzyme bound tritium, leading to a proposed “hidden base” that only exchanged with solvent infrequently.

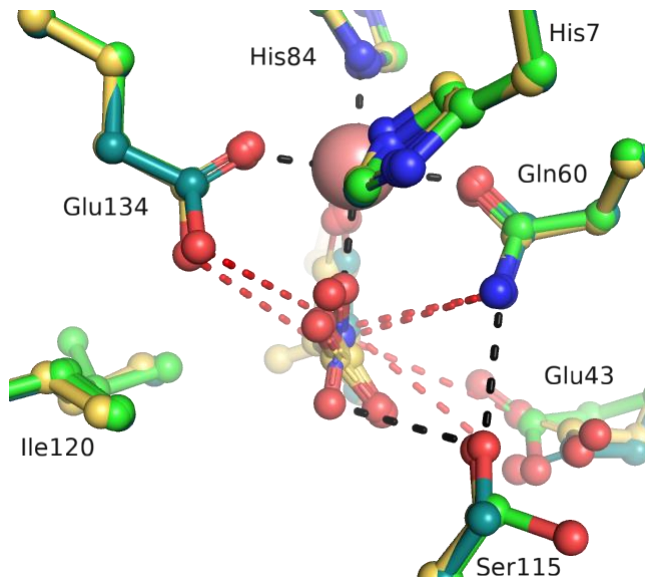


Figure 3.2 Overlay of apo-ScMMCE structure (green), methylmalonyl-CoA bound in ScMMCE (yellow), and nitropropionyl-S-CoA bound in ScMMCE (blue) with the pink sphere modeled as nickel.

Structures of MMCE from *P. shermanii*¹²⁻¹³ (PfMMCE), and later a proposed MMCE from *Thermoanaerobacter tengcongensis*¹⁴ suggested that the acid/base catalytic residues could be conserved glutamate residues. In order to elucidate the “hidden base” and clarify the roles of invariant residues, we solved the structure of ScMMCE, with and without mutants, with methylmalonyl-CoA and a planar carbanion intermediate analog with the carboxylate replaced by a nitro group.

We previously synthesized the nitro bearing methylmalonyl-CoA analog for examining the structure-function activities of methylmalonyl-CoA decarboxylase²². In the active site of *E. coli* methylmalonyl-CoA decarboxylase, the nitro analog bound in the form of the nitronate with a deprotonated C2. We hypothesized this analog would perfectly mimic the planar carbanion transition state to reveal the nature of the proposed catalytic general acids/bases.

3.3 Structures of MMCE with methylmalonyl-CoA and nitro analog and mutant assays suggest acid/base catalysis is not the catalytic mechanism

Three structures of ScMMCE were solved in the apo-conformation, methylmalonyl-CoA bound conformation, and transition state analog bound conformation, Figure 3.2. The apo-structure

was solved to a resolution of 1.4 Å with an R-factor of 15.8% and R-free of 18.1% (5% data excluded). The substrate, methylmalonyl-CoA, bound structure was solved to a resolution of 1.55 Å with an R-factor of 15.5% and R-free of 17.4% (5% data excluded). The transition state analog, nitropropionyl-S-CoA, bound structure was solved to a resolution of 1.37 Å with an R-factor of 15.0% and an R-free of 17.7% (5% data excluded). Each of these structures are solved at a high resolution with clear visibility for all of the active site residues and ligands for the respective structures. A metal was bound in each structure, coordinated by the side chains of His7, Gln60, His84, and Glu134. The substrate and transition state analog bound structures also coordinate with the metal at the thioester carbonyl and carboxylate/carboxylate isostere.

In the structure of ScMMCE, methylmalonyl-CoA is bound in the neutral state, rather than enolate, as C2 is sp³ hybridized, with density for both epimers visible in the electron density maps. Methylmalonyl-CoA bound in the active site reveals there are no acids or bases within proton abstraction or donation distance C2, Figure 3.1 and 3.2. In an overlay of methylmalonyl-CoA and Co²⁺ bound structures, the Glu134 and Glu43 residues are further in the bound structures, Figure 3.2. Thus upon substrate binding the predicted acid-base pairs move away from the substrate, rather than toward. The structure with the nitro analog bound reaffirms the observation that Glu134 and Glu43 are even further from the C2 position than in the substrate bound structure, Figure 3.2. Water molecules are absent from ScMMCE active sites with methylmalonyl-CoA and transition state analog bound structures, excluding water acting as a cryptic acid-base. The substrate and nitro analog bound structures suggest that since the acid/base catalytic residues are too far for proton transfer, acid/base catalysis does not explain the epimerization mechanism.

To test our surprising structural results, we mutated the amino acids in the active site to better understand their roles. We made MMCE E134A, E134Q, E43L, and E43Q mutations because E134 and E43 are the predicted acid/base catalytic residues. The MMCE Q60A, Q60E, S115A, S115T, and I120V mutants were made because they were the only other amino acids interacting with or are in close proximity to the ligands. To test the activity of MMCE and mutants we set up an assay with racemic methylmalonyl-CoA incubated with LnmK, a stereospecific (2R)-methylmalonyl-CoA decarboxylase discussed in chapter 5, for 30 minutes. After 30 minutes the percentage of methylmalonyl-CoA compared to propionyl-CoA were monitored by HPLC. To this point we see a 50% mixture of (2S)-methylmalonyl-CoA and propionyl-CoA. At this point, we add MMCE or mutant to the reaction mixture and incubate for 30 minutes. After 60 minutes we

monitor the percentage of methylmalonyl-CoA compared to propionyl-CoA again. The percentages of methylmalonyl-CoA and propionyl-CoA do not add up to 100% because LnmK has some side hydrolysis activity. The negative control with no MMCE enzyme added at the 30-minute mark results in a consistent 50% mixture of methylmalonyl-CoA and propionyl-CoA at 60 minutes. The positive control with MMCE WT added at 30 minutes results in nearly 100% conversion to propionyl-CoA. We used this assay to test our MMCE mutants for possible epimerase activity, Table 3.1. The results are shown as total percentages of compounds and these percentages don't add to 100% because there is hydrolysis which leads to free CoA.

Table 3.1 MMCE WT and mutant epimerization assays.

	30 minutes		60 minutes	
	methylmalonyl-CoA	propionyl-CoA	methylmalonyl-CoA	propionyl-CoA
MMCE WT	47%	46%	0.2%	84%
MMCE (-MMCE)	47%	46%	43%	42%
MMCE E134A	47%	46%	43%	48%
MMCE E134Q	47%	46%	44%	49%
MMCE E43L	47%	46%	36%	51%
MMCE E43Q	47%	46%	33%	50%
MMCE Q60A	47%	46%	0.2%	84%
MMCE Q60E	47%	46%	0.2%	81%
MMCE S115A	47%	46%	38%	48%
MMCE S115T	47%	46%	0.1%	79%
MMCE I120V	47%	46%	0.2%	78%

The MMCE mutants Q60A, Q60E, S115T, and I120V showed similar results to WT MMCE suggesting the mutated residues are not necessary for epimerization. MMCE E43L and E43Q revealed similar results that they were able to epimerize methylmalonyl-CoA, but at a reduced rate compared to WT. The E134A and E134Q mutants were similar in that they had a drastically reduced epimerization. The conversion of methylmalonyl-CoA to propionyl-CoA for E43A, E43Q, E134A, and E134Q suggest that the glutamate residues are important for

epimerization but not necessary. MMCE S115A also had slow epimerization. It is possible that this mutation is affecting substrate positioning which leads to decreased epimerization. We also incubated methylmalonyl-CoA with our MMCE mutants to test for a confounding decarboxylase and hydrolase activity, which we found none. Taking the structures and mutagenesis data together, it suggests that acid/base catalysis is not the catalytic mechanism for MMCE.

3.4 Other possible mechanisms for MMCE epimerization

Excluding acid/base catalysis, this leaves two possible mechanisms, one where the substrate itself participates via enolization (1,3-H shift), or there is decarboxylation and recarboxylation, Figure 3.1. The decarboxylation/recarboxylation mechanism is precluded as this mechanism doesn't account for exchange of the C2 hydrogen. Alternatively, the "hidden base" might be the thioester or carboxylate oxygens. The enolization mechanism should not be possible as keto-enol tautomerization by sigmatropic 1,3-H shifts are typically forbidden by transition state geometry. However, the metal in MMCE likely favors the enolate intermediate, enabling the 1,3-H shift. Another option is that the water molecules bound to the metal in the apo-state are deprotonated. Upon forming the substrate enzyme complex, these waters deprotonate the substrate, generating an enolate intermediate. The reverse reaction incorporates hydrogen from the solvent on either side. Our crystal structure with methylmalonyl-CoA bound supports the mechanism where the 1,3-shift happens upon substrate exiting the active site, rather than upon entrance, due to the sp³ nature of C2.

The epimerase reaction is acid catalyzed in solution, suggesting a proton shared by the thioester-oxygen and carboxylate oxygen contribute to deprotonation of C2, likely due to a relatively stable pericyclic intermediate. While the active site does not contain any water within distance to act as a acid/base, it is still somewhat water accessible. The active site catalivity penetrates the entire monomer, but the substrate only enters half way. This leaves a

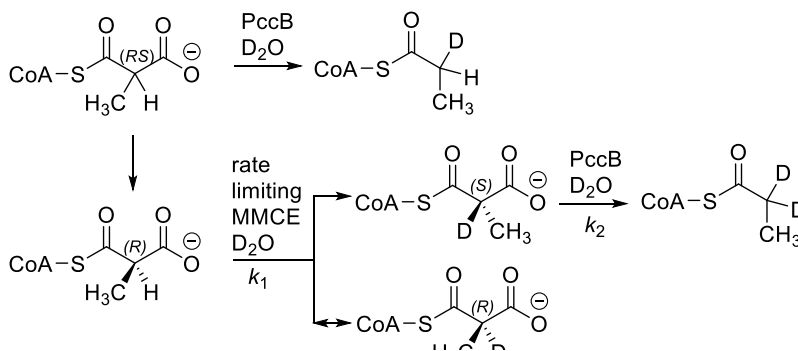


Figure 3.3 NMR analysis of (2*RS*)-methylmalonyl-CoA conversion to propionyl-CoA via MMCE and PccB.

water accessible cavity that can interact with the carboxylate. It is possible that this solvent interaction with the carboxylate and the formation of the enol intermediate eject the molecule into solution for enol tautomerization to complete the reaction.

3.5 Proposed experiments to test directional or mixed epimerase activity

The rate of epimerization and solvent exchange are related by 50% in theory. In the NMR, the C2 methyl group is easily visible and split by the C2 hydrogen, which is buried under the water solvent peak. Exchange of the hydrogen with deuterium leads to the C2 methyl group becoming a singlet. Monitoring the splitting pattern thus allows quantitation of enzyme turnover for enolization. Linking this turnover to a downstream enzyme performing decarboxylation allows quantitation of enolization vs epimerization. We propose to use *S. coelicolor* propionyl-CoA carboxylase or methylmalonyl-CoA:pyruvate transcarboxylase to stereospecifically decarboxylate (2*S*)-methylmalonyl-CoA, Figure 3.3. During this reaction, the carboxylate is replaced by a solvent proton or deuteron, Figure 3.1. If MMCE catalysis mimicked that of proline racemase with a pair of catalytic general acids/bases, the rate of propionyl-CoA formation would equal the rate of deuterium incorporation into methylmalonyl-CoA, if enolization is the mechanism the rate of formation of propionyl-CoA will be 50% of deuterium incorporation into malonyl-CoA.

3.6 Experiments to test substrate engineering potential

Since there is much interest in engineering PKS enzymes to accept larger α -carbon substituents, MMCE is a strong platform to optimize the α -carbon epimerization for better incorporation into PKSs²⁻³. MMCE has the potential to accept larger substrates upon active site engineering. Mutating Ile120 and Gln39 to smaller amino acids may provide the active site cavity necessary to accept larger α -carbon substituents for epimerization. I would recommend mutating these positions to open the active site cavity, followed by assays with larger α -carbon substituents such as ethyl/propyl-malonyl-CoA, 2-aminomalonyl-CoA, and 2-methoxymalonyl-CoA.

3.7 Conclusions

The structures of ScMMCE in complex with methylmalonyl-CoA and the nitro-bearing transition state analog reveal two structural states where the predicted acid-base glutamate residues

are positioned 4 Å from the C_α. This distance is too far for a hydrogen bond, let alone a proton abstraction or donation. Mutant ScMMCE activity assays revealed that while Glu134 and Glu43 are important for epimerization, they are not necessary. When the glutamate residues are mutated, the epimerization activity is still obtained, albeit much slower. The substrate and transition state analog bound structural states combined with the mutant ScMMCE data suggest that ScMMCE does not undergo acid-base catalysis to perform epimerization. These results disclose the possibility of ScMMCE performing epimerization through an unknown catalytic mechanism that requires further experimentation, highlighted in section 3.6. A possible mechanism for epimerization is through an enol or enolate intermediate as we propose in Figure 3.1 C and E. Results from our proposed experiment in Figure 3.3 will begin to yield insight into a possible new mechanism for epimerization. These proposed mechanistic intermediates start to raise the question of how does ScMMCE stabilize methylmalonyl-CoA to proceed through an enol or enolate intermediate without decarboxylation or hydrolysis side products? Is it possible to reverse engineer the active site to accept larger 2-substituted substrates without altering the mechanism of epimerization? A thorough understanding of the catalytic mechanism will provide more information to engineering ScMMCE to accept larger 2-substituted substrates for PKS engineering.

3.8 References

1. Fenton, W. A.; Rosenberg, L. E., Disorders of propionate and methylmalonate metabolism. *In The Metabolic and Molecular Bases of Inherited Disease*, C.R. Scriver, A.L. Beaudet, W.S. Sly, and D. Valle, eds. (New York: McGraw-Hill) **1995**, 1423–1449.
2. Marsden, A. F.; Caffrey, P.; Aparicio, J. F.; Loughran, M. S.; Staunton, J.; Leadlay, P. F., Stereospecific acyl transfers on the erythromycin-producing polyketide synthase. *Science* **1994**, 263 (5145), 378-80.
3. Pfeifer, B. A.; Admiraal, S. J.; Gramajo, H.; Cane, D. E.; Khosla, C., Biosynthesis of complex polyketides in a metabolically engineered strain of E. coli. *Science* **2001**, 291 (5509), 1790-2.
4. Kalkreuter, E.; CroweTipton, J. M.; Lowell, A. N.; Sherman, D. H.; Williams, G. J., Engineering the Substrate Specificity of a Modular Polyketide Synthase for Installation of Consecutive Non-Natural Extender Units. *Journal of the American Chemical Society* **2019**, 141 (5), 1961-1969.
5. Koryakina, I.; Williams, G. J., Mutant Malonyl-CoA Synthetases with Altered Specificity for Polyketide Synthase Extender Unit Generation. *Chembiochem : a European journal of chemical biology* **2011**, 12 (15), 2289-2293.

6. Crosby, H. A.; Rank, K. C.; Rayment, I.; Escalante-Semerena, J. C., Structure-guided expansion of the substrate range of methylmalonyl coenzyme A synthetase (MatB) of *Rhodospseudomonas palustris*. *Applied and environmental microbiology* **2012**, *78* (18), 6619-29.
7. Koryakina, I.; McArthur, J.; Randall, S.; Draelos, M. M.; Musiol, E. M.; Muddiman, D. C.; Weber, T.; Williams, G. J., Poly specific trans-acyltransferase machinery revealed via engineered acyl-CoA synthetases. *ACS chemical biology* **2013**, *8* (1), 200-8.
8. Koryakina, I.; McArthur, J. B.; Draelos, M. M.; Williams, G. J., Promiscuity of a modular polyketide synthase towards natural and non-natural extender units. *Organic & biomolecular chemistry* **2013**, *11* (27), 4449-58.
9. Koryakina, I.; Kasey, C.; McArthur, J. B.; Lowell, A. N.; Chemler, J. A.; Li, S.; Hansen, D. A.; Sherman, D. H.; Williams, G. J., Inversion of Extender Unit Selectivity in the Erythromycin Polyketide Synthase by Acyltransferase Domain Engineering. *ACS chemical biology* **2017**, *12* (1), 114-123.
10. Hughes, A. J.; Keatinge-Clay, A., Enzymatic extender unit generation for in vitro polyketide synthase reactions: structural and functional showcasing of *Streptomyces coelicolor* MatB. *Chemistry & biology* **2011**, *18* (2), 165-76.
11. Leadlay, P. F., Purification and characterization of methylmalonyl-CoA epimerase from *Propionibacterium shermanii*. *Biochemical Journal* **1981**, *197* (2), 413-9.
12. McCarthy, A. A.; Baker, H. M.; Shewry, S. C.; Kagawa, T. F.; Saafi, E.; Patchett, M. L.; Baker, E. N., Expression, crystallization and preliminary characterization of methylmalonyl coenzyme A epimerase from *Propionibacterium shermanii*. *Acta crystallographica. Section D, Biological crystallography* **2001**, *57* (Pt 5), 706-8.
13. McCarthy, A. A.; Baker, H. M.; Shewry, S. C.; Patchett, M. L.; Baker, E. N., Crystal structure of methylmalonyl-coenzyme A epimerase from *P. shermanii*: a novel enzymatic function on an ancient metal binding scaffold. *Structure* **2001**, *9* (7), 637-46.
14. Shi, L.; Gao, P.; Yan, X. X.; Liang, D. C., Crystal structure of a putative methylmalonyl-coenzyme A epimerase from *Thermoanaerobacter tengcongensis* at 2.0 Å resolution. *Proteins* **2009**, *77* (4), 994-9.
15. Fuller, J. Q.; Leadlay, P. F., Proton transfer in methylmalonyl-CoA epimerase from *Propionibacterium shermanii*. The reaction of (2R)-methylmalonyl-CoA in tritiated water. *Biochemical Journal* **1983**, *213* (3), 643-50.
16. Leadlay, P. F.; Fuller, J. Q., Proton transfer in methylmalonyl-CoA epimerase from *Propionibacterium shermanii*. Studies with specifically tritiated (2R)-methylmalonyl-CoA as substrate. *Biochemical Journal* **1983**, *213* (3), 635-42.
17. Powers, V. M.; Koo, C. W.; Kenyon, G. L.; Gerlt, J. A.; Kozarich, J. W., Mechanism of the reaction catalyzed by mandelate racemase. 1. Chemical and kinetic evidence for a two-base mechanism. *Biochemistry* **1991**, *30* (38), 9255-63.
18. Babbitt, P. C.; Gerlt, J. A., Understanding Enzyme Superfamilies Chemistry as the fundamental determinant in the evolution of new catalytic activities. *The Journal of biological chemistry* **1997**, *272* (49), 30591–30594.
19. Armstrong, R. N., Mechanistic diversity in a metalloenzyme superfamily. *Biochemistry* **2000**, *39* (45), 13625-32.
20. Cameron, A. D.; Olin, B.; Ridderstrom, M.; Mannervik, B.; Jones, T. A., Crystal structure of human glyoxalase I—evidence for gene duplication and 3d domain swapping. *EMBO Journal* **1997**, *16* (12), 3386–3395.

21. Cameron, A. D.; Ridderstrom, M.; Olin, B.; Kavarana, M. J.; Creighton, D. J.; Mannervik, B., Reaction mechanism of glyoxalase I explored by an X-ray crystallographic analysis of the human enzyme in complex with a transition state analogue. *Biochemistry* **1999**, *38* (41), 13480-90.
22. Stunkard, L. M.; Dixon, A. D.; Huth, T. J.; Lohman, J. R., Sulfonate/Nitro Bearing Methylmalonyl-Thioester Isosteres Applied to Methylmalonyl-CoA Decarboxylase Structure-Function Studies. *Journal of the American Chemical Society* **2019**, *141* (13), 5121-5124.

CHAPTER 4. SYNTHESIS OF MALONYL-THIOESTER ANALOGS WITH SULFONATE CARBOXYLATE ISOSTERES AND ACTIVITY WITH FATTY ACID SYNTHASE KETOSYNTASE

A version of this chapter will be submitted for review.

Contributions: Jeremy R Lohman and Lee M Stunkard designed experiments, interpreted the resulting data and wrote the manuscript. Lee M Stunkard carried out the vast majority of experiments. Aaron B. Benjamin assisted with synthesis and protein preparation. Brendan G. Williams assisted with kinetic experiments.

Note: Literature references and chemical numbers within schemes are unique within this chapter.

4.1 Abstract

Stable analogs of acyl-CoAs are of value for enzyme structure-function studies. We previously reported the synthesis of methylmalonyl-CoA analogs with methylmalonyl-thioester isosteres having nitro and sulfonate replacements of the carboxylate and preserving the thioester or altering it to an ester or amide. Here we generate the respective sulfonate bearing malonyl-thioester analogs, along with -amido(dethia)- and -oxa(dethia)- analogs in order to examine their binding affinity and reactivity with *Escherichia coli* fatty acid synthase β -ketoacylsynthase III (KasIII or FabH).

4.2 Malonyl-thioester reactivity has led to limited structure-function studies

The reactive malonyl-thioester moiety is present in malonyl-CoA, which has been described as “hyperreactive” due to spontaneous acylation of amines¹. The malonyl-thioester is also a β -keto acid that can be irreversibly decarboxylated by enzymes such as fatty acid and polyketide synthases to generate carbon-carbon bonds. This inherent reactivity prevents capture of malonyl-thioesters in enzyme active sites via X-ray crystallography²⁻⁵. These complexes are needed to understand structure-function relationships such as the enzyme-substrate molecular interactions promoting catalysis, and catalytic or allosteric conformational changes that are necessary for drug design and protein engineering.

A major question in fatty acid synthase catalysis is how the malonyl-thioester substrate interacts with the β -ketoacyl synthase (KS) active site. One of the simplest KS initiates fatty acid biosynthesis in *Escherichia coli*, FabH or KASIII. FabH accepts an acetyl-group from CoA onto a conserved active site cysteine in a transthioylation reaction, generating acetyl-S-KS. Next the KS binds an acyl carrier protein (ACP) loaded with a malonate bound via a thioester to a phosphopantetheine posttranslational modification, Figure 4.1. The KS decarboxylates the malonyl-thioester followed by a Claisen condensation with the acetyl-S-KS thioester to generate acetoacetyl-S-ACP⁶. Mutation of the FabH active site cysteine to a glutamine mimics the acetyl-S-KS acyl-enzyme intermediate, which we determined generates a malonyl-thioester decarboxylase⁷. Therefore, stable malonyl-isostere analogs are necessary to overcome the inherent reactivity of the substrate⁸⁻¹⁰. These analogs will elucidate how the malonyl-thioester interacts with the KS active site.

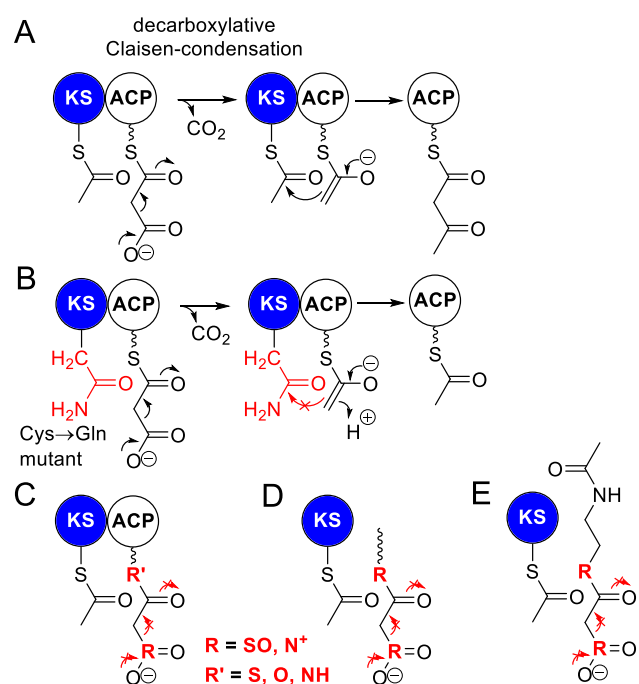
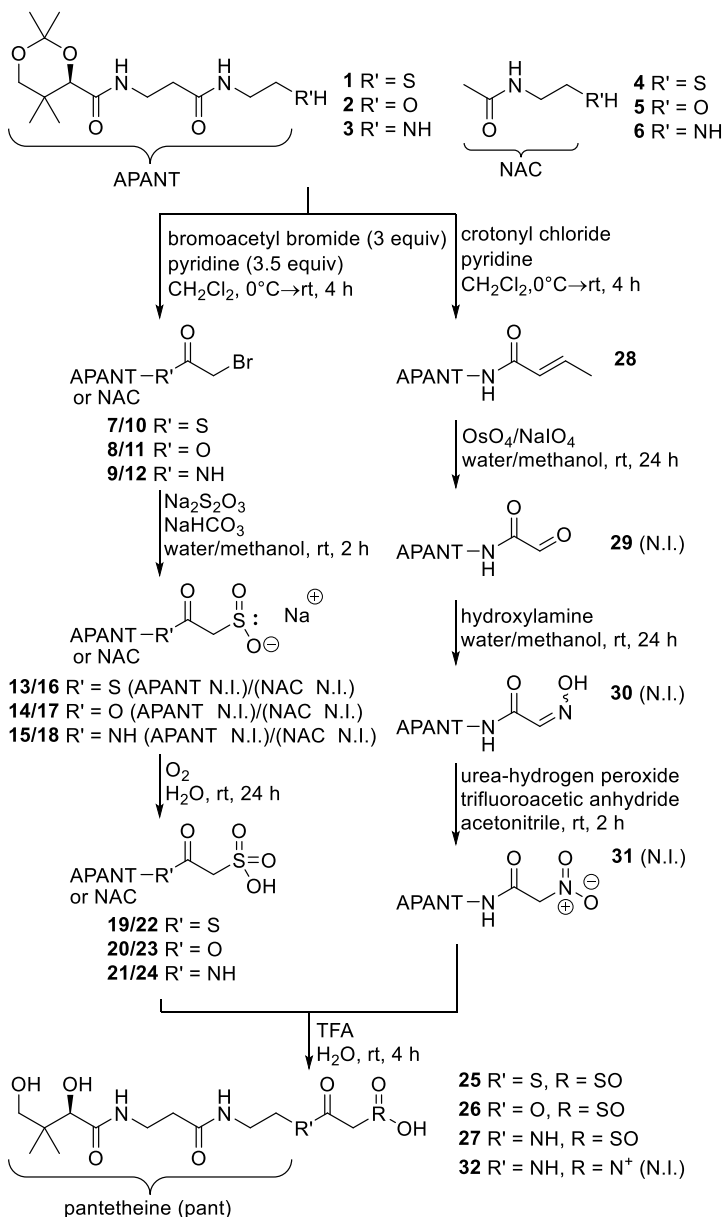


Figure 4.1 A) Carbon-carbon bond forming activity of FabH. B) FabH C→Q mutant decarboxylation activity. C) Possible inhibition of FabH by stable malonyl-thioester analogs. Squiggly line represents phosphopantetheine.

4.3 Synthesis of malonyl-thioester analogs overcomes substrate reactivity

We recently reported synthesis of a six methylmalonyl-CoA analog panel and use in methylmalonyl-CoA decarboxylase structure-function studies¹¹. These analogs had methylmalonyl-thioester isosteres where the carboxylate was represented by a sulfonate or nitro group and the thioester was retained or represented by an ester or amide. Our report of methylmalonyl-CoA analogs established the potential use of sulfonate and nitro groups as carboxylate isosteres of malonyl-CoAs. Here we report a malonyl-thioester panel more suited for the study of fatty acid synthase enzymes and demonstrate the ability of these analogs to inhibit the activity of *E. coli* FabH.

We synthesized stable malonyl-thioester analogs using a diversity oriented synthetic strategy as in scheme



Scheme 4.1 Synthesis of sulfonate-bearing and nitro-bearing malonyl-thioester analogs.

similar to our previous synthesis of stable methylmalonyl-CoA analogs, which was inspired by previous syntheses of acyl-CoAs and analogs. Acetonide protected pantetheine (**1**), oxy(dethia)pantetheine (**2**) and amino(dethia)pantetheine (**3**) were generated as previously published. The acetonide pantetheine analogs **1-3**, N-acetylcysteamine (**4**, SNAC), N-acetylethanolamine (**5**) and N-acetylethylenediamine (**6**) were treated with bromoacetyl bromide with pyridine as a base to give

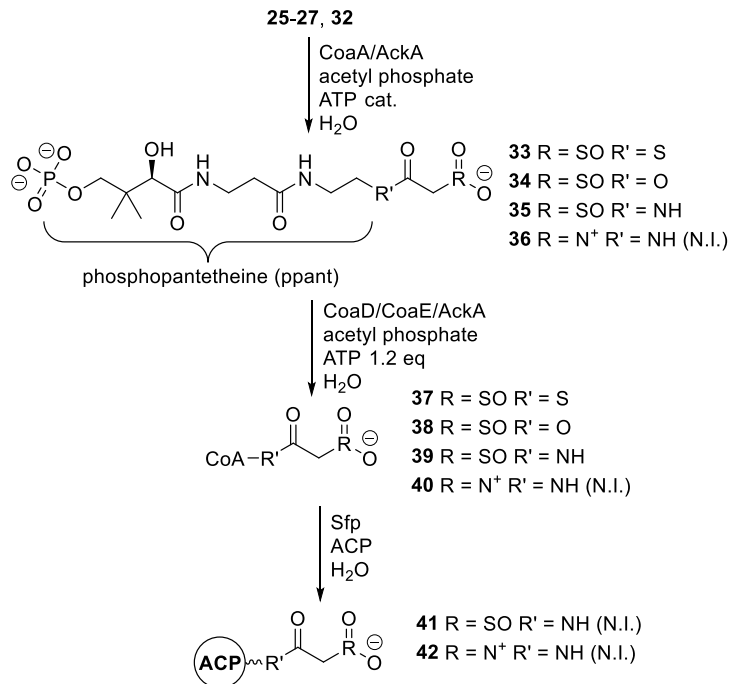
bromoacetyl-pantetheine acetonides (**7-9**), and bromoacetyl-SNACs (**10-12**). The bromoacetyl pantethine analogs **7-12** were treated with sodium dithionite to yield 2-sulfinateacetyl-pantethine analogs (**13-18**). Upon sitting overnight, the sulfonates oxidize to the sulfonates (**19-24**). Finally, the acetonides are deprotected in TFA/water and the sulfonic acids are purified by reverse phase preparative chromatography.

Our previous synthetic route

to nitro-bearing methylmalonyl-CoA analogs, via acetonide protected 2-

bromopropionyl-pantetheine intermediates was not applicable to generating the respective malonyl-CoA analogs. Reaction of the 2-bromopropionyl group with potassium nitrite in DMF with the presence of phloroglucinol led to reasonable yields of the nitro product. The same reaction with bromoacetyl-pantetheine results in very poor yields. Therefore, we had to take a new approach. Alternatively, **3** was treated with crotonyl chloride to give crotonyl-amido(dethia)pantethine acetonide (**28**), which was treated with osmium tetroxide and sodium periodate in water to give glyoxylate-amido(dethia)pantetheine acetonide (**29**). The glyoxylate was converted to an oxime (**30**) upon treatment with hydroxylamine. We are currently working on converting the oxime to the nitro (**31**) with trifluoroacetic peroxide via urea-hydrogen peroxide complex with trifluoroacetic anhydride. The acetonides **7-10** and were deprotected with TFA in water and chemoenzymatically converted to the CoA or phosphopantetheine analogs, using the improved method developed in the accompanying paper, Scheme 4.2.

Our 2-sulfonate-acetyl-CoAs can also be prepared from bromoacetyl-CoA, which have been previously synthesized. This creates an opportunity to generate the sulfonates *in situ*, due to their essentially complete conversion.



Scheme 4.2 Chemoenzymatic synthesis of ppant, CoA and ACP containing malonyl-thioester analogs

4.4 Stability and inhibition assays of malonyl-thioester analogs with FabH

In order to determine the suitability of our analogs for structure-function studies we subjected the malonyl-CoA analogs (**37-39**) to stability assays in the presence of FabH and FabH C→Q, Appendix A Figure 4.2. The sulfonateacetyl-S-CoA (**37**) had partial hydrolysis upon purification and storage (~20% hydrolyzed) and sulfonateacetyl-oxa(dethia)-CoA (**38**) had significant hydrolysis (~50% hydrolyzed). Therefore, the stability assays and inhibition assays are not optimized for these compounds, which is currently being worked on for manuscript submission. The sulfonateacetyl-CoA and sulfonateacetyl-oxy(dethia)-CoA analogs were slightly degraded by 10 μM FabH with little difference seen between degradation with and without enzyme present. The 2-sulfonate-amido(dethia)-CoA analogs were stable over the course of 24 hours with no difference with and without enzyme present.

Using ITC, none of these analogs generated enough signal to determine binding constants. Therefore, we obtained inhibition constants for the malonyl-thioester analogs generated here using the assay described in Appendix A, Table 4.1¹². General trends can be extrapolated from the inhibition data. Malonyl-phosphopantetheine analogs are better inhibitors than malonyl-pantetheine analogs. Malonyl-CoA analogs inhibit differently depending on the thioester atom. The thioester-CoA inhibits the best, followed by the ester-CoA and amido-CoA. This suggests that there is a specific adenosine binding interaction. When this adenosine is bound, however, the pantetheine and malonyl moieties have more restricted movement within the active site. The restricted movement can explain why alteration of the thioester bond to an ester or amide bond weakens the inhibition due to the change in geometry combating with the restricted movement to orient within the oxyanion hole. The pantetheine and malonyl moieties are under much less restrictive movement when they aren't attached to adenosine as seen in the phosphopantetheine and pantetheine analog inhibition. The freedom of movement allows for the alteration of the thioester bond to an ester or amide bond to be overcome which can explain why the pantetheine analogs group and the phosphopantetheine analogs group.

Taken together these experiments reveal there isn't a huge advantage with using phosphopantetheine analogs over the corresponding pantetheine analogs. This is key as addition of the phosphate group makes purification much more difficult.

4.5 Synthesis of malonyl-ACP analogs

The inhibition and stability assays reported in this chapter should be recognized as not optimized and experiments performed with impure starting materials. Therefore, to prepare this data for manuscript submission the compounds need to be re-purified to have pure starting material. The inhibition and stability assays will be optimized with pure starting compounds. Synthesis of the nitro-bearing compounds needs to be completed and purified. These compounds will be tested for stability and inhibition with FabH and FabH C→Q. In order for these compounds to maximize their inhibition and structure-function potential, they will need to be synthesized as the ACP-bearing analogs. The ACP from *E. coli* will need to be expressed and purified. Using ACPH and ACPS you can transfer the malonyl-CoA analogs to malonyl-ACP analogs. Synthesis and purification of malonyl-ACP analogs will give the greatest potential for structure-function studies with FabH and other KSs.

4.6 Conclusions

Our previous studies have demonstrated how sulfono-bearing methylmalonyl-CoA analogs can be used in structure-function studies; and this study expands the sulfono-bearing compounds to include malonyl-CoA, malonyl-phosphopantetheine, and malonyl-pantetheine analogs. We used a similar synthetic scheme for the methyl- and malonyl-analogs. To test the stability and inhibition of our new malonyl-thioester analogs we tested them against FabH. The CoA-tethered analogs revealed an adenosine mode of binding as the inhibition was different depending on the thioester, ester, or amide carbonyl. This phenomenon was not seen with the phosphopantetheine or pantetheine analogs. These results suggest that sulfono-bearing analogs tethered to the ACP will have the most specific binding interactions. Synthesis of the sulfono-bearing ACP analogs could provide the missing information of the protein-protein interactions between the KS-ACP with a substrate analog bound in the active site. Experimentation is being done to synthesize the sulfono-bearing ACP analogs for crystallization experiments with FabH and other KS.

4.7 Appendix A. Stability and inhibition assays of malonyl-thioester analogs with FabH

The stability reactions were performed in a 500 μL reaction mixture which contained 100 mM potassium phosphate buffer ($\text{KH}_2\text{PO}_4/\text{K}_2\text{HPO}_4$) at pH 7.0, 10 mM MgCl_2 , 20 μM enzyme (FabH wt or FabH C \rightarrow Q), and 600 μM malonyl-thioester analog. Reaction mixtures were incubated at 25 $^\circ\text{C}$, 75 μL aliquots taken at times 0 hour, 30 minutes, 1 hour, 2 hours, 4 hours, and 24 hours were quenched with 25 μL of 50% TFA v/v, precipitating the protein. Centrifugation at 2000 rpm at 25 $^\circ\text{C}$ for 10 minutes was used to pellet the protein and the supernatant was analyzed via the procedure outlined below. General procedure for determination of malonyl-thioester analog or hydrolyzed product. Malonyl-thioester analog and hydrolyzed product were determined using HPLC with detection at A254 over the 250 x 4.6 mm C18(2) column. The analytes were separated with a 2 \rightarrow 25% gradient of 0.1% TFA in water \rightarrow ACN over 20 min. Peak areas of malonyl-thioester analogs and hydrolyzed product were determined and plotted over time, Figure 4.2.

The inhibition reactions were performed in a 500 μL reaction mixture which contained 100 mM potassium phosphate buffer ($\text{KH}_2\text{PO}_4/\text{K}_2\text{HPO}_4$) at pH 7.0, 10 mM MgCl_2 , 600 μM malonyl-CoA, 300 μM acetyl-CoA, 5 mM or 1 mM malonyl-thioester analog, and the reaction was initiated with the addition of 5 μM FabH. Reaction mixtures were incubated at 25 $^\circ\text{C}$, 75 μL aliquots taken at times 0 hour, 1 minute, 5 min, 10 min, 15 min, and 30 min were quenched with 25 μL of 50% TFA v/v, precipitating the protein. Centrifugation at 2000 rpm at 25 $^\circ\text{C}$ for 10 minutes was used to pellet the protein and the supernatant was analyzed via the procedure outlined below. General procedure for determination of malonyl-CoA, acetyl-CoA and CoA concentrations in FabH catalyzed assays. Substrate and product concentrations were determined using HPLC with detection at A254 over the 250 x 4.6 mm C18(2) column. The analytes were separated with a 2 \rightarrow 25% gradient of 0.1% TFA in water \rightarrow ACN over 20 min. Peak areas of substrate and products were converted to concentration by summing their areas and dividing each peak by this total to give relative percentages that were converted to concentration by adjusting to the starting concentration of methylmalonyl-CoA. This procedure gave essentially the same values as using a standard curve to generate concentrations for each peak, but enhanced reproducibility due to small differences in recovery from the reaction quenching step outlined above. Inhibition of FabH by malonyl-thioester analogs was determined by fitting initial rate data to equation (4), which describes competitive inhibition and V_{ii} describes the V_i in the presence

of inhibitor.¹⁵ The values of $(V_{ii} \cdot V_{is}) / (V_{ii} - V_{is})$ and K_m / k_{cat} were determined from the initial slopes of V_i or V_{ii} versus substrate concentration rather than from the full assay. A minimum of two concentrations were used, 1 or 5 mM of each malonyl-thioester analog and the experiments need to be repeated at least twice.

The initial rates (V_i) of decomposition of malonyl-CoA were determined by fitting the data to equation (1), with the rate of formation of CoA being fitted to equation (2). Taking the derivative at time 0 and dividing by enzyme concentration gave the initial rates V_i . Using this method rather than an estimation from the early data points gave similar values for experiments performed at high concentrations. However, it allowed more accurate determination of V_i at low substrate concentrations.

$$\text{Equation (1)} \quad [S] = [S]_t \cdot e^{-k \cdot t}$$

$$\text{Equation (2)} \quad [S] = [S]_t \cdot (1 - e^{k \cdot t})$$

Data for the V_i versus substrate concentration was fit to equation (3) which describes substrate inhibition.

$$\text{Equation (3)} \quad V_i = (k_{cat} \cdot [S]) / (K_m + [S]^{(1 + \frac{[S]}{K_i})})$$

Inhibition of FabH by each malonyl-thioester analog was determined by fitting the data to equation (4), which describes competitive inhibition and V_{ii} describes the V_i in the presence of inhibitor. These experiments were performed at substrate concentrations below where significant substrate inhibition is present. The values of $(V_{ii} \cdot V_{is}) / (V_{ii} - V_{is})$ and K_m / k_{cat} were determined from the initial slopes of V_i or V_{ii} versus substrate concentration rather than from the full assay.

$$\text{Equation (4)} \quad K_i = \frac{V_{ii} \cdot V_{is}}{V_{ii} - V_{is}} \cdot \frac{[I]}{[E] \cdot [S]} \cdot \frac{K_m}{k_{cat}}$$

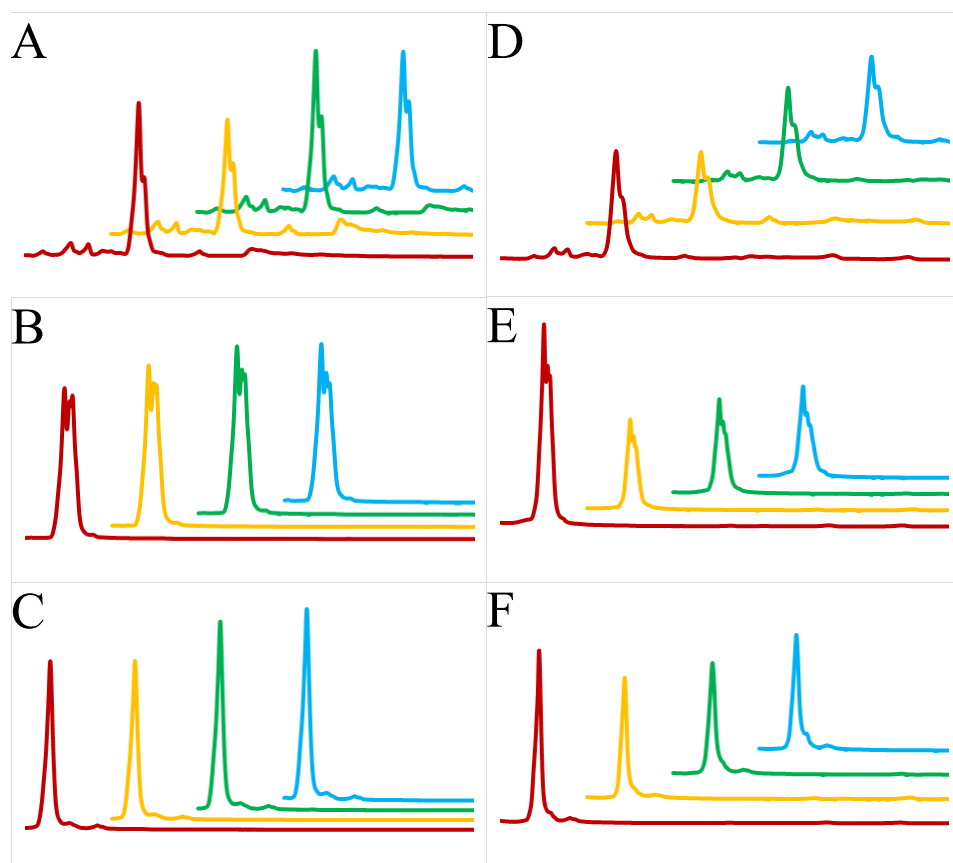
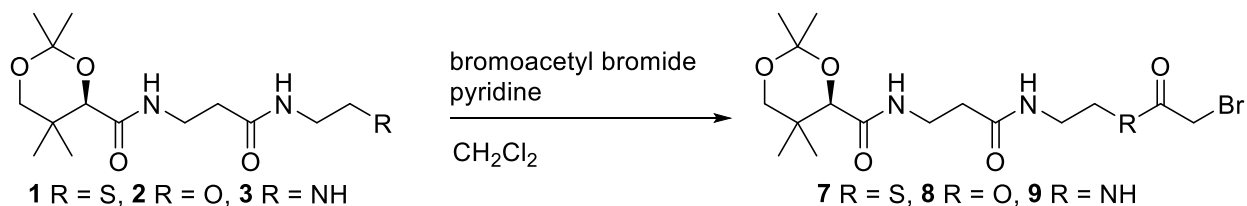


Figure 4.2 Stability assays of sulfonate-bearing analogs with FabH. Red is 1 hour without enzyme, orange is 24 hours without enzyme, green is 1 hour with enzyme, and blue is 24 hours with enzyme. A) **37** with FabH wt B) **38** with FabH wt C) **39** with FabH wt D) **37** with FabH C→Q E) **38** with FabH C→Q F) **39** with FabH C→Q.

Table 4.1 FabH inhibition constants for malonyl-thioester analogs.

Analog	Platform R', R	K_i (μM)	Rate of decay
22	NAC S, SO	TBD	
23	NAC O, SO	TBD	
24	NAC NH, SO	TBD	
25	Pant S, SO	3 ± 1	
26	Pant O, SO	1 ± 0.1	
27	Pant NH, SO	1 ± 0.2	
32	Pant NH, N+	TBD	
33	Ppant S, SO	0.8 ± 0.1	
34	Ppant O, SO	7 ± 3	
35	Ppant NH, SO	0.9 ± 0.1	
36	Ppant NH, N+	TBD	
37	CoA S, SO	0.5 ± 0.1	Stable with enzyme over 24 hours
38	CoA O, SO	2 ± 0.1	Stable with enzyme over 24 hours, 50% hydrolyzed starting material
39	CoA NH, SO	8 ± 4	Stable with enzyme over 24 hours
40	CoA NH, N+	TBD	
41	ACP N, SO	TBD	
42	ACP N, N+	TBD	

4.8 Appendix B. Experimental synthesis procedures



Preparation of 7-9 via 1-3:

General procedure

A solution of DCM containing **1-3** pyridine was added slowly to a solution of DCM containing bromoacetyl bromide. The reaction was allowed to stir for 12 hours at room temperature. The solution was transferred to a separatory funnel, except for 3/9. The solution was washed with brine, copper sulfate, and sodium thiosulfate, repeatedly. The solvent was removed and the remaining red/orange oil was subjected to flash chromatography (0 → 100% gradient of DCM → acetone or MeOH) affording **7-9**.

2-bromoacetyl-S-pantetheine acetonide (**7**):

1 (8.0 g, 25.12 mmol) was reacted with pyridine (8 mL, 99.3 mmol) and bromoacetyl bromide (6 mL, 68.87 mmol) according to the general procedure above affording **7** (yellow oil, 9.0 g, 20.48 mmol 81.5%).

¹H NMR (500 MHz, CDCl₃) δ 7.08 (br, 1H, NH), 6.92 (br, 1H, NH), 4.08 (s, 1H), 4.07 (s, 2H), 3.69 (d, J = 11.7 Hz, 1H), 3.61 – 3.47 (m, 2H), 3.47 – 3.38 (m, 2H), 3.28 (d, J = 11.7 Hz, 1H), 3.10 (t, J = 6.7 Hz, 2H), 2.46 (t, J = 6.3 Hz, 2H), 1.46 (s, 3H), 1.43 (s, 3H), 1.03 (s, 3H), 0.97 (s, 3H).

¹³C NMR (126 MHz, CDCl₃) δ 192.76, 171.37, 170.14, 99.04, 76.91, 71.31, 38.80, 35.75, 34.85, 33.44, 32.90, 29.60, 29.45, 22.11, 18.91, 18.69. LRMS (ESI) *m/z* calculated for C₁₆H₂₇BrN₂O₅SH ([M+H]⁺) 439.37 and 441.37, found 439.0 and 441.0.

2-bromoacetyl-oxa(dethia)pantetheine acetonide(8):

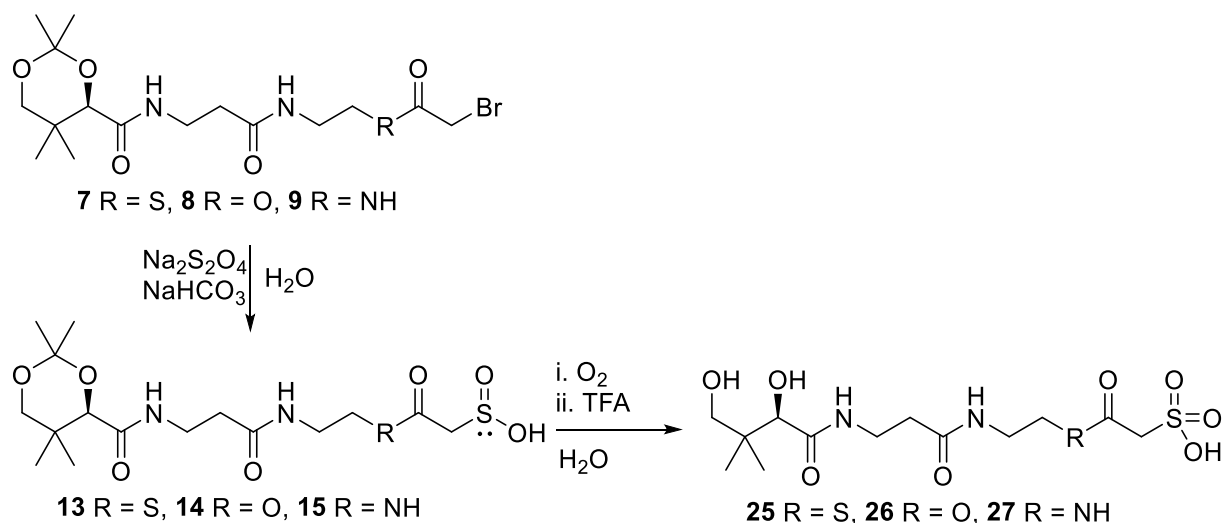
2 (8.0 grams, 26.46 mmol) was reacted with pyridine (8 mL, 99.3 mmol) and bromoacetyl bromide (6 mL, 68.87 mmol) according to the general procedure above affording **8** (oil, 1.8 g, 4.25 mmol 16.1%).

¹H NMR (500 MHz, CDCl₃) δ 7.12 (br, 1H, NH), 6.88 (br, 1H, NH), 4.26 (t, J = 6.0, 4.9, 1.2 Hz, 2H), 4.08 (s, 1H), 3.89 (s, 2H), 3.69 (d, J = 11.7 Hz, 1H), 3.63 – 3.44 (m, 4H), 3.28 (d, J = 11.7 Hz, 1H), 2.48 (t, J = 6.3 Hz, 2H), 1.47 (s, 3H), 1.43 (s, 3H), 1.02 (s, 3H), 0.97 (s, 3H). **¹³C NMR** (126 MHz, CDCl₃) δ 171.45, 170.34, 167.24, 99.08, 76.88, 71.30, 64.77, 38.22, 35.90, 34.89, 32.91, 29.41, 25.76, 22.09, 18.85, 18.68. LRMS (ESI) *m/z* calculated for C₁₆H₂₇BrN₂O₆H ([M+H]⁺) 423.20 and 425.20, found 423.0 and 425.0.

2-bromoacetyl-amino(dethia)pantetheine acetonide (9):

3 (3 g, 9.95 mmol) was reacted with pyridine (1.5 mL, 18.62 mmol) and bromopropionyl bromide (2.25 mL, 25.82 mmol) according to the general procedure above affording **9** (oil, 520 mg, 1.23 mmol 12.4%).

¹H NMR (500 MHz, CDCl₃) δ 7.02 (br, 1H, NH), 6.72 (br, 1H, NH), 4.07 (s, 1H), 3.85 (s, 1H), 3.67 (d, J = 11.7 Hz, 1H), 3.62 - 3.48 (m, 2H), 3.46 – 3.35 (m, 4H), 3.27 (d, J = 11.7 Hz, 1H), 2.46 (t, J = 6.2 Hz, 2H), 1.46 (s, 3H), 1.42 (s, 3H), 1.02 (s, 3H), 0.96 (s, 3H). **¹³C NMR** (126 MHz, CDCl₃) δ 172.09, 170.43, 166.65, 99.14, 76.78, 71.38, 40.81, 39.34, 36.35, 34.92, 32.98, 29.50, 28.87, 22.15, 18.90, 18.72. LRMS (ESI) *m/z* calculated for C₁₆H₂₈BrN₃O₅H ([M+H]⁺) 422.32 and 424.32, found 422.1 and 424.1.



Preparation of 25-27 via 13-15 via 7-9:

General procedure

A solution of water containing equimolar sodium dithionite and sodium bicarbonate is allowed to stir for 5 minutes, followed by an addition of a solution of water containing 2-bromoacetyl pantetheine acetonide (**7-9**). The reaction was allowed to stir at room temperature. After stirring for 30 minutes, HPLC-MS analysis indicated complete conversion of bromides (**7-9**) to sulfinates (**13-15**). After stirring for 18 hours, sulfinates (**13-15**) oxidize to sulfonates (**19-21**) as indicated by HPLC-MS analysis. The acetonides were deprotected with 15% TFA in water. The resulting solution was subjected to preparative HPLC with a 0 → 20% gradient of 1% TFA in water → methanol over 30 minutes. Solvent was removed affording **25-27**.

2-sulfiniateacetyl-S-pantetheine acetonide (**13**):

7 (1.0 g, 2.28 mmol) was reacted with sodium dithionite (2.35 g, 13.50 mmol) and sodium bicarbonate (1.13 g, 13.50 mmol) according to the general procedure above affording **13** (off white powder which was used directly in the next reaction). MS (ESI) *m/z* calculated for C₁₆H₂₈N₂O₇S₂ ([M-H]⁻) 423.13, found 423.0.

2-sulfonateacetyl-S-pantetheine (**25**):

The deprotection of **13** yielded **25** (off white powder, 251.3 mg, 0.63 mmol 27.6%, **7** → **25**).

¹H NMR (500 MHz, D₂O) δ 4.08 (s, 2H), 3.87 (s, 1H), 3.43 – 3.35 (m, 3H), 3.35 – 3.23 (m, 3H), 3.16 (q, 1H), 3.03 – 2.98 (m, 1H), 2.43 – 2.34 (m, 2H), 0.81 (s, 3H), 0.77 (s, 3H). ¹³C NMR (126

MHz, D₂O) δ 192.66, 175.06, 174.09, 75.72, 68.32, 62.53, 38.56, 38.36, 35.34, 35.15, 28.71, 20.47, 19.05. MS (ESI) m/z calculated for C₁₃H₂₄N₂O₈S₂ ([M-H]⁻) 399.10, found 399.0.

2-sulfinateacetyl-oxa(dethia)pantetheine acetone (14):

8 (1.0 g, 2.36 mmol) was reacted with sodium dithionite (2.44 g, 14.00 mmol) and sodium bicarbonate (1.18 g, 14.00 mmol) according to the general procedure above affording **14** (off white powder which was used directly in the next reaction). MS (ESI) m/z calculated for C₁₆H₂₈N₂O₈S ([M-H]⁻) 407.16, found 407.0.

2-sulfonateacetyl-oxa(dethia)pantetheine (26):

The deprotection of **14** yielded **26** (off white powder, 539.9 mg, 1.40 mmol 59.3%, **14** → **26**).

¹H NMR (500 MHz, D₂O) δ 4.20 (t, 2H), 3.93 – 3.88 (m, 3H), 3.49 – 3.36 (m, 6H), 3.30 (d, 1H), 2.42 (t, 2H), 0.83 (s, 3H), 0.79 (s, 3H). ¹³C NMR (126 MHz, D₂O) δ 175.07, 174.16, 166.77, 75.75, 68.37, 64.37, 55.78, 38.57, 38.13, 35.39, 35.23, 20.49, 19.06. MS (ESI) m/z calculated for C₁₃H₂₄N₂O₉S ([M-H]⁻) 383.12, found 383.4.

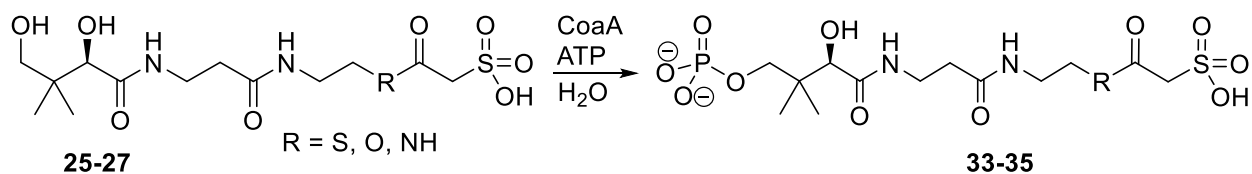
2-sulfinateacetyl-amino(dethia)pantetheine acetone (15):

9 (500 mg, 1.18 mmol) was reacted with sodium dithionite (1.22 g, 7.0 mmol) and sodium bicarbonate (590 mg, 7.0 mmol) according to the general procedure above affording **15** (off white powder which was used directly in the next reaction). MS (ESI) m/z calculated for C₁₆H₂₉N₃O₇S ([M-H]⁻) 407.17, found 407.1.

2-sulfonateacetyl-amino(dethia)pantetheine (27):

The deprotection of **15** yielded **27** (off white powder, 572.5 mg, 1.49 mmol 100%, **9** → **27**).

¹H NMR (500 MHz, D₂O) δ 4.26 (s, 1H), 4.05 – 3.95 (m, 1H), 3.88 (d, J = 12.6, 1.6 Hz, 1H), 3.42 – 3.34 (m, 4H), 3.30 – 3.23 (m, 7H), 2.37 (t, J = 6.2, 1.7 Hz, 3H), 0.80 (s, 3H), 0.76 (s, 3H). ¹³C NMR (126 MHz, D₂O) δ 175.07, 174.20, 166.71, 76.89, 75.75, 75.47, 68.32, 57.09, 38.84, 38.50, 35.40, 20.44, 19.02. MS (ESI) m/z calculated for C₁₃H₂₅N₃O₈S ([M-H]⁻) 382.14, found 382.1.



Chemoenzymatic preparation of 33-35 via 25-27:

General procedure

A solution containing 100 mM Tris (pH 8.0), 10 mM MgCl₂, 50 mM NaCl, 10 mM TCEP (pH 8.0) and 20 μM ATP was used to dissolve the malonyl-pantetheine analogs **25-27** at a final concentration of 5.5 mM, ~60-150 mL total. Then CoaA was added to a final concentration of 2.7 μM and the reaction allowed to mix at room temperature overnight. The reaction was quenched with 10% TFA, precipitating the protein out of solution, which was removed by filtration. Reverse phase HPLC was used to purify the final products using a 0 → 10% gradient of 0.1% TFA in water → methanol or ACN over 30 minutes. Fractions were pooled, rotary evaporated and lyophilized.

2-sulfonatacetyl-S-phosphopantetheine (**33**):

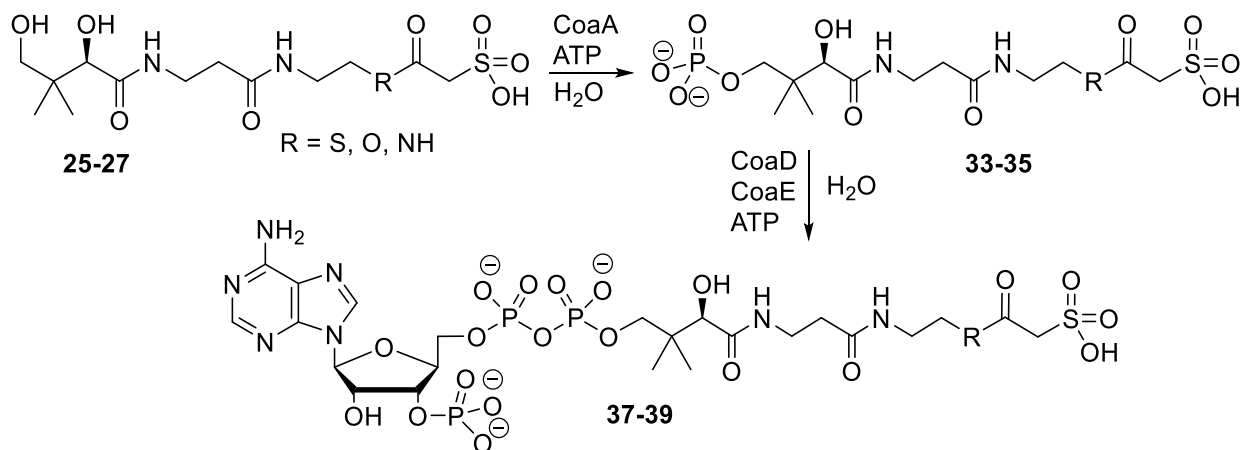
25 (22 mg, 0.05 mmol) was used as starting material to afford **33** (off white powder, 12 mg, 0.02 mmol 40%). ¹H NMR (500 MHz, D₂O) δ 4.08 (s, 2H), 3.93 (s, 1H), 3.74 – 3.64 (m, 1H), 3.62 (s, 2H), 3.47 (m, 1H), 3.42 – 3.36 (m, 2H), 3.30 (t, J = 6.4 Hz, 1H), 3.01 (t, J = 6.4 Hz, 1H), 2.37 (m, J = 7.4 Hz, 2H), 0.86 (s, 3H), 0.78 (s, 3H). ¹³C NMR (126 MHz, D₂O) δ 192.65, 174.83, 174.10, 74.44, 71.07, 62.52, 59.28, 38.36, 35.37, 28.69, 20.69, 18.51, 13.35. MS (ESI) m/z calculated for C₁₃H₂₅N₂O₁₁PS₂ ([M-H]⁻) 479.06, found 479.0.

2-sulfonatacetyl-oxa(dethia)-phosphopantetheine (**34**):

24 (42 mg, 0.11 mmol) was used as starting material to afford **34** (off white powder, 51.4 mg, 0.11 mmol 100%). ¹H NMR (500 MHz, D₂O) δ 8.50 (br, 1H, NH), 8.32 (br, 1H, NH), 4.15 (t, J = 5.2 Hz, 2H), 3.88 (d, J = 15.0 Hz, 2H), 3.58 – 3.48 (m, 2H), 3.38 (m, 4H), 3.19 (t, J = 5.5 Hz, 1H), 2.38 (q, J = 6.3 Hz, 2H), 0.85 (s, 3H), 0.78 (s, 3H). MS (ESI) m/z calculated for C₁₃H₂₅N₂O₁₂PS ([M-H]⁻) 463.09, found 463.0. ¹³C NMR (126 MHz, D₂O) δ 174.78, 174.13, 166.65, 74.58, 70.17, 64.29, 59.27, 55.75, 41.42, 38.09, 35.36, 20.52, 18.54.

2-sulfonatacetyl-amino(dethia)-phosphopantetheine (**35**):

25 (200 mg, 0.52 mmol) was used as starting material to afford **35** (off white powder, 223 mg, 0.48 mmol 92.3%). MS (ESI) m/z calculated for $C_{13}H_{26}N_3O_{11}PS$ ($[M-H]^-$) 462.1, found 462.0.



Chemoenzymatic preparation of **37-39**:

General procedure

A solution containing 100 mM Tris (pH 8.0), 10 mM MgCl₂, 50 mM NaCl, 10 mM TCEP (pH 8.0) and 20 μM ATP was used to dissolve the malonyl-pantetheine analogs **25-27** at a final concentration of 5.5 mM, ~60-150 mL total. Then CoaA was added to a final concentration of 2.7 μM and the reaction allowed to mix at room temperature for 2 hours. Then CoaD was added to a concentration of 5.6 μM and allowed to mix at room temperature for 1 hour. Then CoaE was added to a final concentration of 13.1 μM and allowed to mix at room temperature overnight. The reaction was quenched with 10% TFA, precipitating the protein out of solution, which was removed by filtration. Reverse phase HPLC was used to purify the final products using a 0 → 20% gradient of 0.1% TFA in water → methanol or ACN over 30 minutes. Fractions were pooled, rotary evaporated and lyophilized.

2-sulfonateacetyl-S-CoA (**37**):

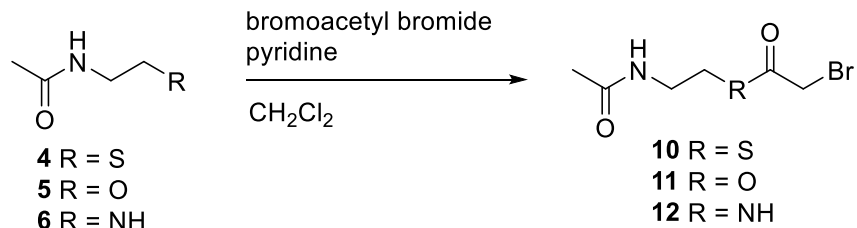
25 (250 mg, 0.62 mmol) was used as starting material to afford **37** (off white powder, 81 mg, 0.09 mmol 14.5%). NMR being processed

2-sulfonateacetyl-oxa(dethia)CoA (**38**):

26 (434.3 mg, 1.13 mmol) was used as starting material to afford **38** (off white powder, 62.3 mg, 0.07 mmol 6.2%). ¹H NMR (500 MHz, D₂O) δ 8.43 (s, 1H), 8.26 (s, 1H), 6.03 (d, J = 5.6, 2.7 Hz, 1H), 4.79 (d, 2H), 4.14 – 4.10 (m, 2H), 4.09 – 4.05 (m, 2H), 3.82 – 3.78 (m, 2H), 3.72 (d, J = 9.7, 5.0 Hz, 1H), 3.55 – 3.47 (m, 2H), 3.29 (q, J = 5.4, 4.0 Hz, 4H), 2.30 (q, J = 6.9 Hz, 2H), 0.76 (s, 3H), 0.65 (s, 3H). ¹³C NMR (126 MHz, D₂O) δ 174.60, 174.03, 166.57, 149.72, 148.35, 144.61, 142.37, 114.84, 87.50, 74.48, 74.06, 73.50, 72.31, 65.14, 64.19, 59.23, 55.68, 38.22, 38.03, 35.31, 35.11, 20.56, 18.18. LRMS (ESI) m/z calculated for C₂₃H₃₈N₇O₂1P₃S ([M-H]⁻) 872.11, found 872.0.

2-sulfonateacetyl-amino(dethia)CoA (**39**):

27 (150 mg, 0.39 mmol) was used as starting material to afford **39** (off white powder, 44.7 mg, 0.05 mmol 12.8%). NMR being processed. LRMS (ESI) m/z calculated for C₂₃H₃₉N₈O₂0P₃S ([M-H]⁻) 871.12, found 871.0.



Preparation of 10-12 via 4-6:

General procedure

A solution of DCM containing **10-12** pyridine was added slowly to a solution of DCM containing bromoacetyl bromide. The reaction was allowed to stir for 12 hours at room temperature. The solution was transferred to a separatory funnel, **except for 6/12**. The solution was washed with brine, copper sulfate, and sodium thiosulfate, repeatedly. The solvent was removed and the remaining red/orange oil was subjected to flash chromatography (0 → 100% gradient of DCM → acetone or MeOH) affording **10-12**.

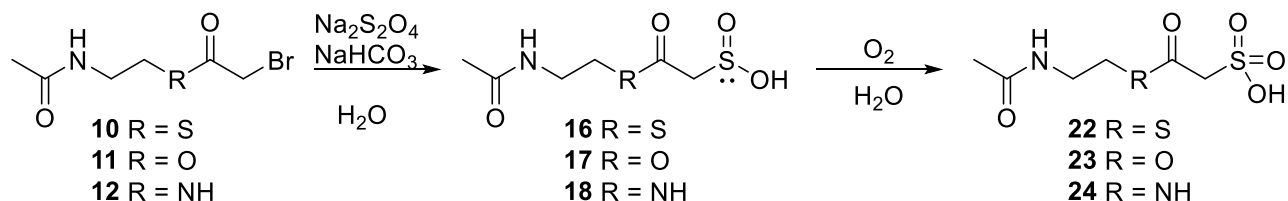
2-bromoacetyl-S-NAC (**10**):

4 (2 mL, 18.8 mmol) was reacted with pyridine (4 mL, 49.65 mmol) and bromoacetyl bromide (3 mL, 34.43 mmol) according to the general procedure above affording **10** (yellow oil, 3.23 g, 13.45 mmol 71.5%). ¹H NMR (500 MHz, CDCl₃) δ 6.67 (br, 1H, NH), 3.99 (s, 2H), 3.37 (q, J = 6.4 Hz, 2H), 3.03 (t, J = 6.6 Hz, 2H), 1.92 (s, 3H). ¹³C NMR (126 MHz, CDCl₃) δ 192.90, 170.85, 38.93, 33.48, 29.65, 23.07. LRMS (ESI) *m/z* calculated for C₆H₁₀BrNO₂S ([M+H]⁺) 240.12 and 242.12, found 240.0 and 242.0.

2-bromoacetyl-oxa(dethia)-NAC (**11**):

5 (2 mL, 21.72 mmol) was reacted with pyridine (4 mL, 49.65 mmol) and bromoacetyl bromide (3 mL, 34.43 mmol) according to the general procedure above affording **11** (yellow oil, 400 mg, 1.79 mmol 8.2%). ¹H NMR (500 MHz, CDCl₃) δ 6.56 (br, 1H, NH), 4.19 (t, J = 5.5 Hz, 2H), 3.81 (s, 2H), 3.46 (q, J = 5.6 Hz, 2H), 1.93 (s, 3H). ¹³C NMR (126 MHz, CDCl₃) δ 170.91, 167.34, 64.77, 38.36, 25.79, 23.04. LRMS (ESI) *m/z* calculated for C₆H₁₀BrNO₃ ([M+H]⁺) 224.05 and 226.05, found 224.0 and 226.0.

2-bromoacetyl-amino(dethia)-NAC (**12**): Needs to be synthesized



Preparation of **22-24** via **16-18** via **10-12**:

General procedure

A solution of water containing equimolar sodium dithionite and sodium bicarbonate is allowed to stir for 5 minutes, followed by an addition of a solution of water containing 2-bromoacetyl N-acetylcysteamine (**10-12**). The reaction was allowed to stir at room temperature. After stirring for 30 minutes, HPLC-MS analysis indicated complete conversion of bromides (**10-12**) to sulfates (**16-18**). After stirring for 18 hours, sulfates (**16-18**) oxidize to sulfonates (**22-24**) as indicated by HPLC-MS analysis. The resulting solution was subjected to preparative HPLC with a 0 → 10% gradient of 1% TFA in water → methanol over 30 minutes. Solvent was removed affording **22-24**.

2-sulfinylacetyl-S-NAC (16): Needs to be purified

MS (ESI) m/z calculated for C₆H₁₀NO₄S⁻ ([M-H]⁻) 224.01, found 224.0.

2-sulfonateacetyl-S-NAC (22): Needs to be purified

MS (ESI) m/z calculated for C₆H₁₁NO₅S⁻ ([M-H]⁻) 240.01, found 240.0.

2-sulfinylacetyl-oxa(dethia)-NAC (17): Needs to be purified

MS (ESI) m/z calculated for C₆H₁₀NO₅S⁻ ([M-H]⁻) 208.03, found 208.1.

2-sulfonateacetyl-oxa(dethia)-NAC (23): Needs to be purified.

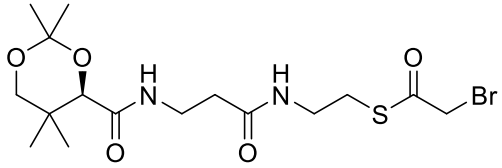
MS (ESI) m/z calculated for C₆H₁₁NO₆S ([M-H]⁻) 224.03, found 224.1.

2-sulfinylacetyl-amino(dethia)-NAC (38): Needs to be synthesized

2-sulfonateacetyl-amino(dethia)-NAC (41): Needs to be synthesized

4.9 Appendix C. NMR characterization.

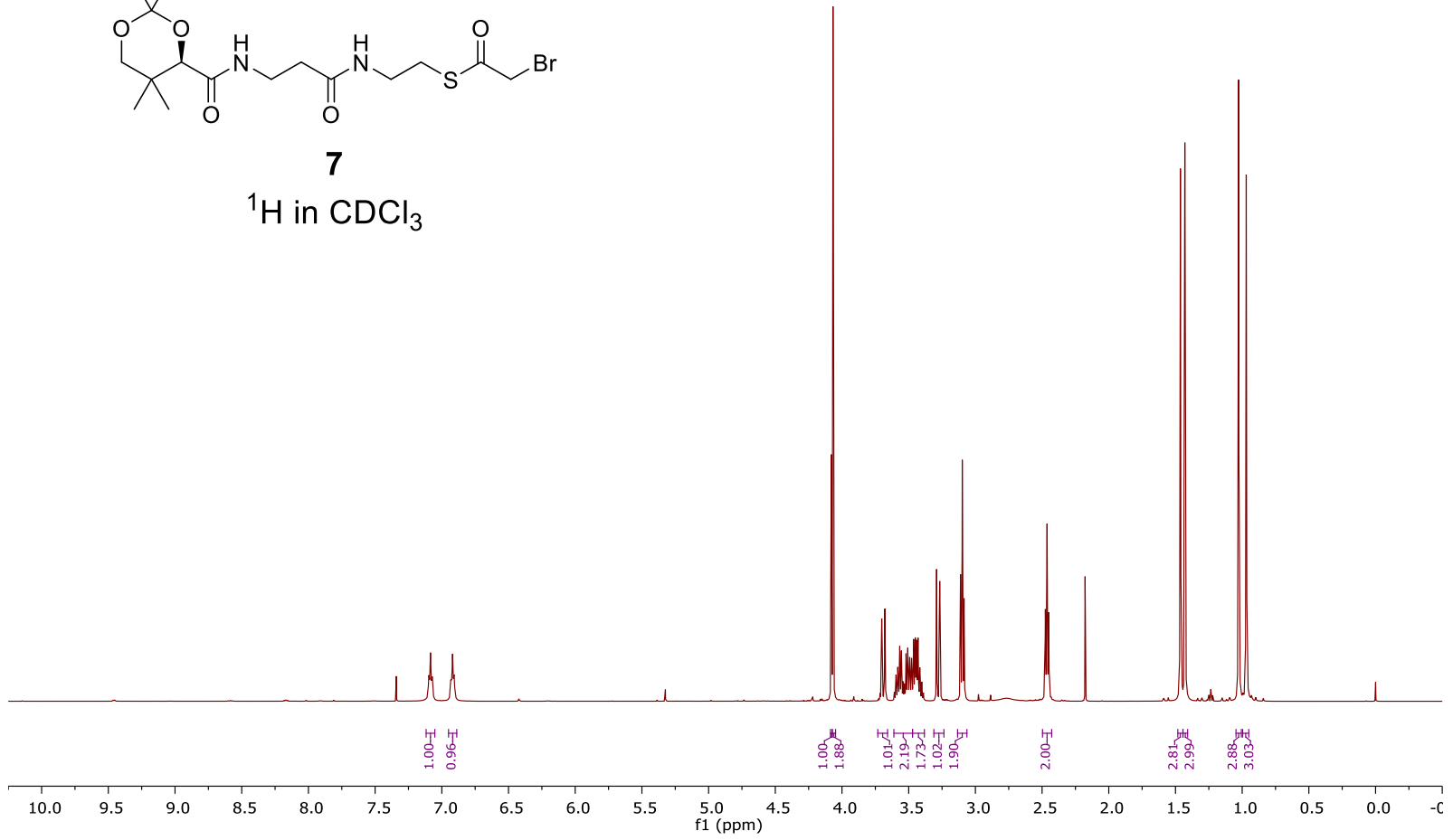
Nmr characterizations of synthetic intermediates and products:

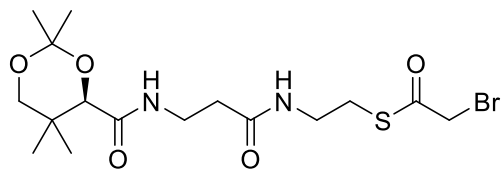
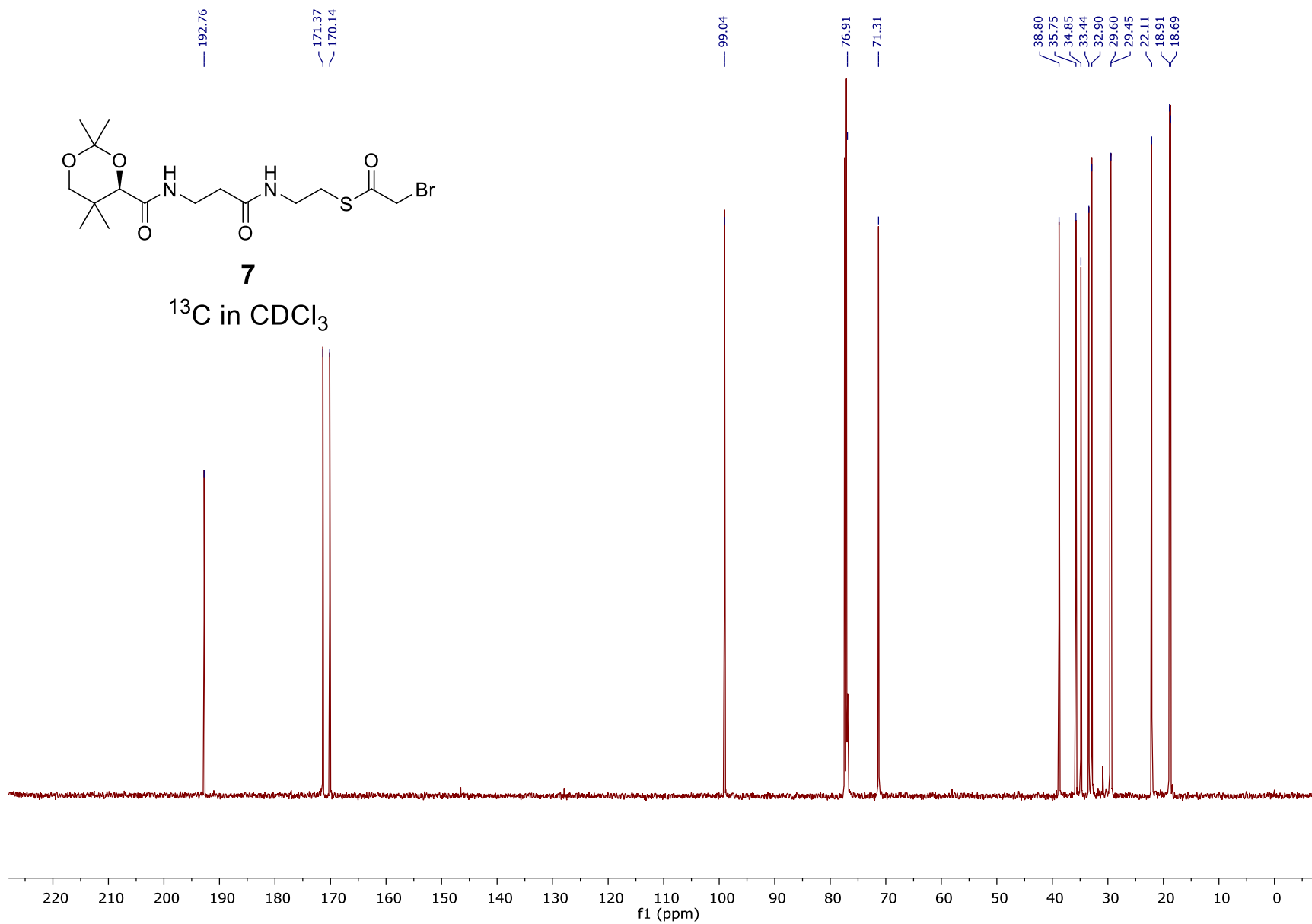


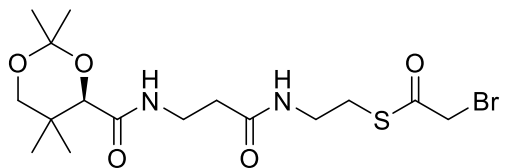
7

^1H in CDCl_3

99

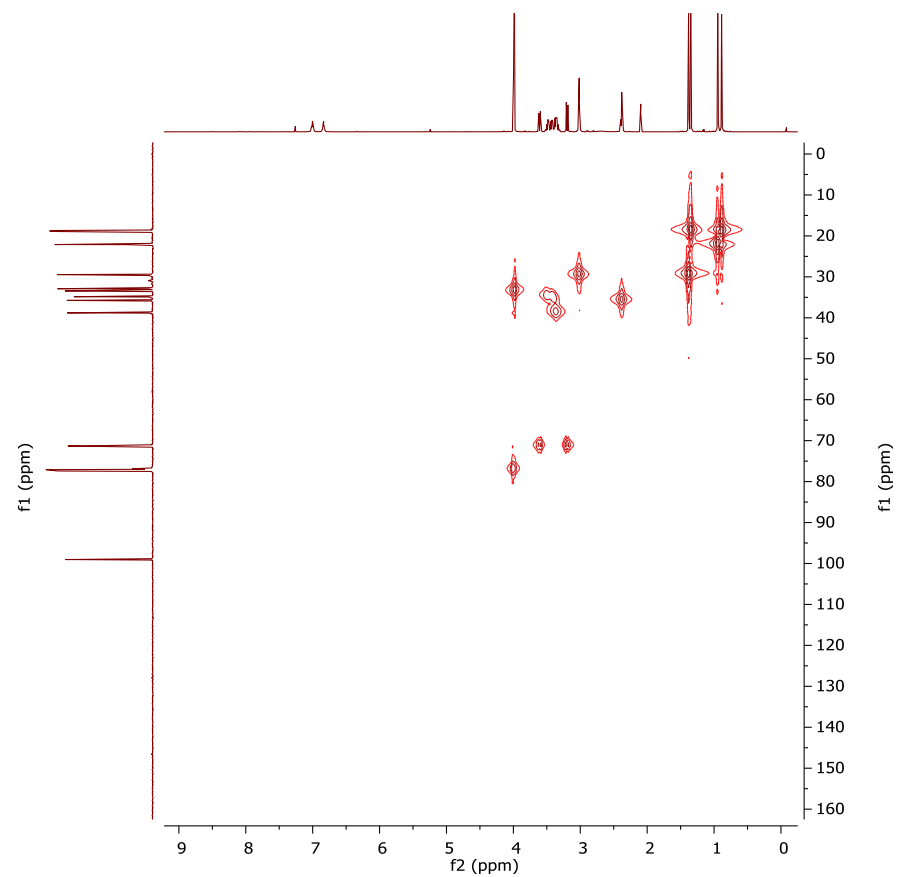
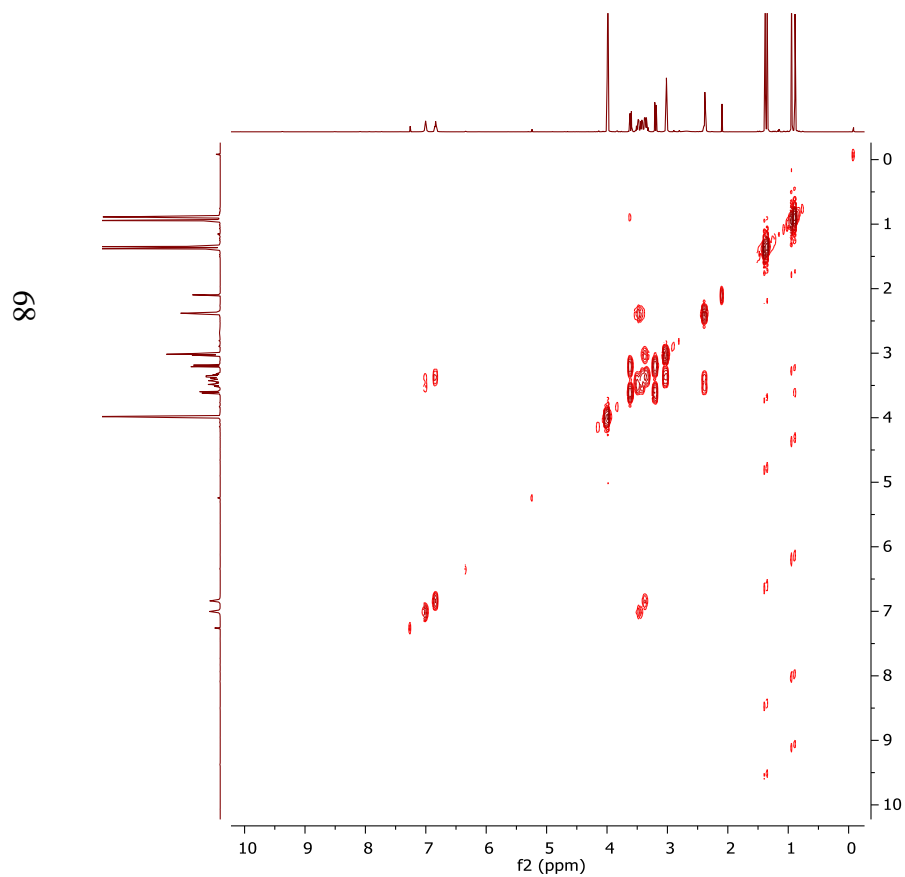


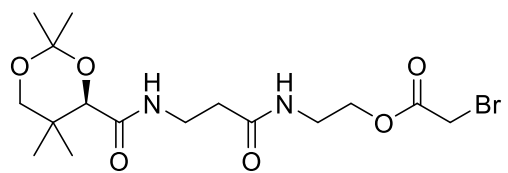
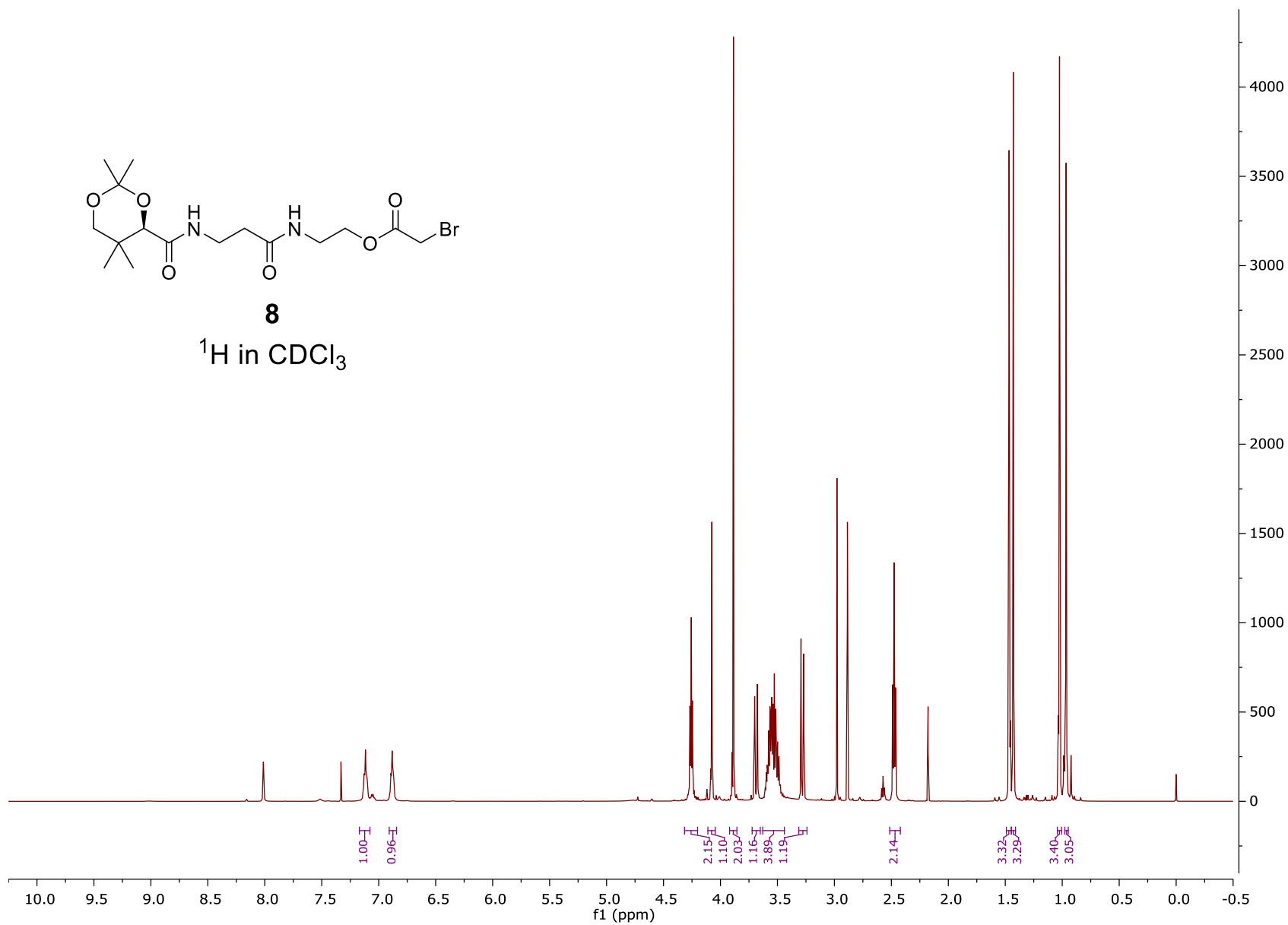
**7** ^{13}C in CDCl_3 

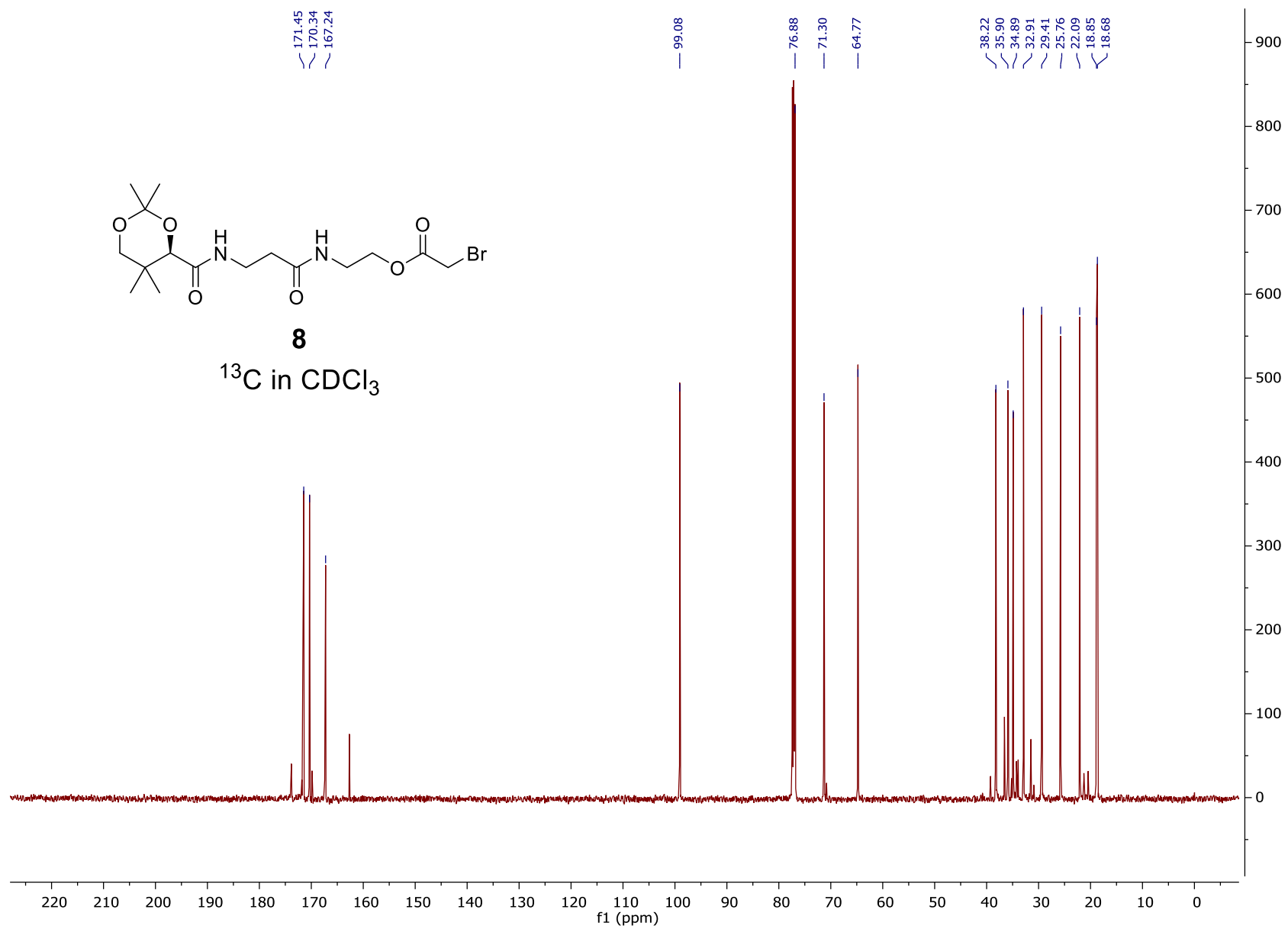


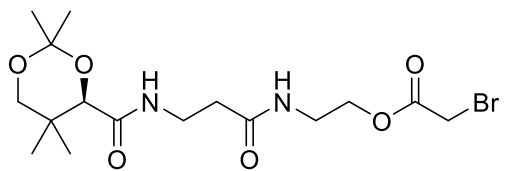
7

COSY and HMQC in CDCl₃



**8** ^1H in CDCl_3 

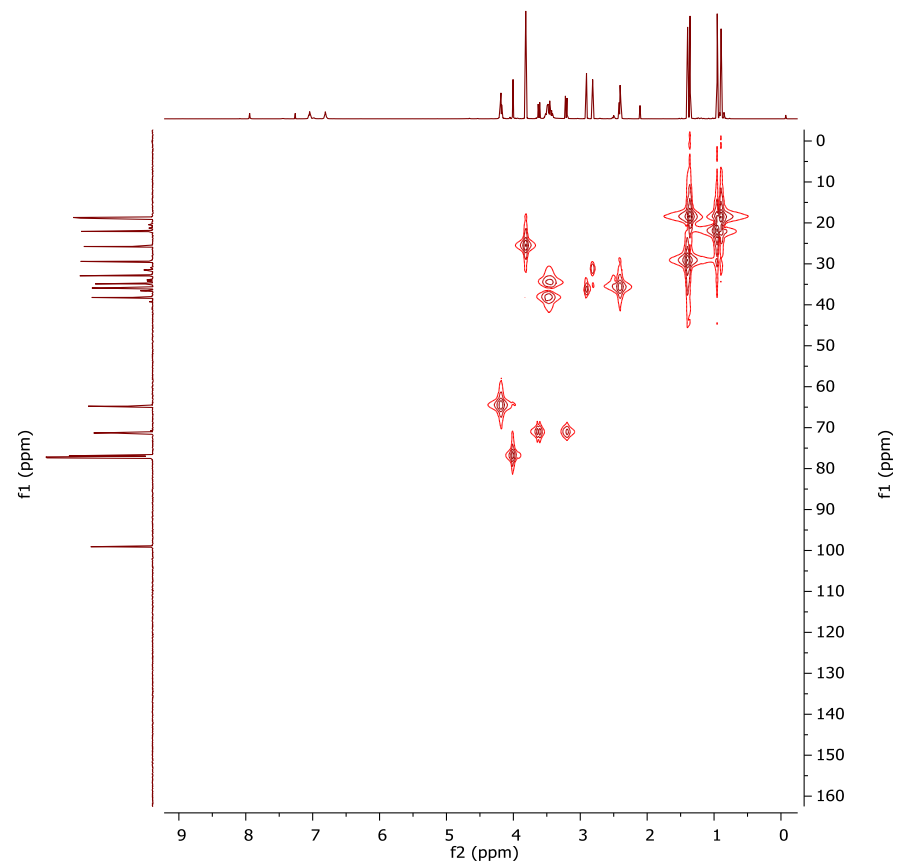
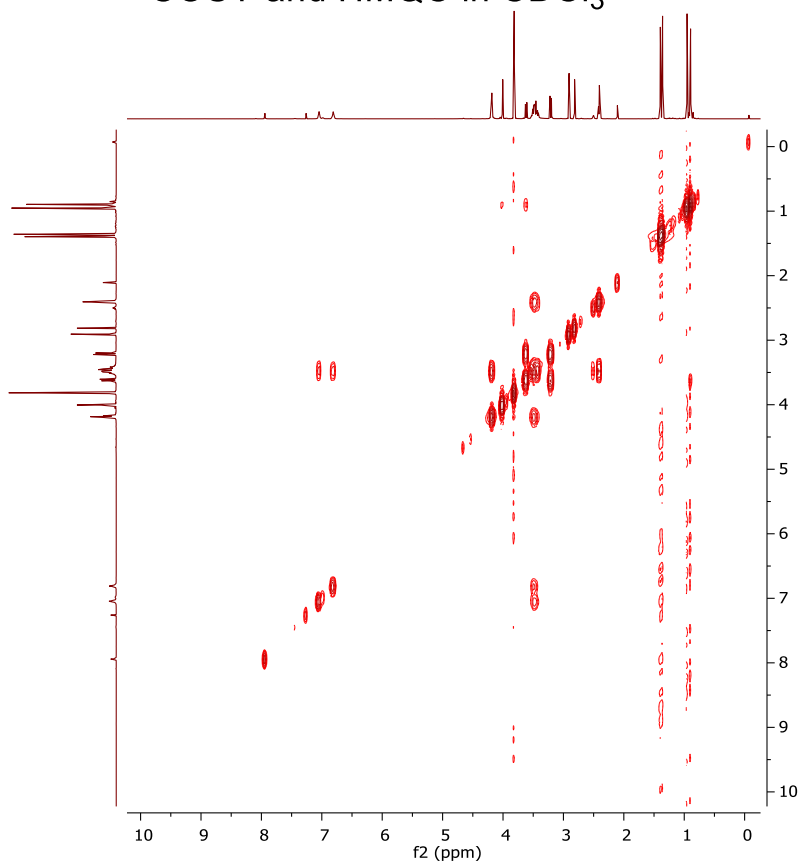


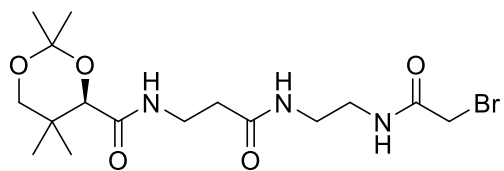


8

COSY and HMQC in CDCl₃

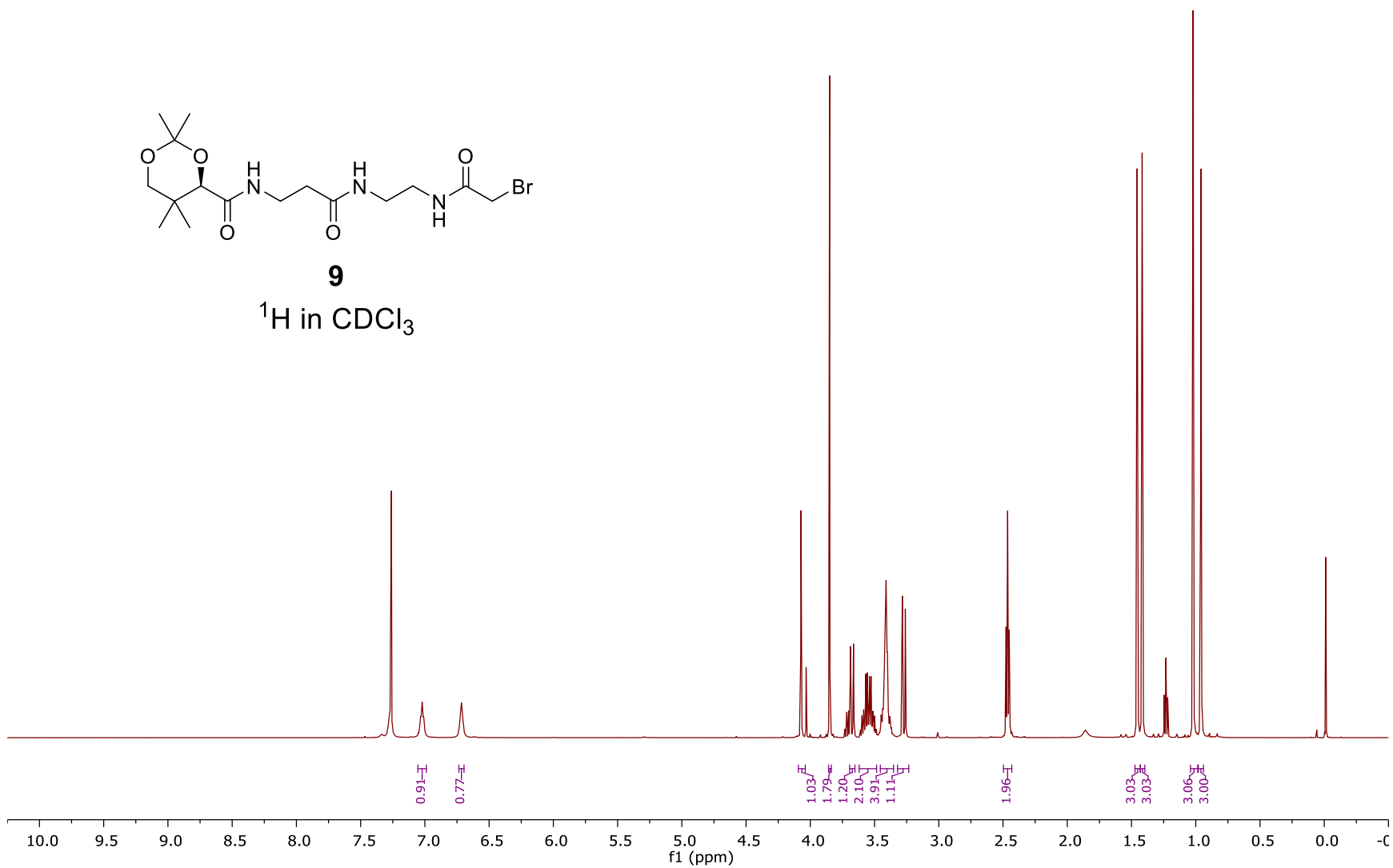
71

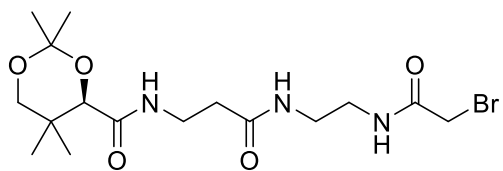
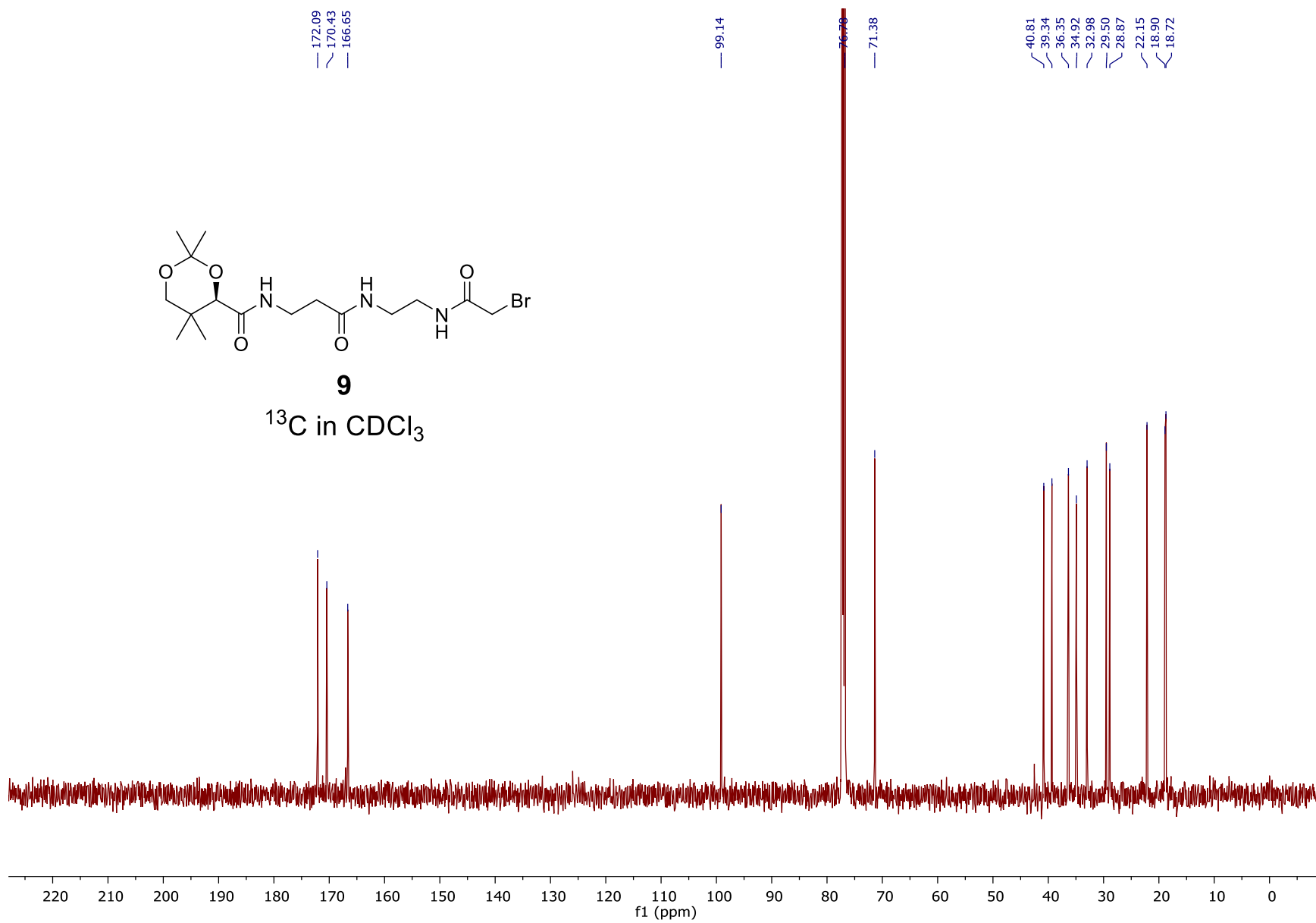


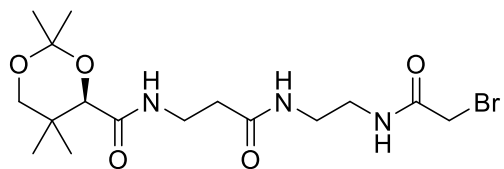


9

^1H in CDCl_3



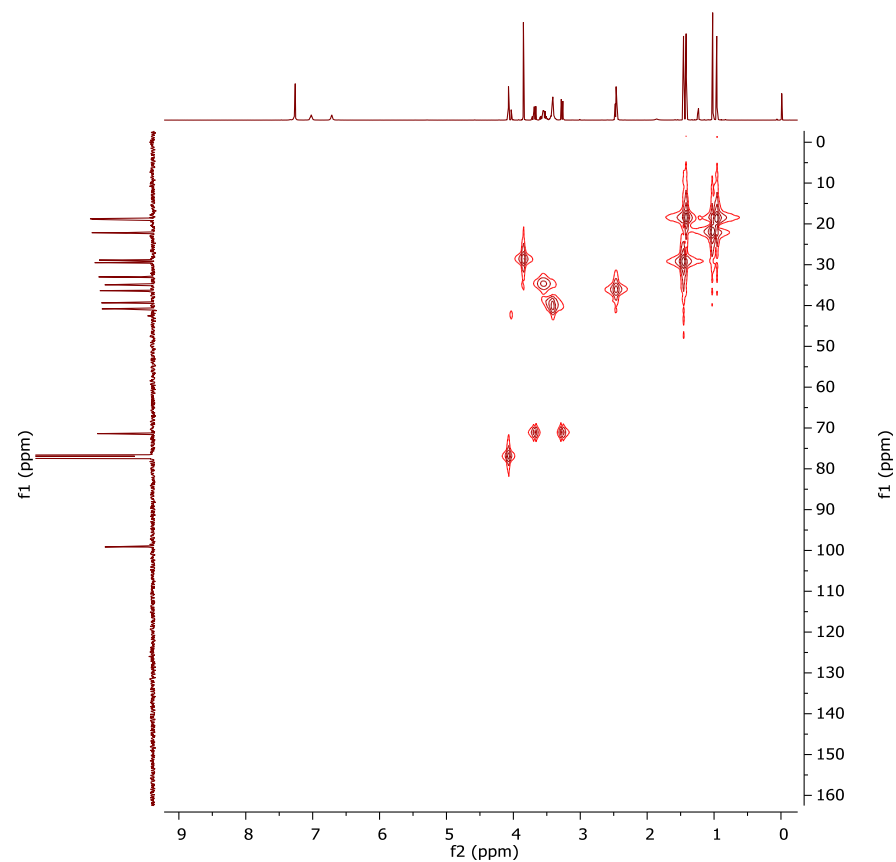
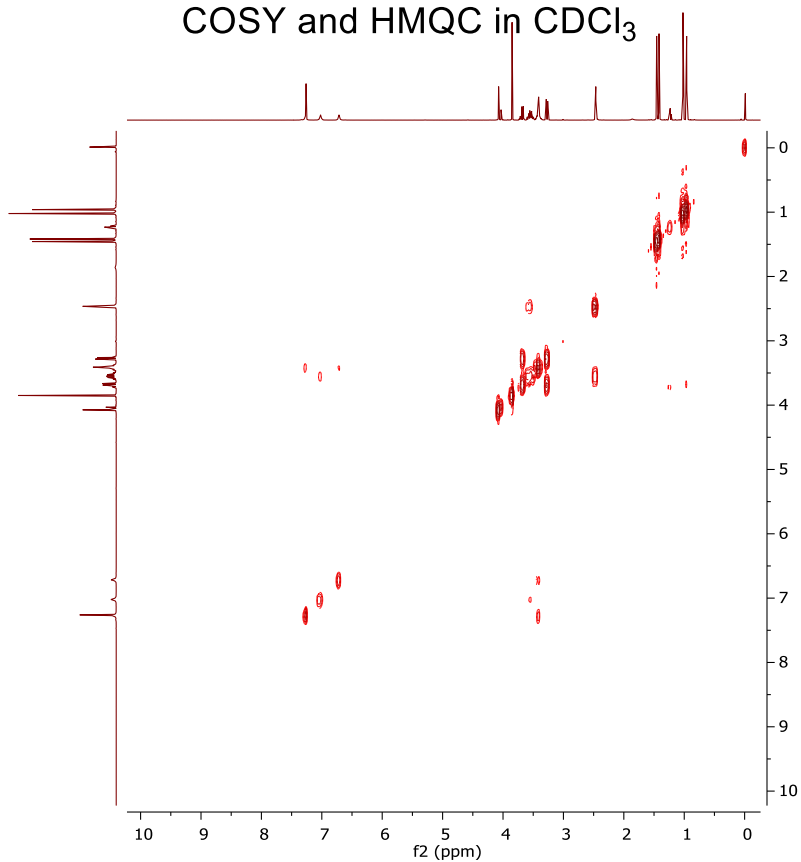
**9** ^{13}C in CDCl_3 

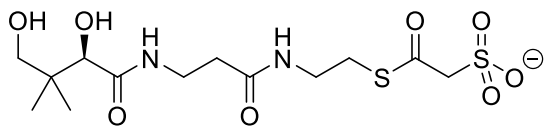


9

COSY and HMQC in CDCl₃

74

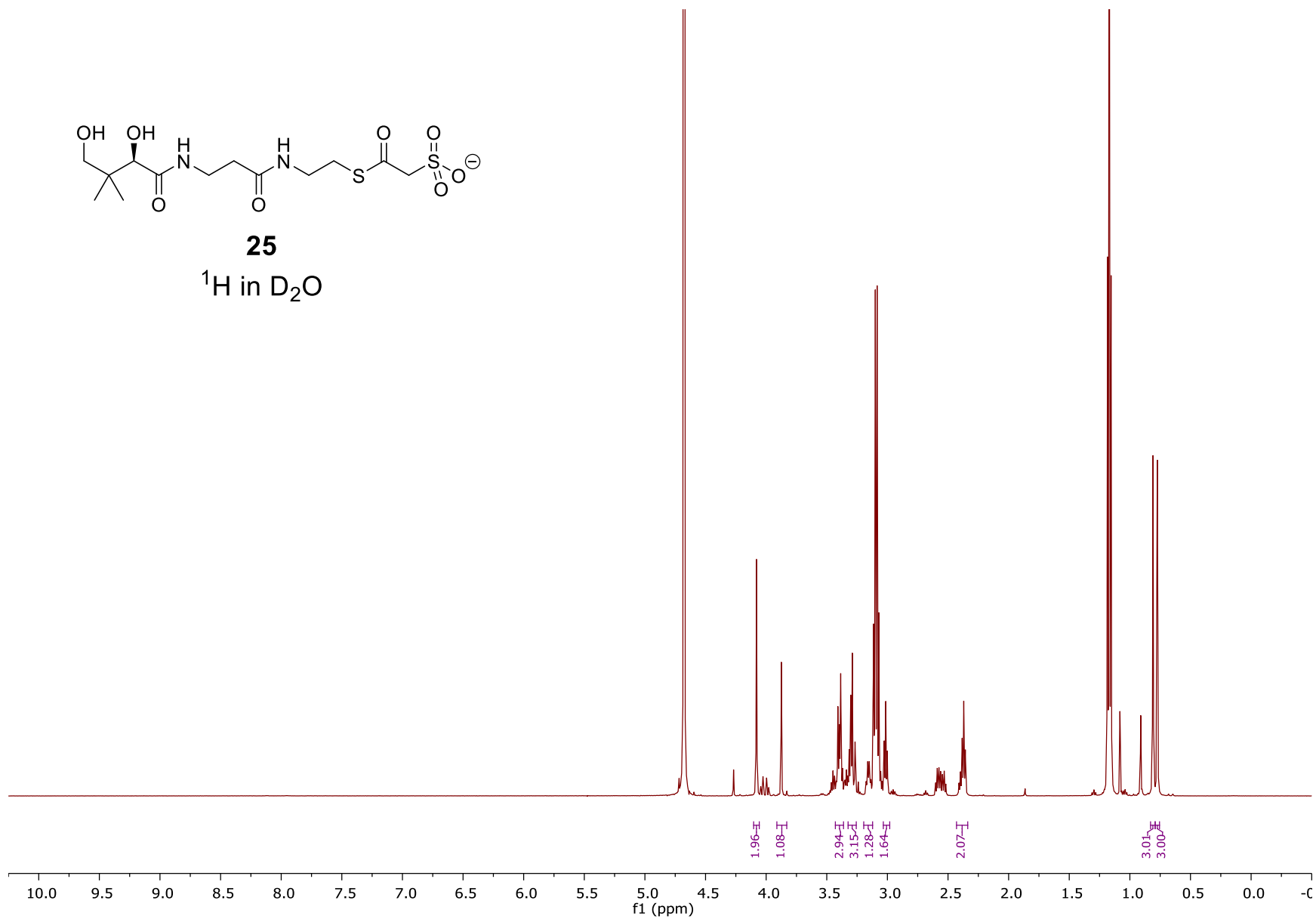


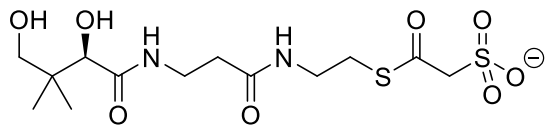
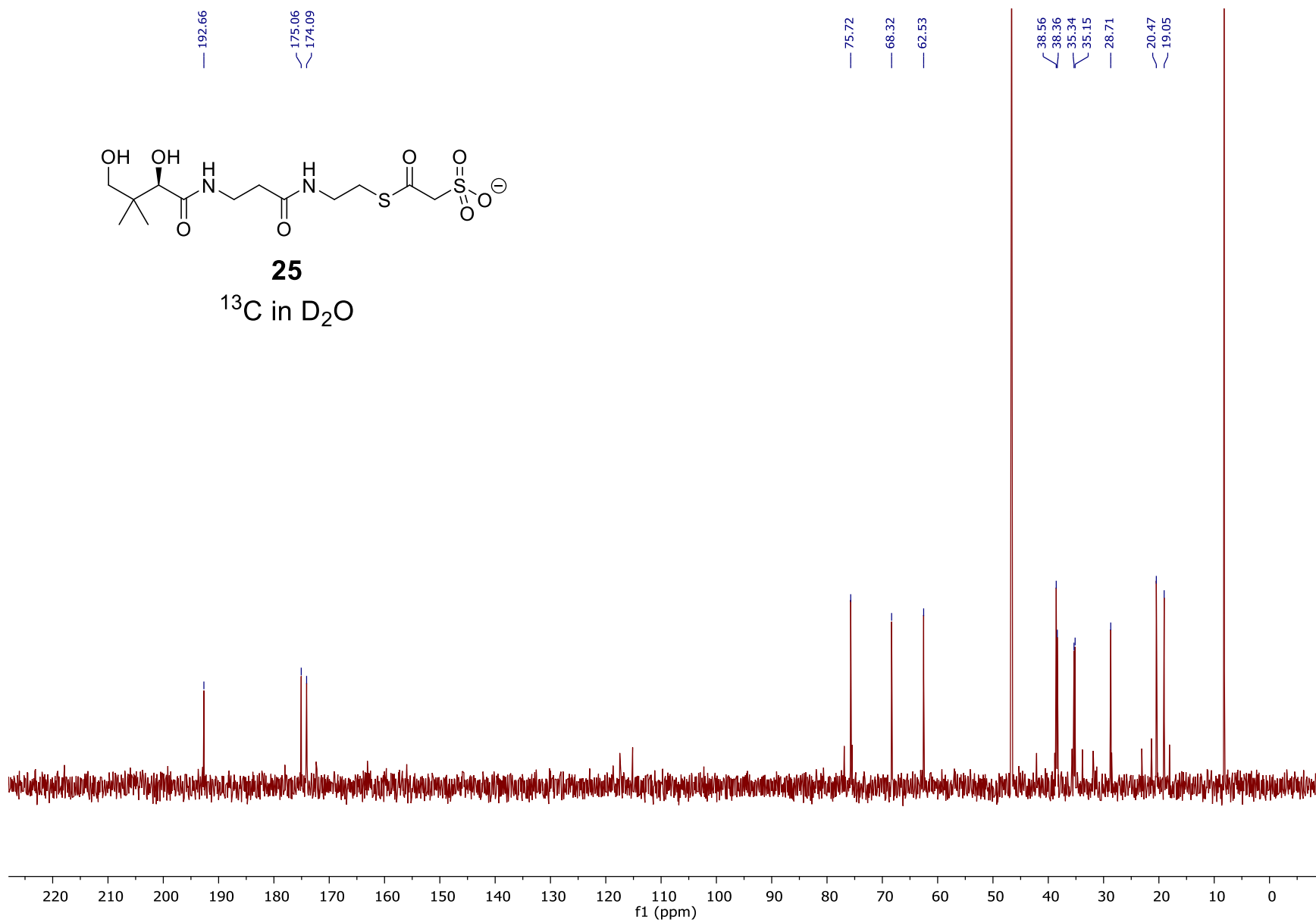


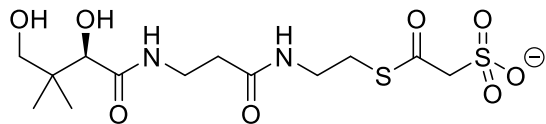
25

^1H in D_2O

75

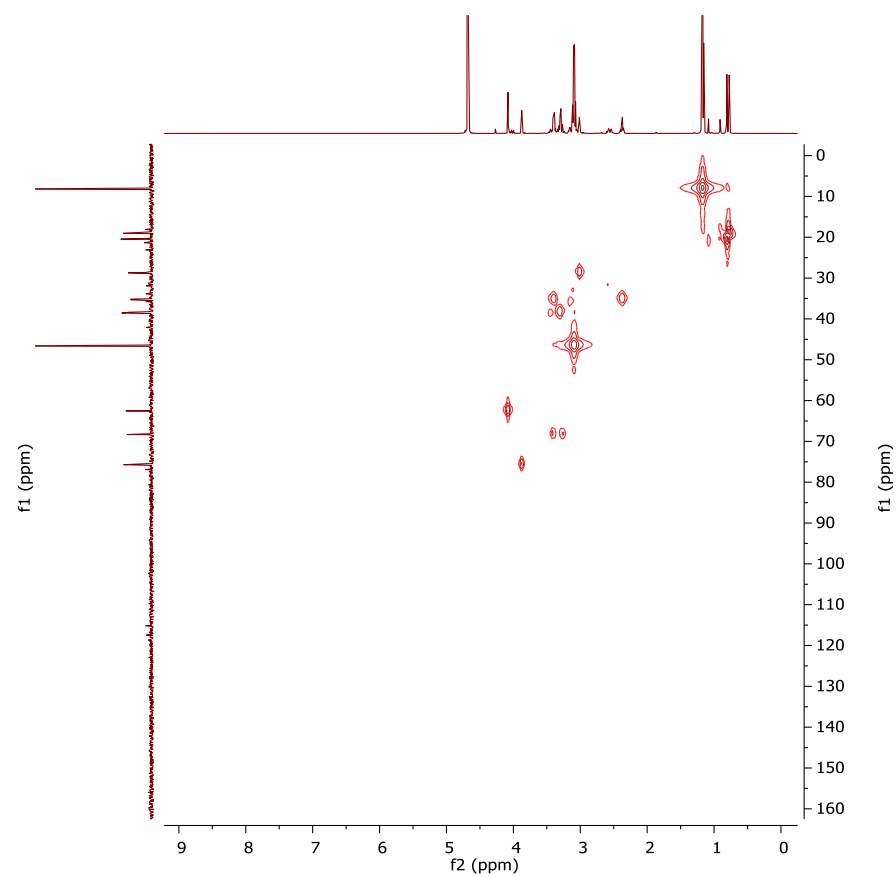
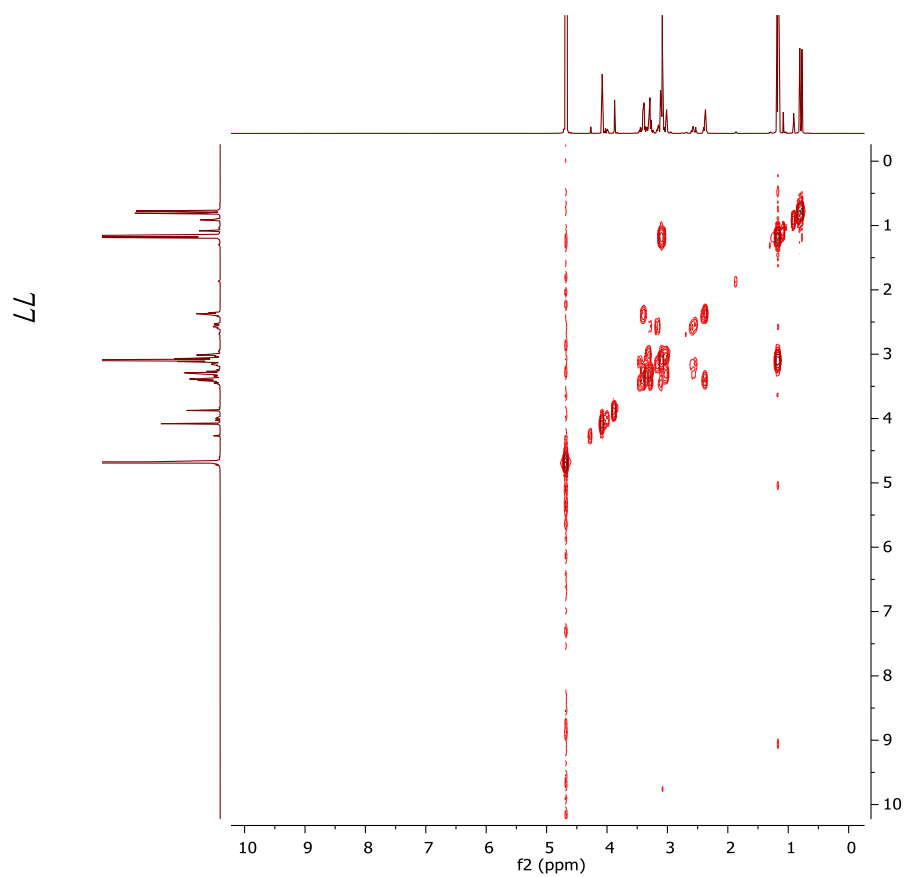


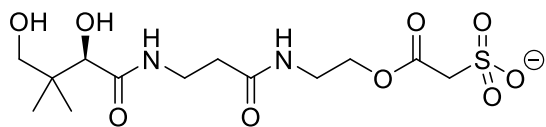
**25** ^{13}C in D_2O 



25

COSY and HMQC in D₂O

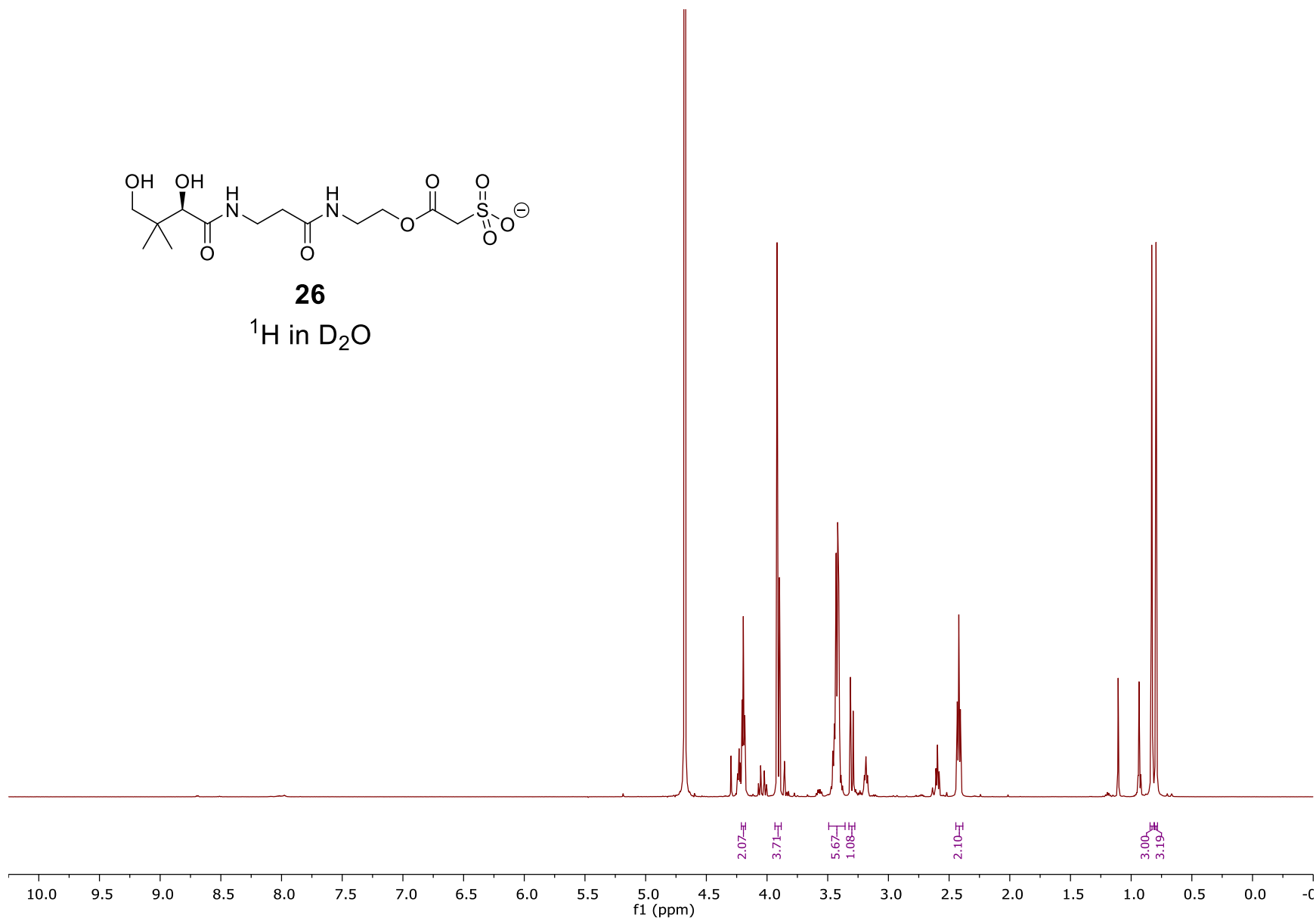


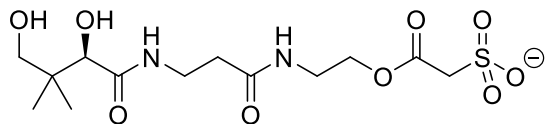
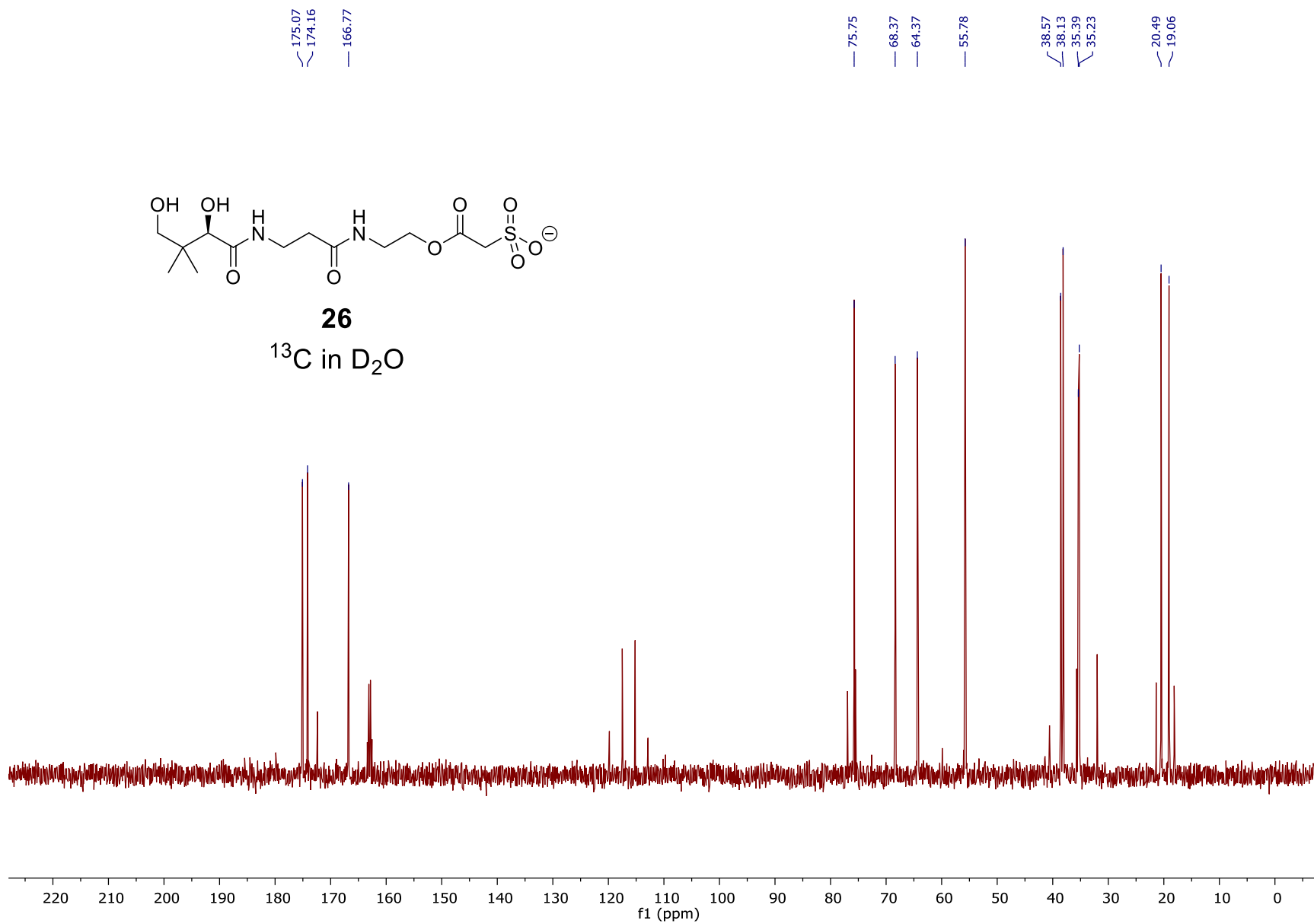


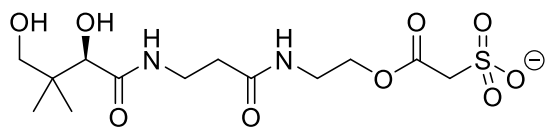
26

¹H in D₂O

78

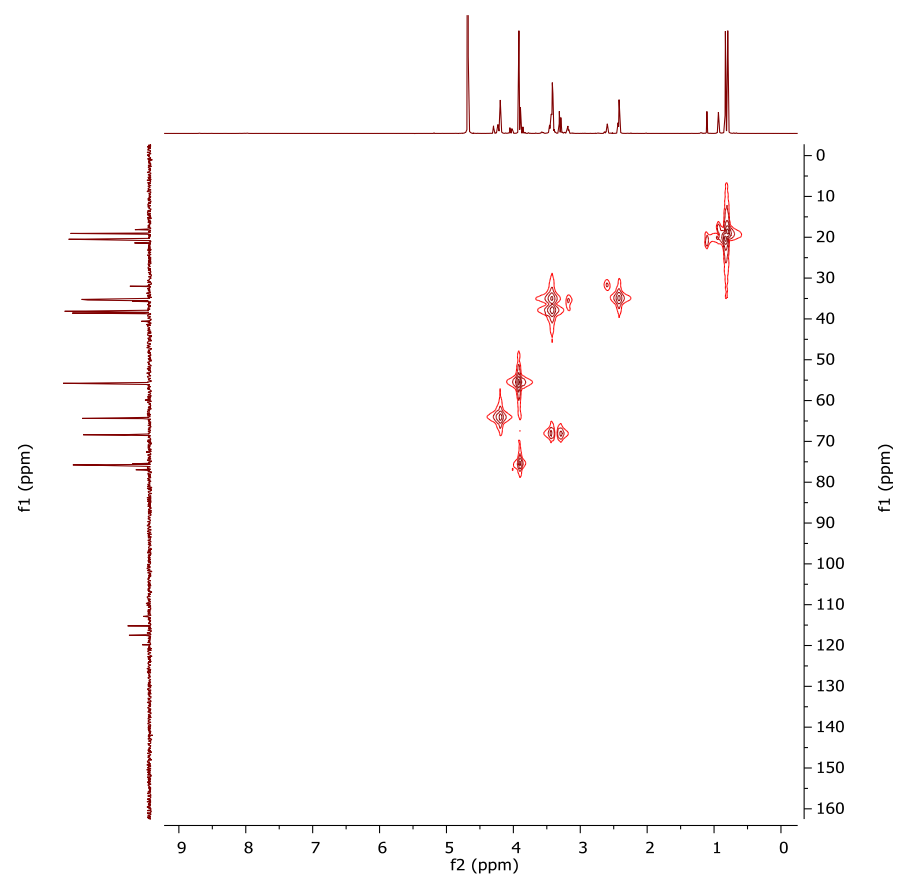
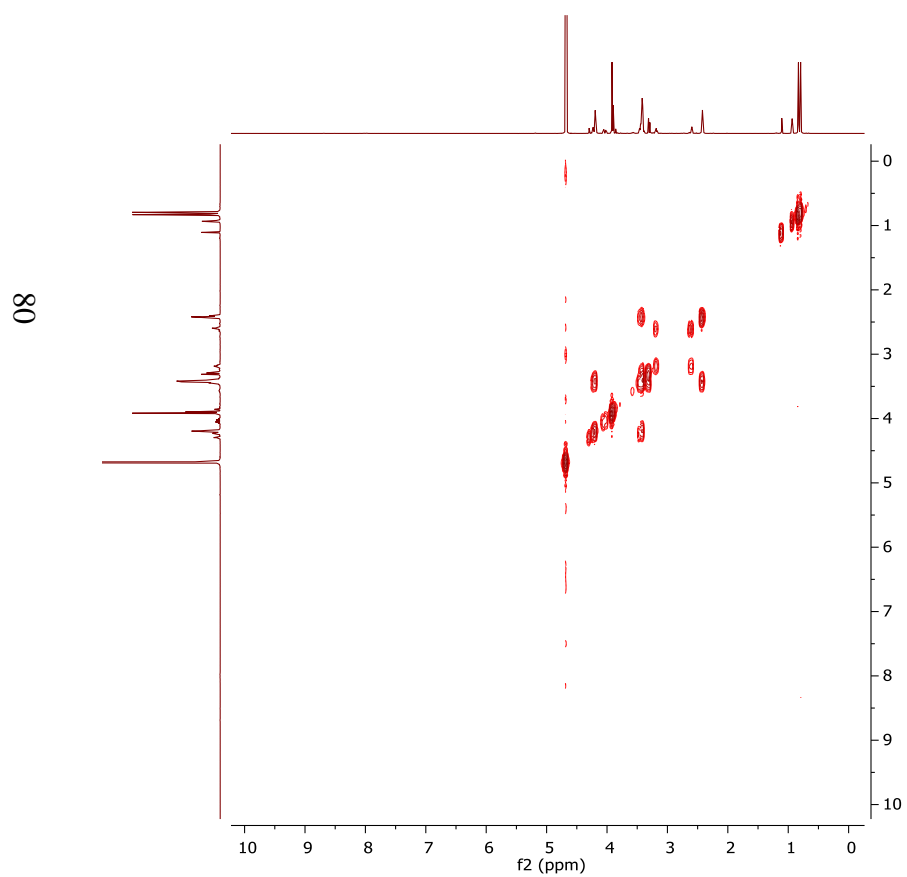


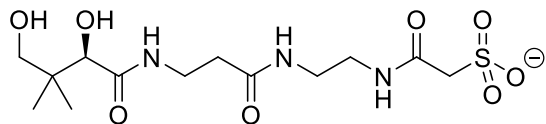
**26** ^{13}C in D_2O 



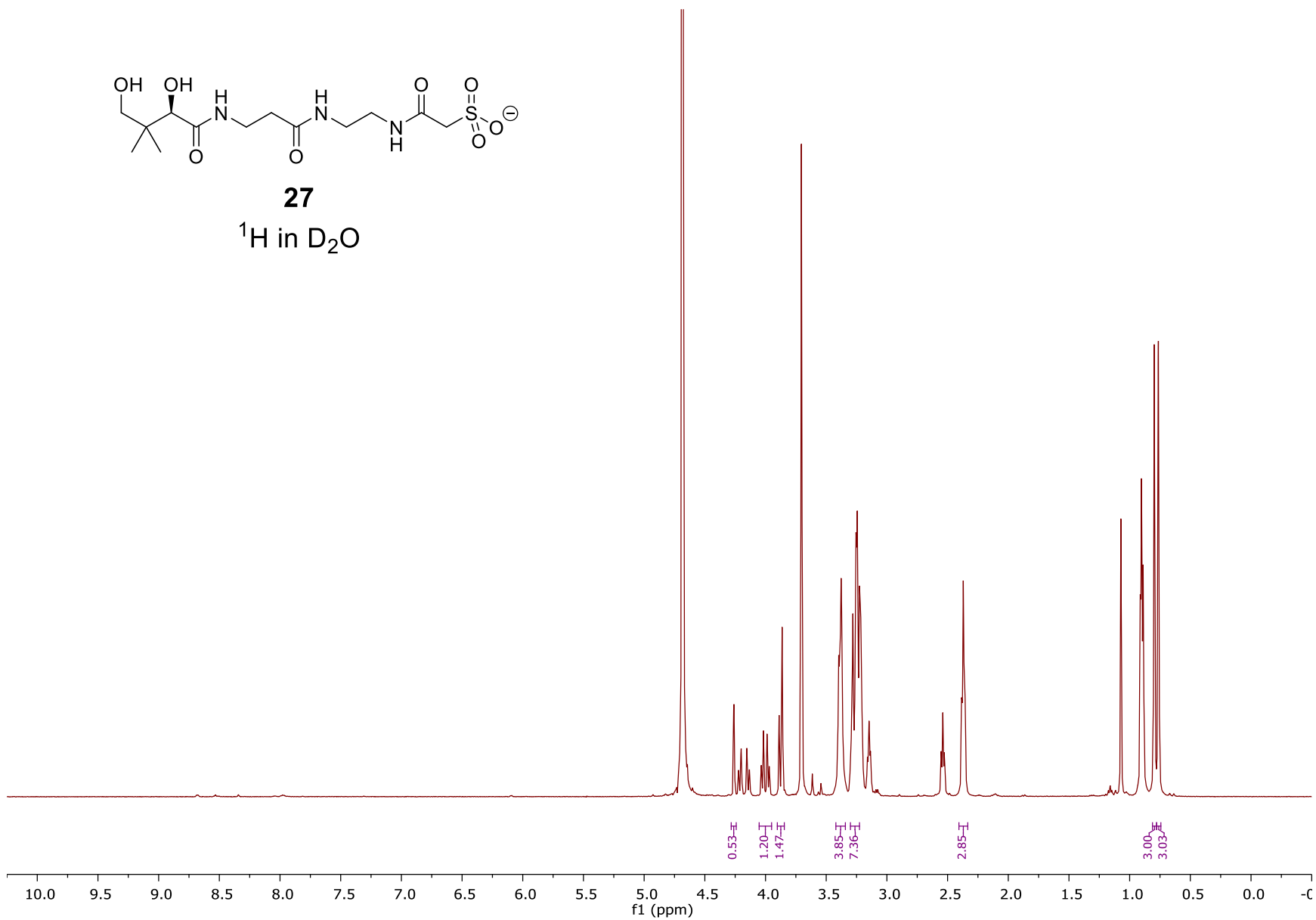
26

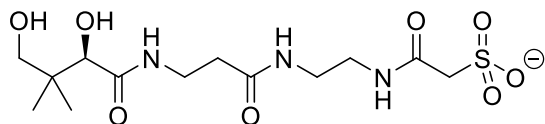
COSY and HMQC in D₂O





27
¹H in D₂O





27

¹³C in D₂O

175.07
174.20

166.71

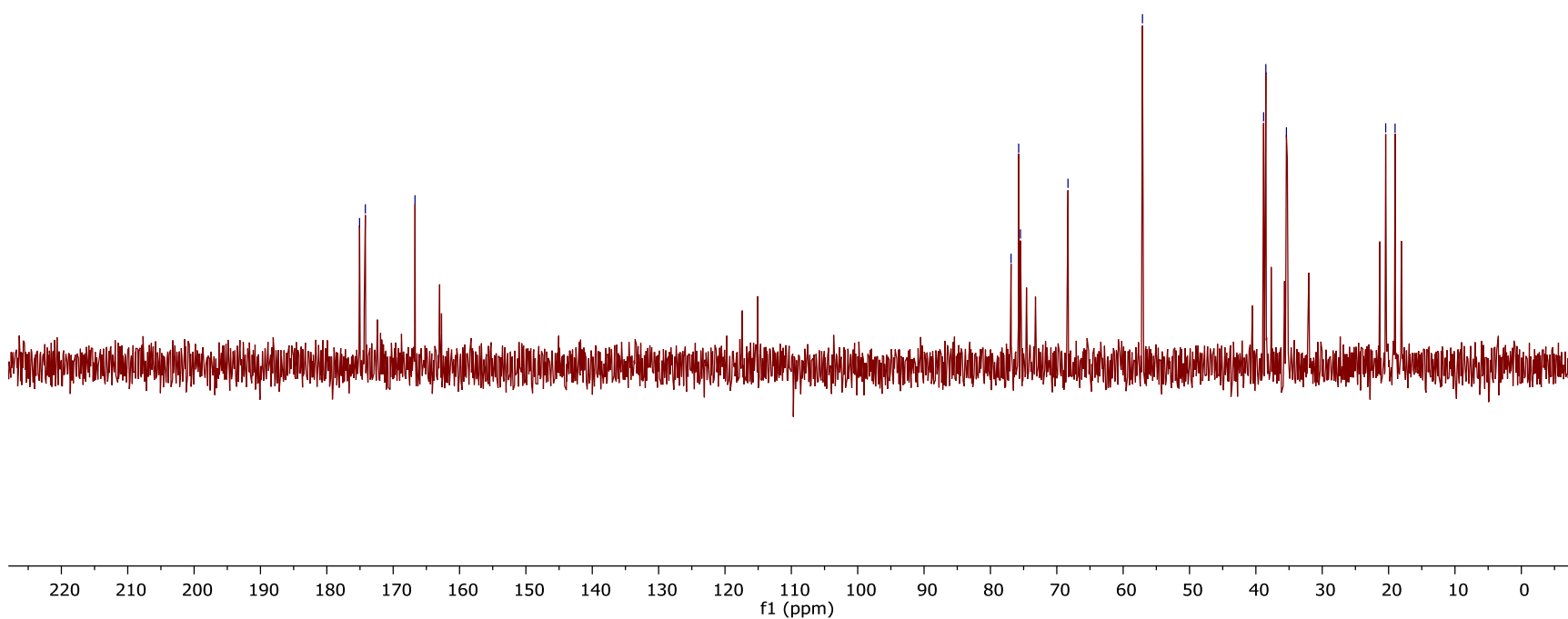
76.89
75.75
75.47

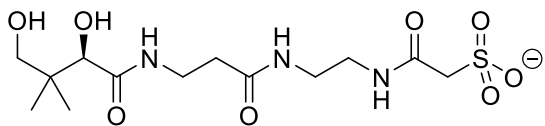
68.32

57.09

38.84
38.50
35.40

20.44
19.02

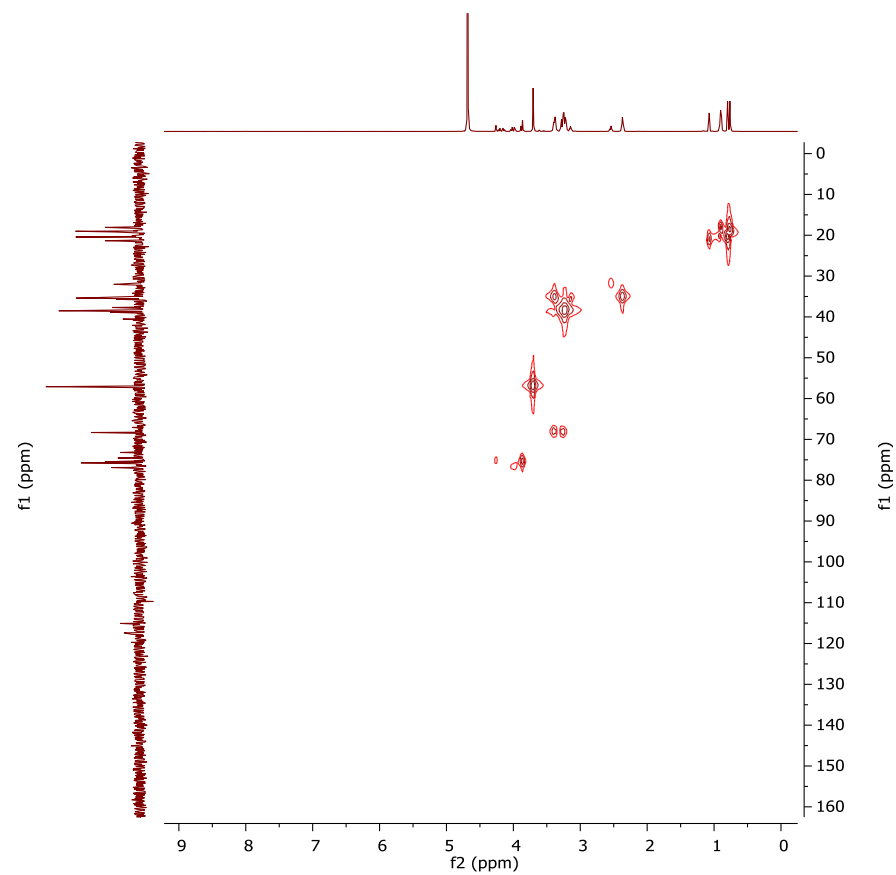
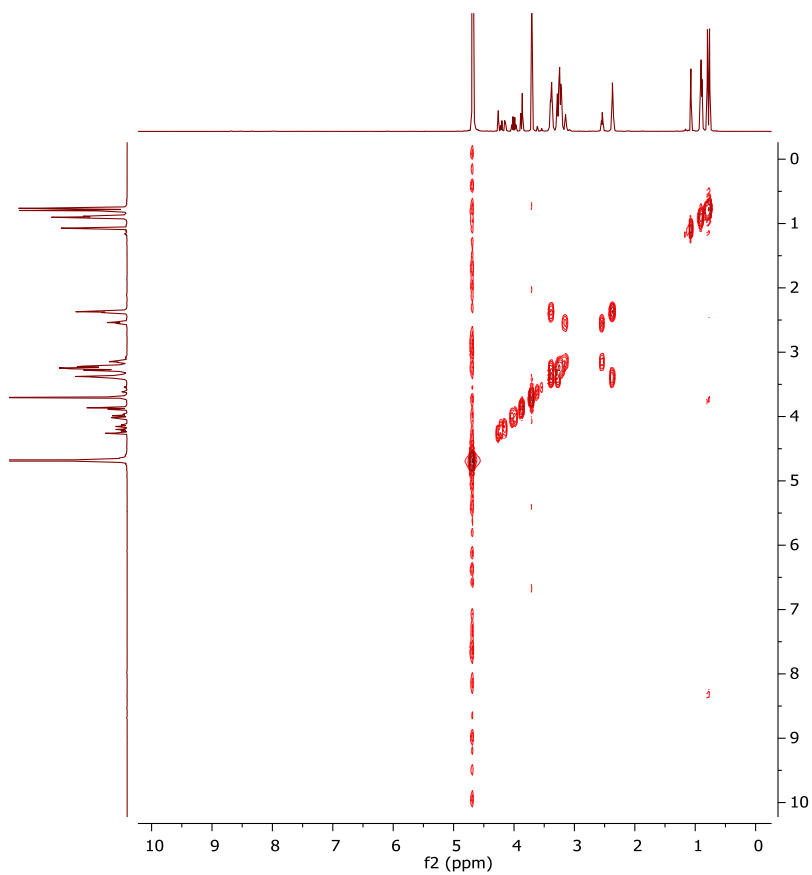


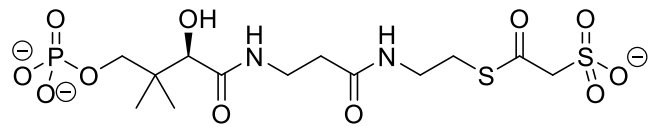
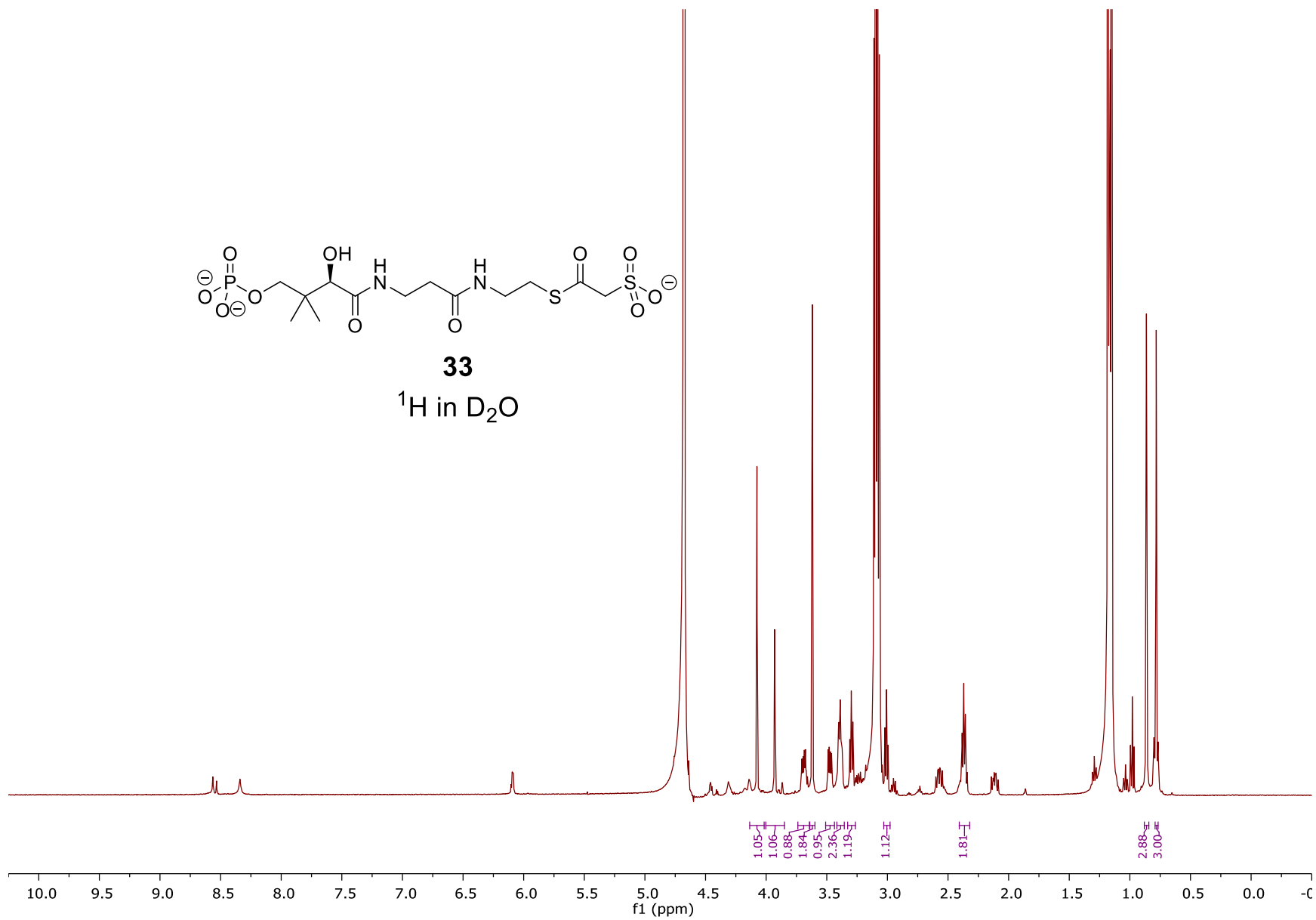


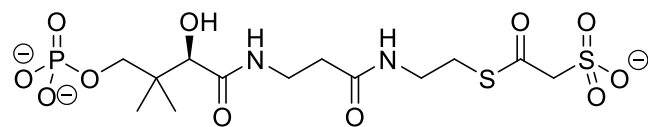
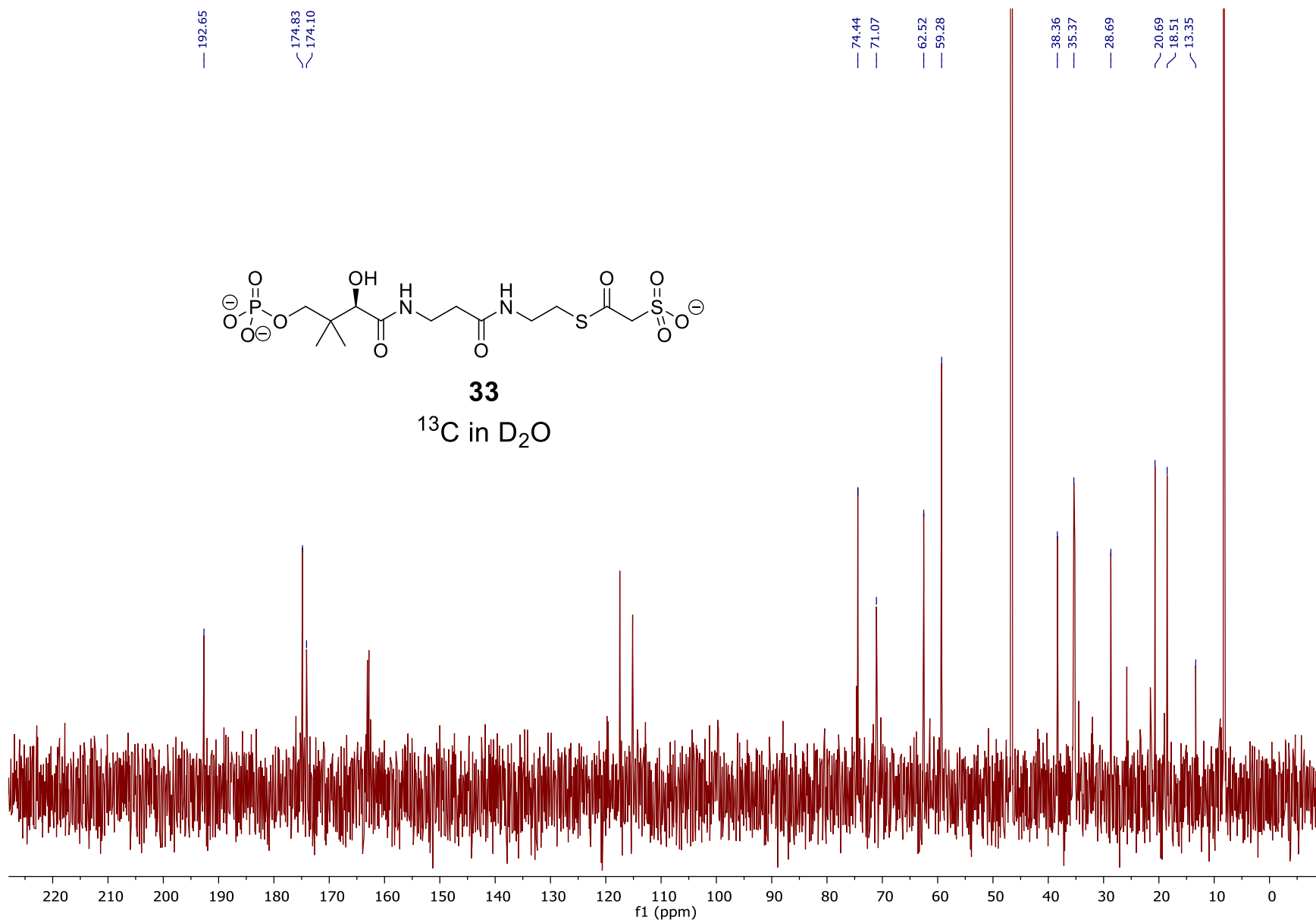
27

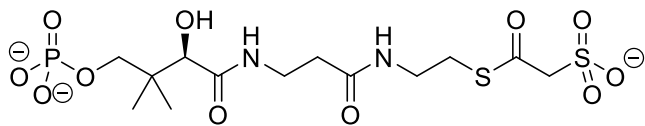
COSY and HMQC in D₂O

83



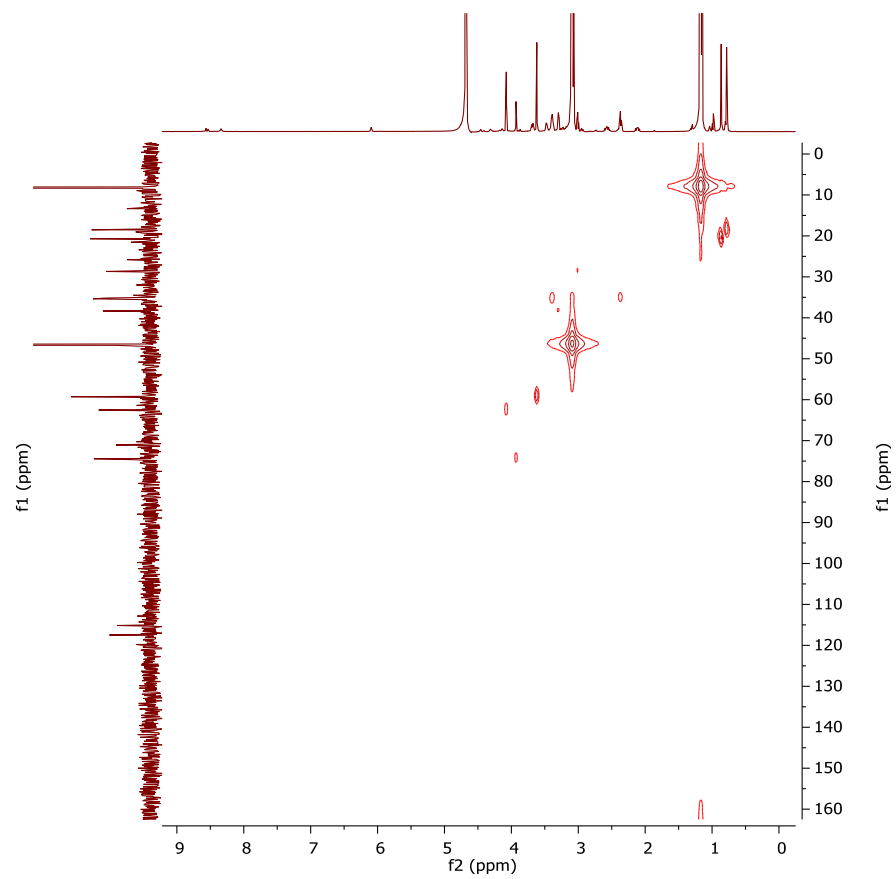
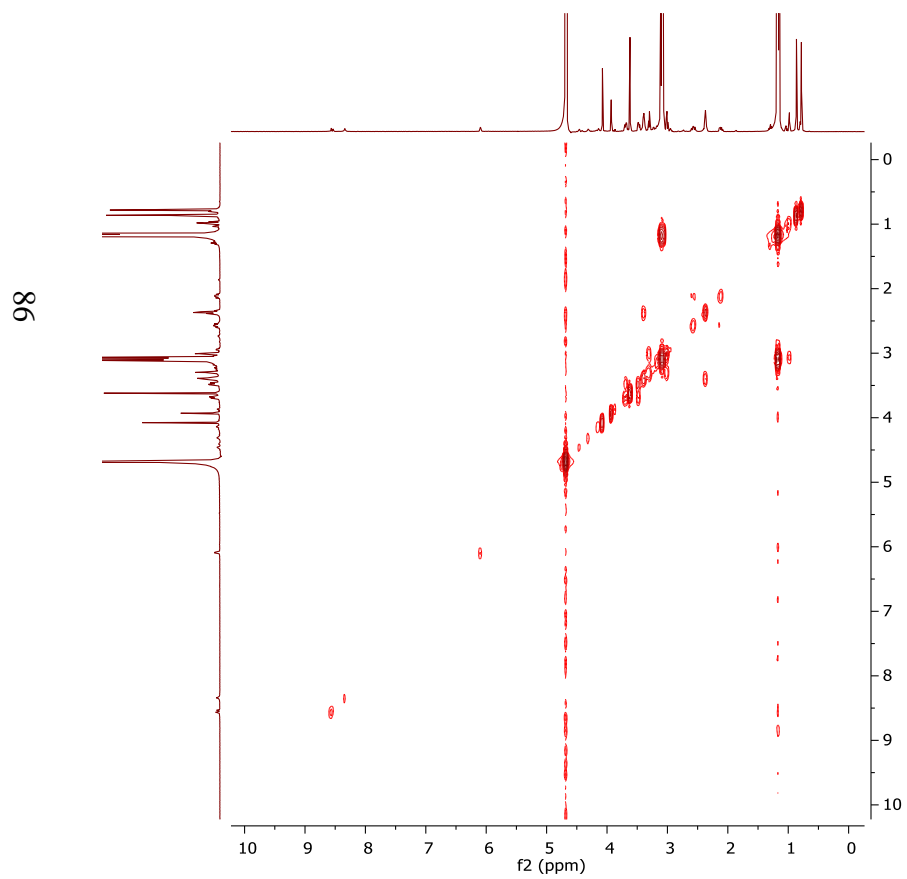
**33**¹H in D₂O

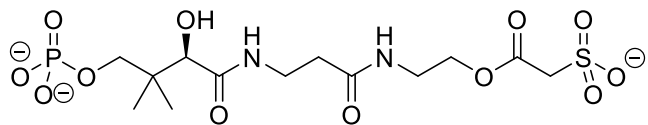
**33** ^{13}C in D_2O 



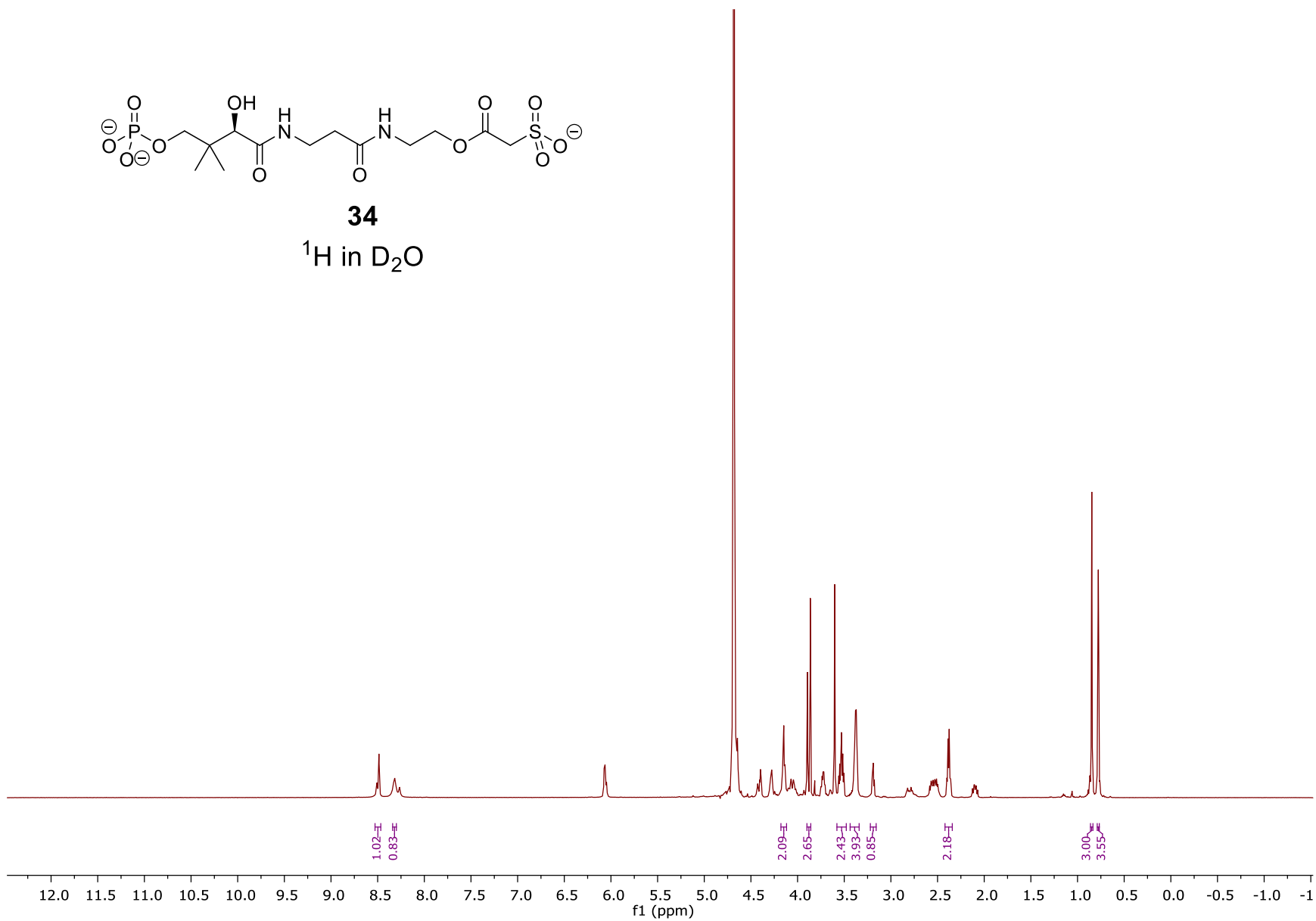
33

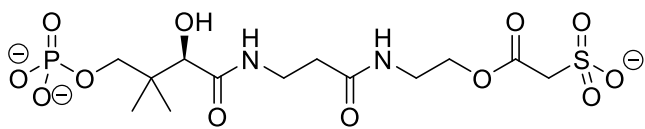
COSY and HMQC in D₂O





34
 ^1H in D_2O





34

¹³C in D₂O

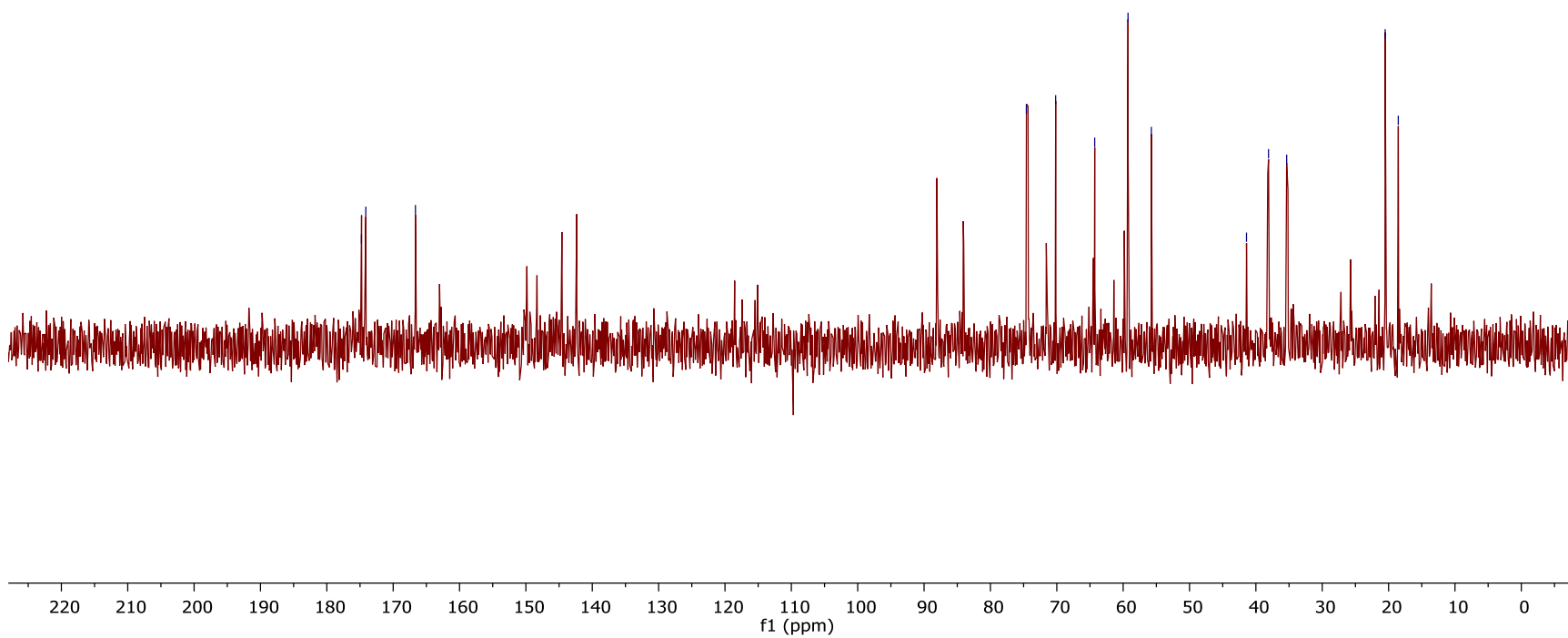
174.78
174.13
166.65

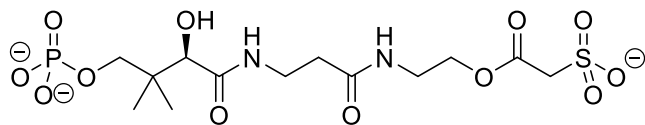
74.58
70.17
64.29
59.27
55.75

41.42
38.09
35.36

20.52
18.54

88

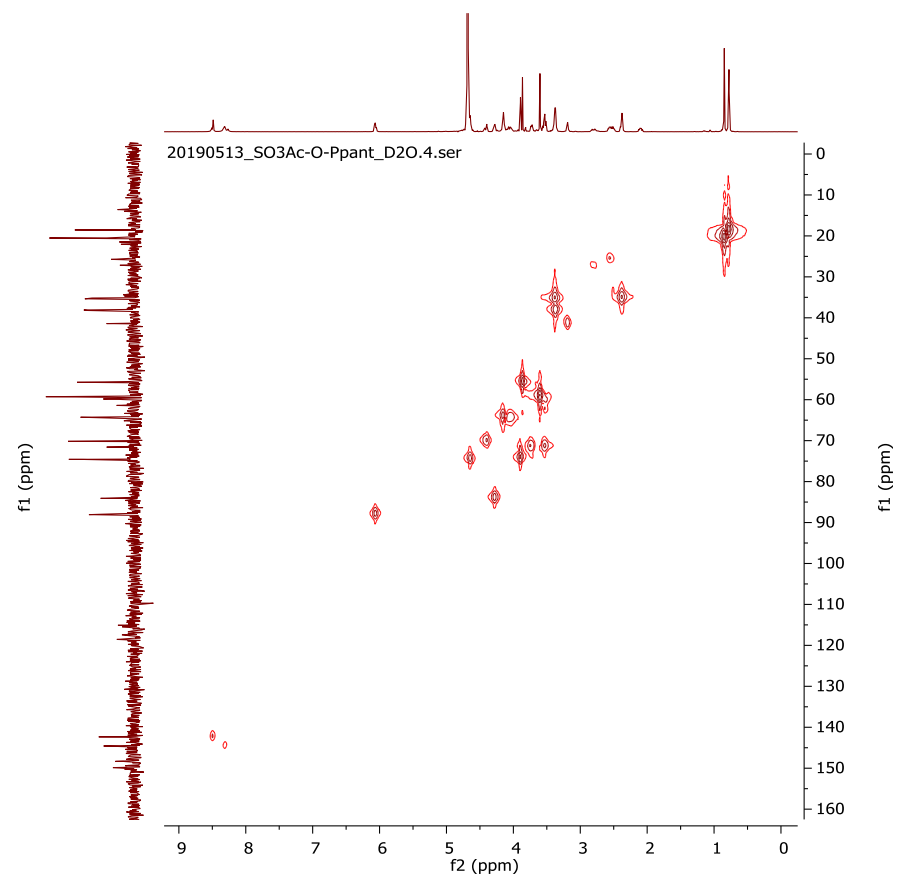
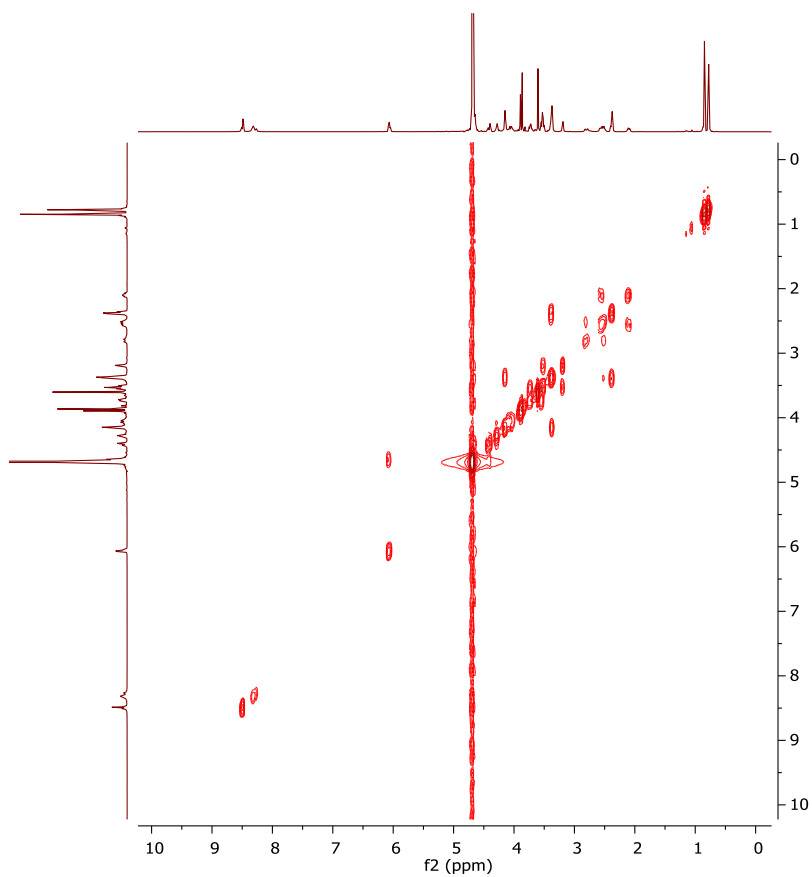


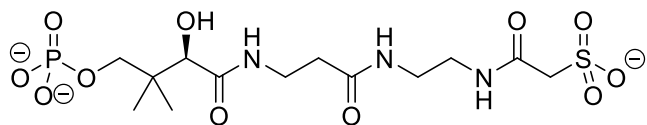
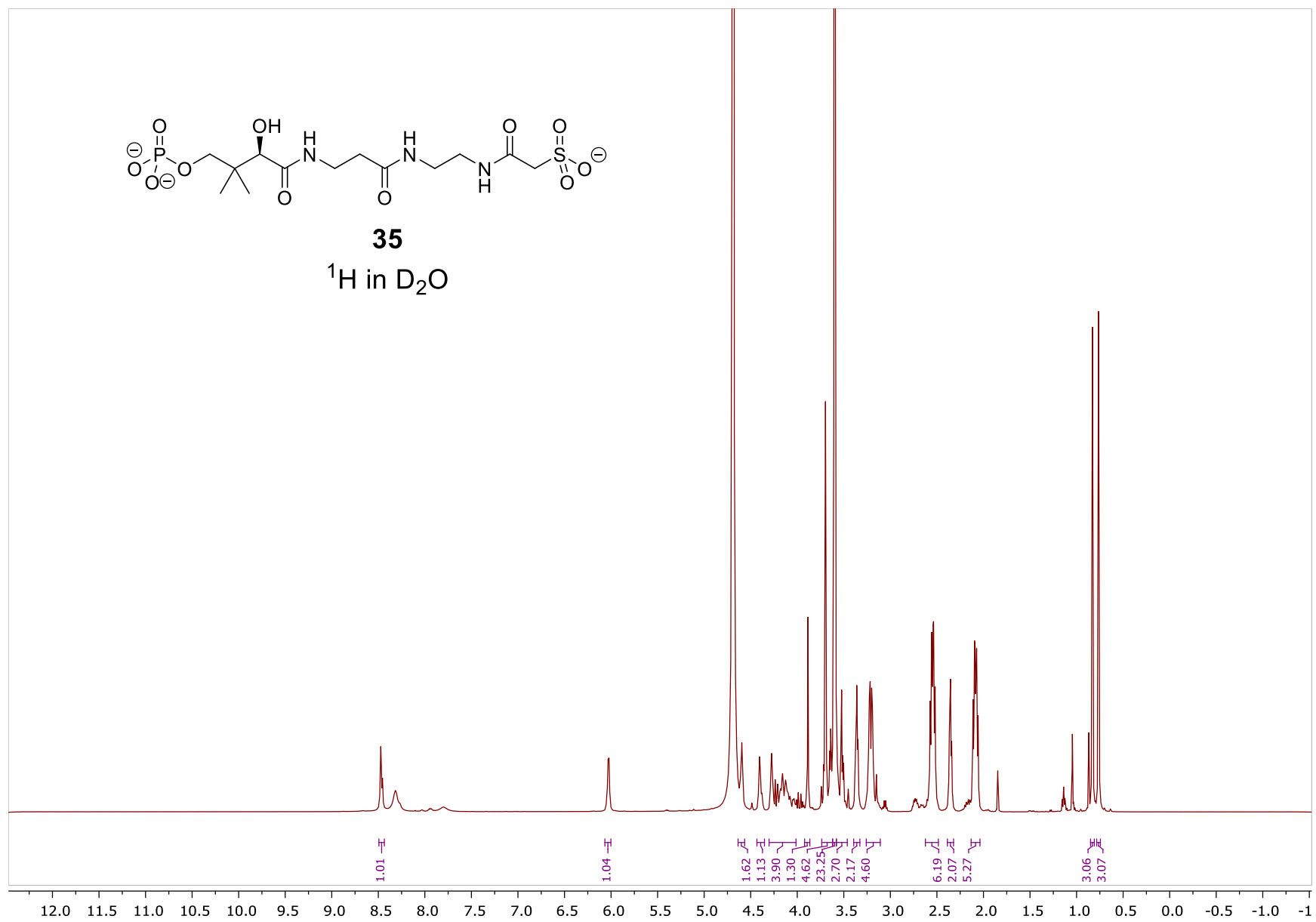


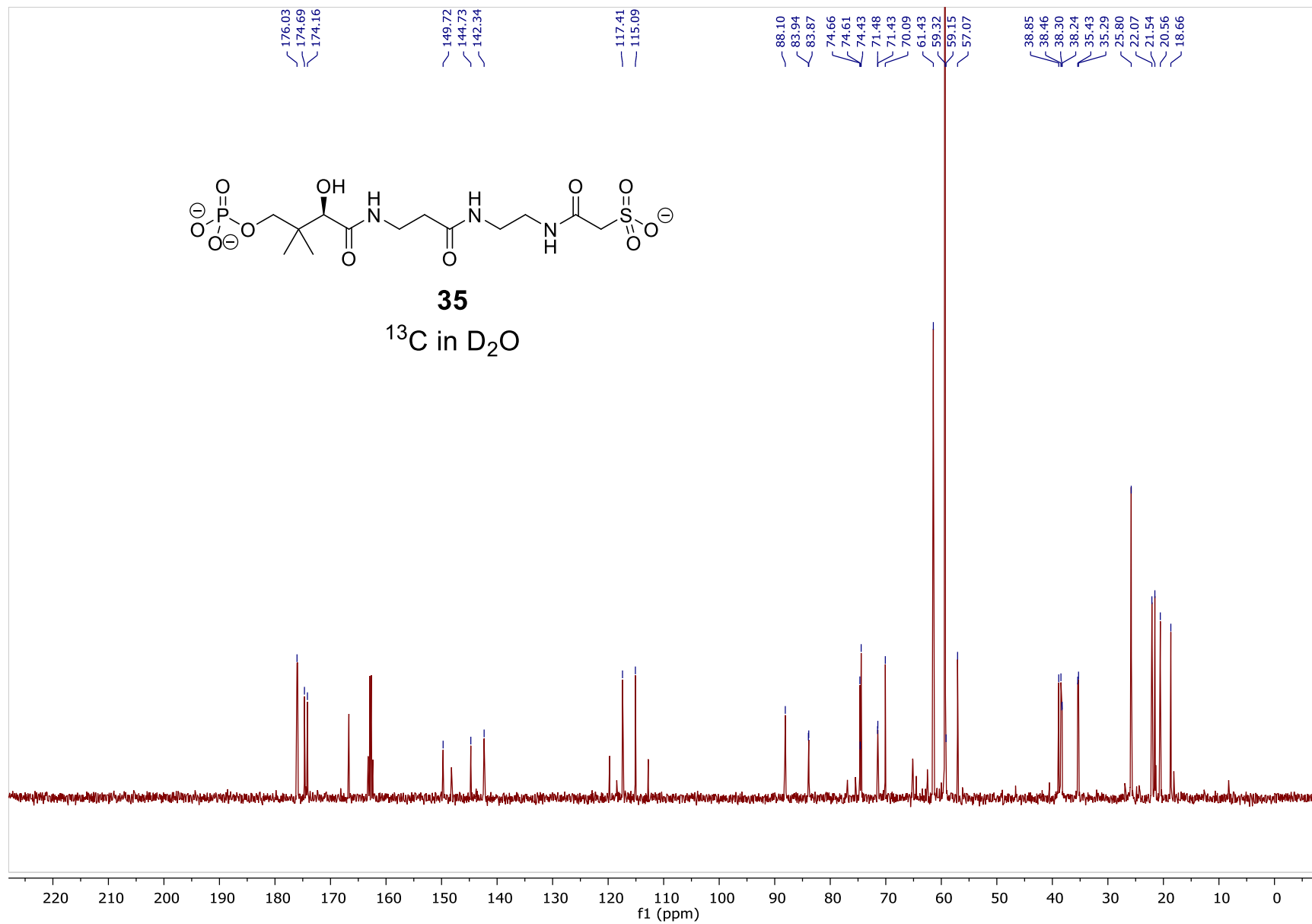
34

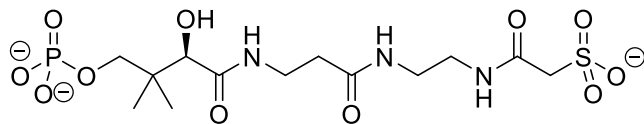
COSY and HMQC in D₂O

68



**35** ^1H in D_2O 

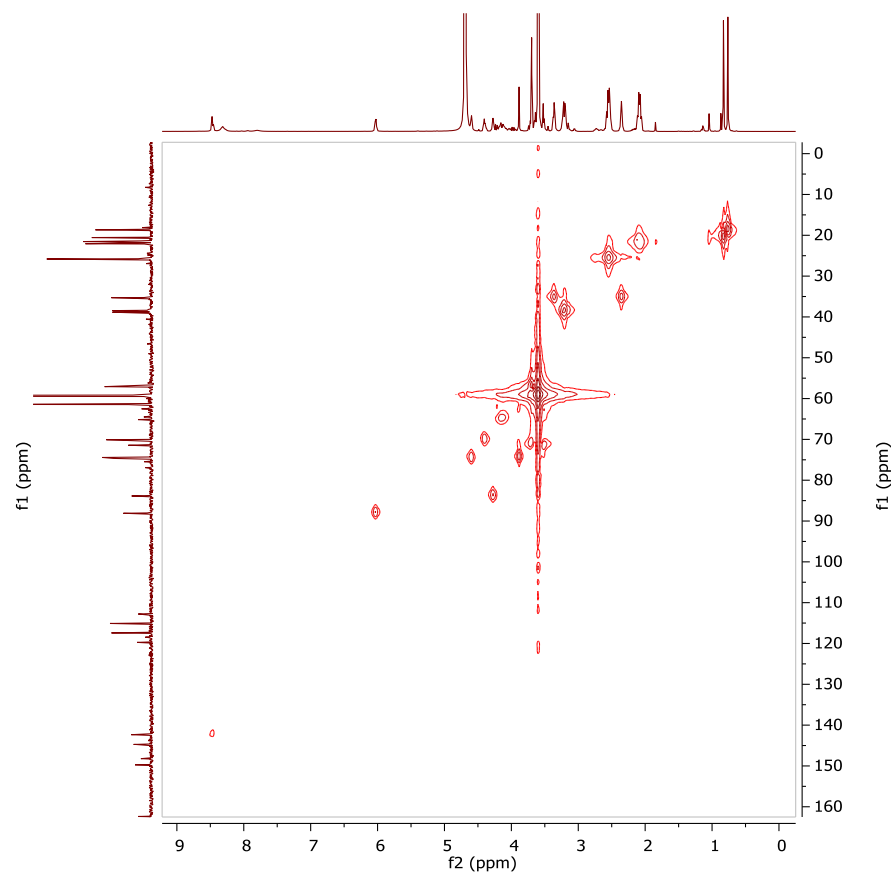
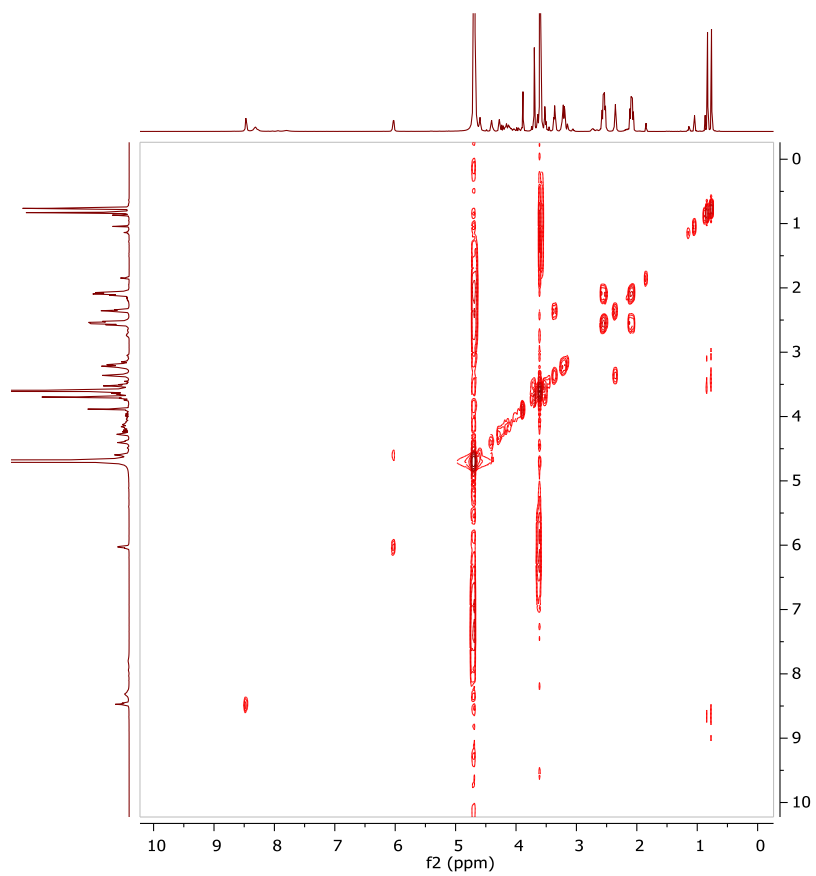


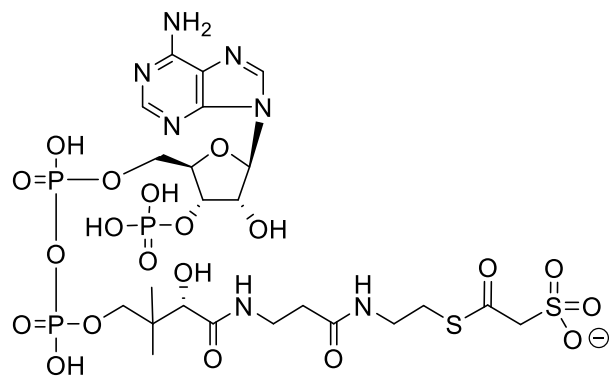
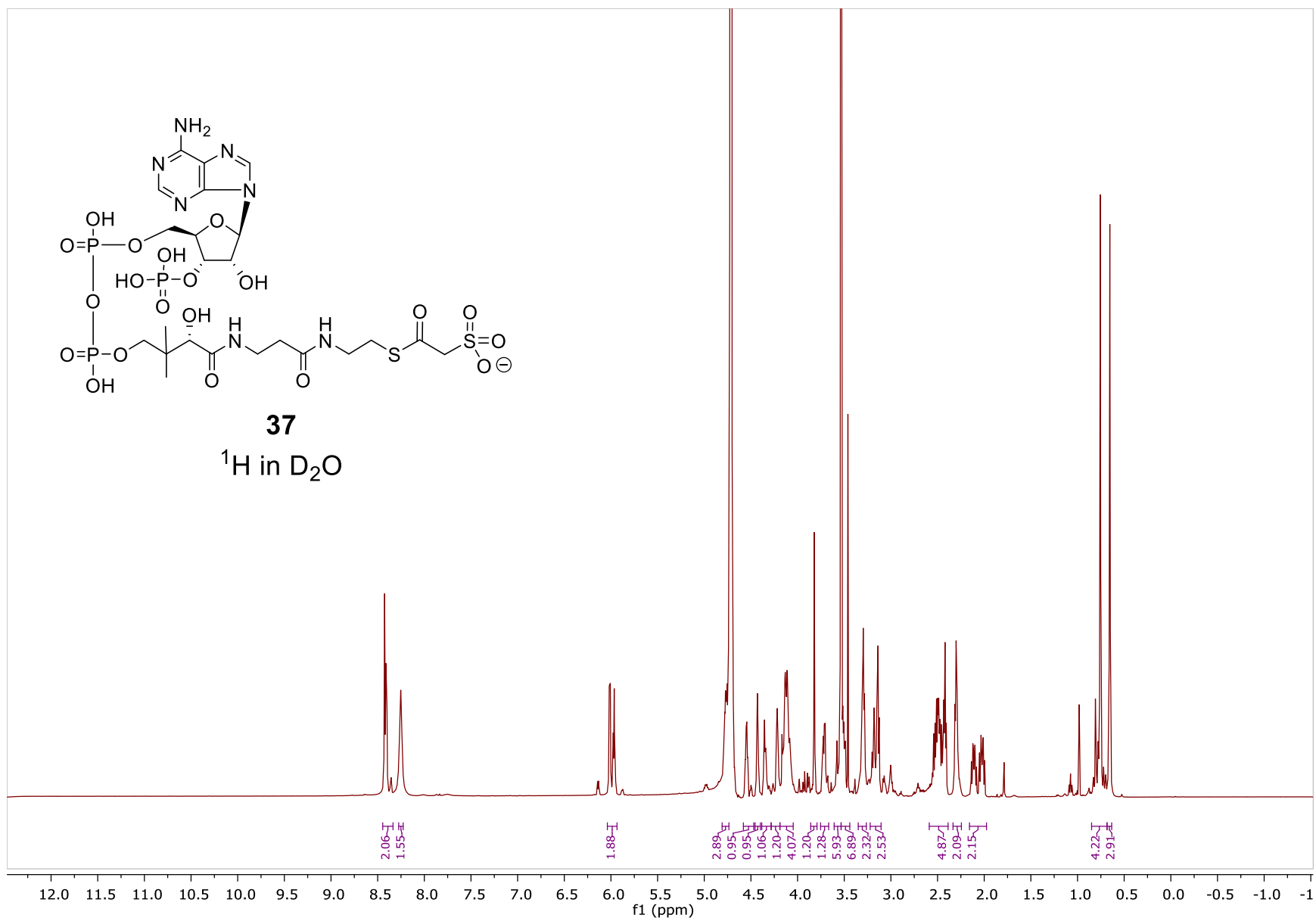


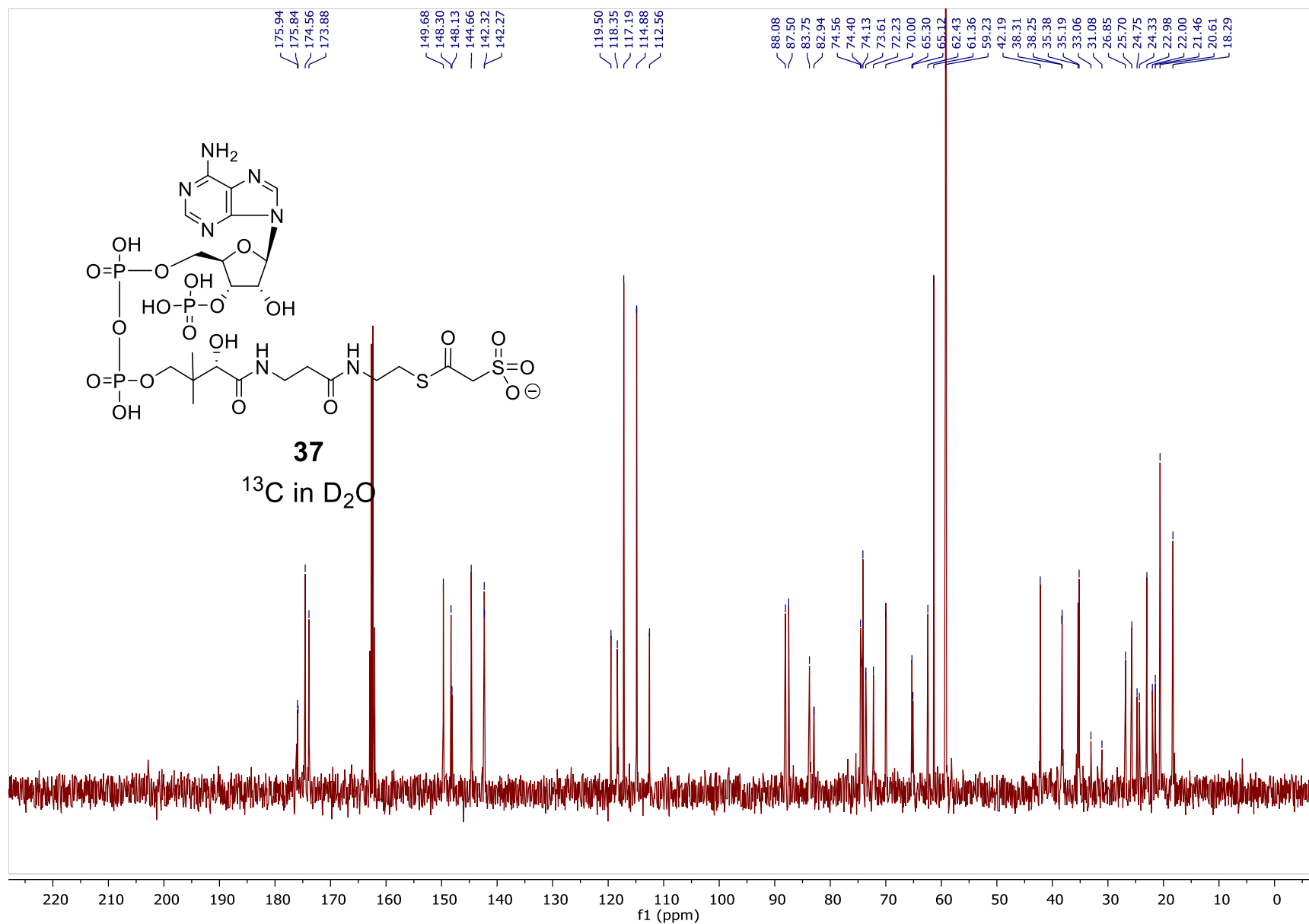
35

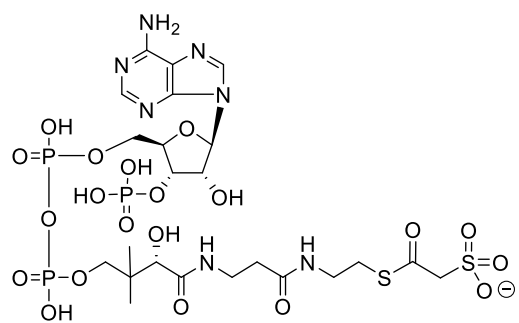
COSY and HMQC in D₂O

92



**37** ^1H in D_2O 

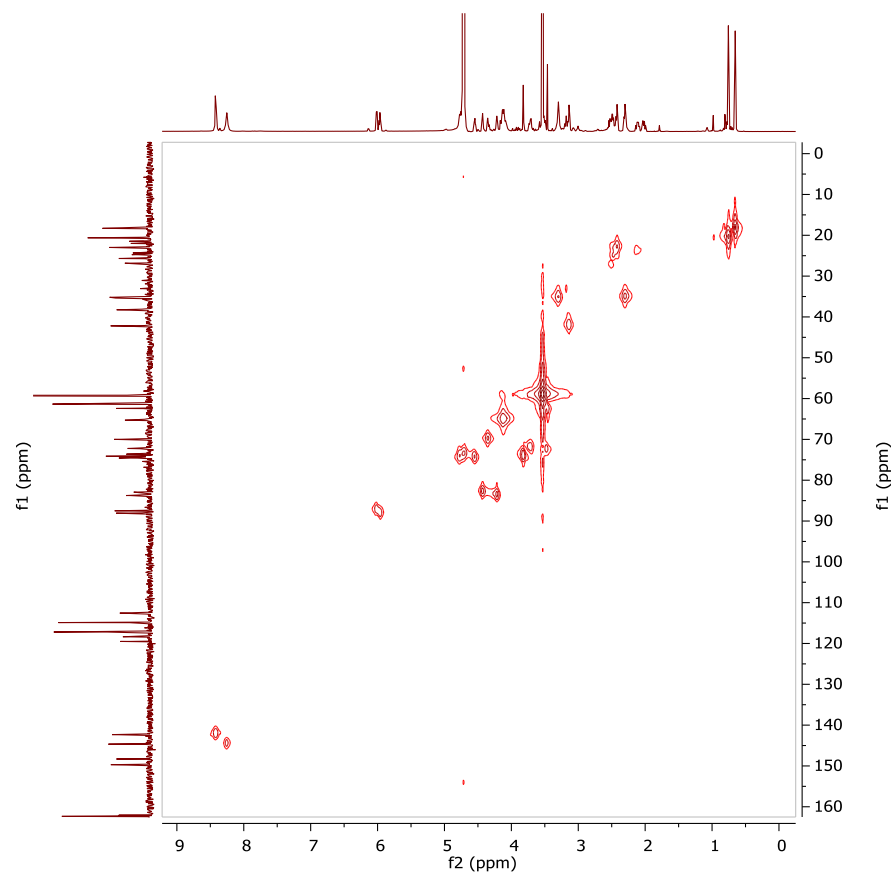
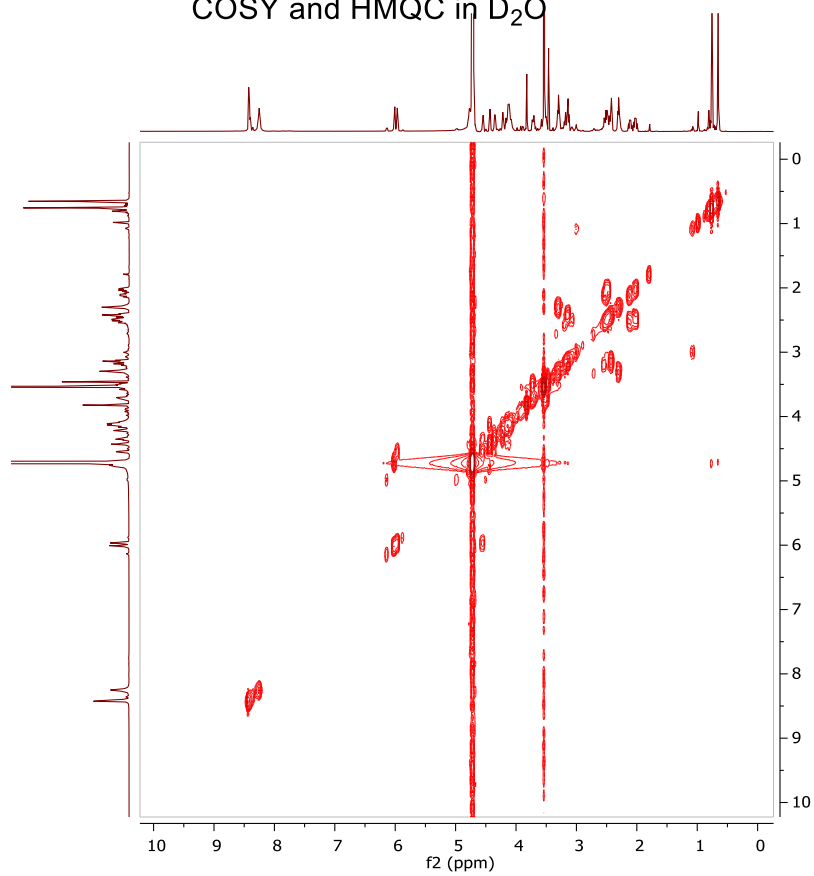


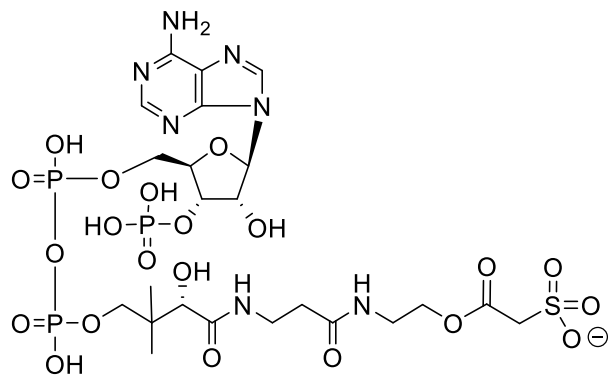
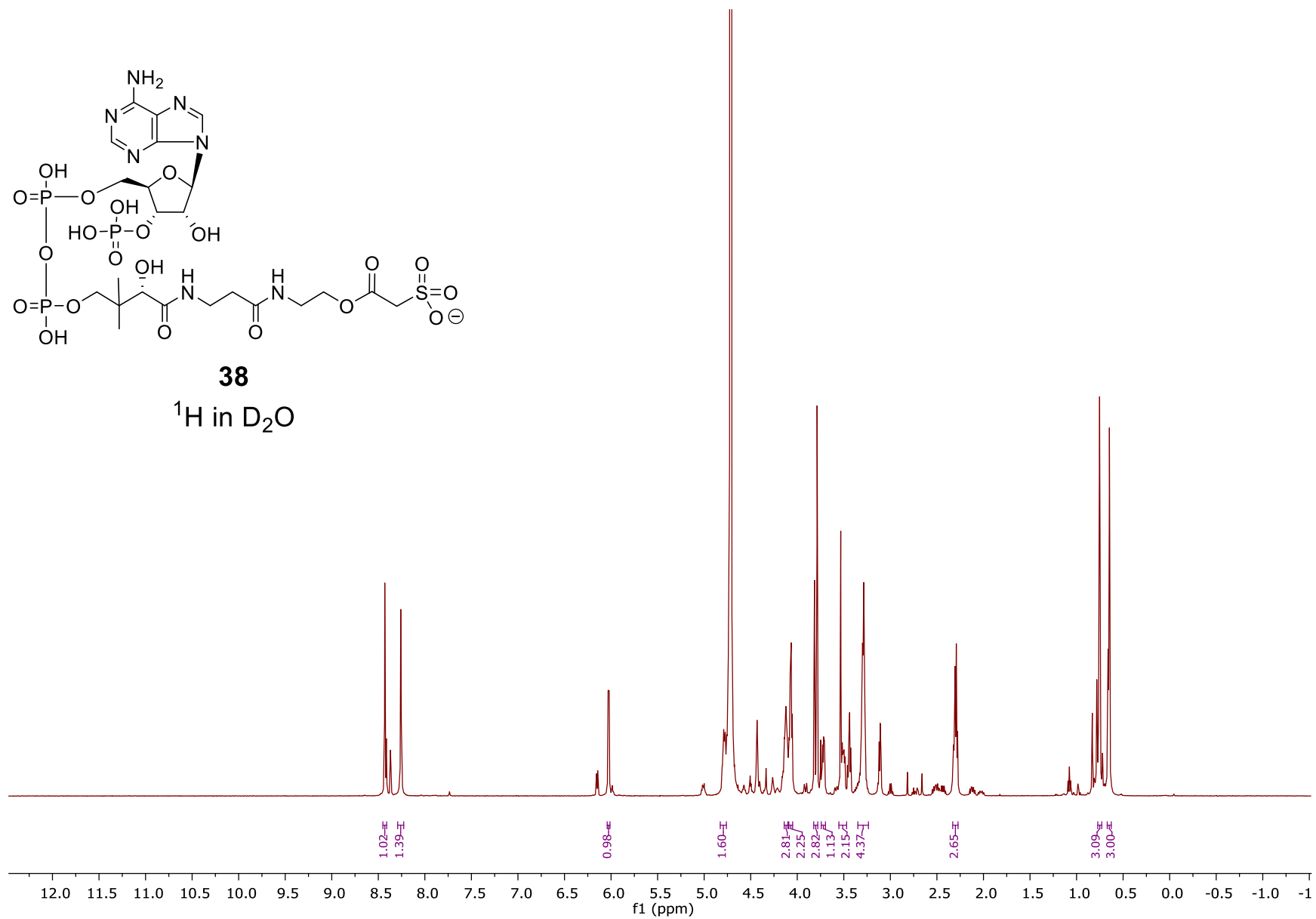


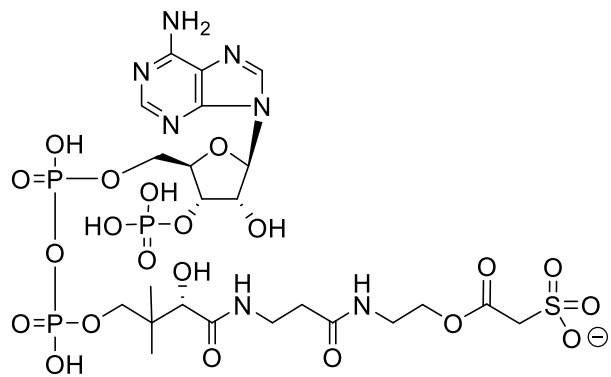
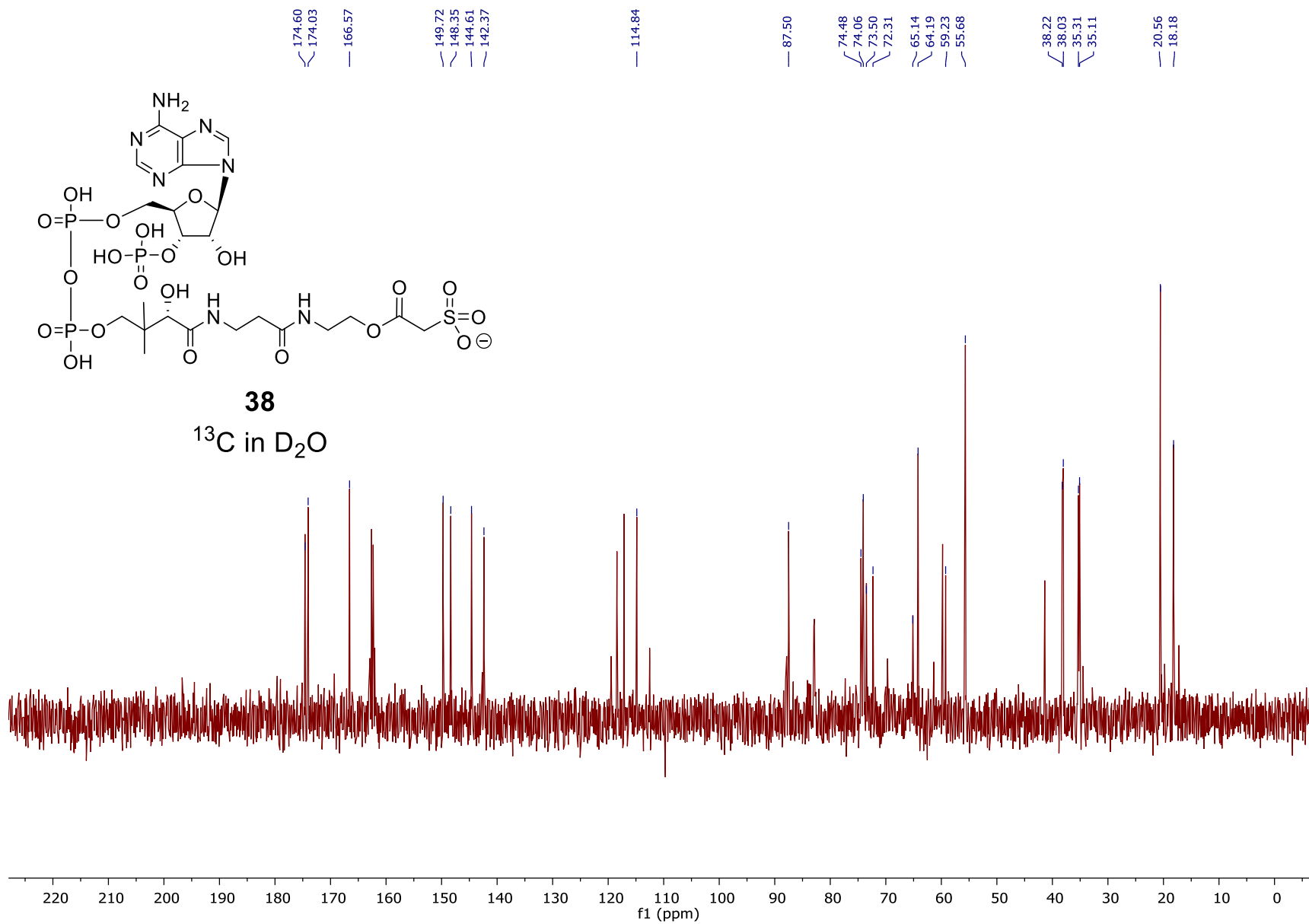
37

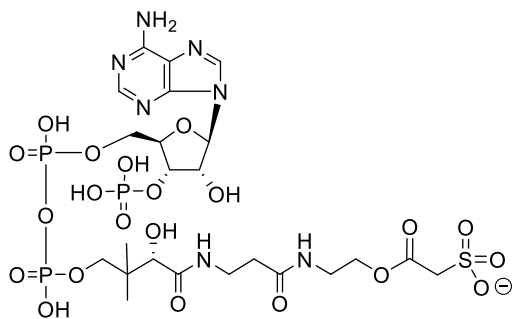
COSY and HMQC in D₂O

95



**38**¹H in D₂O

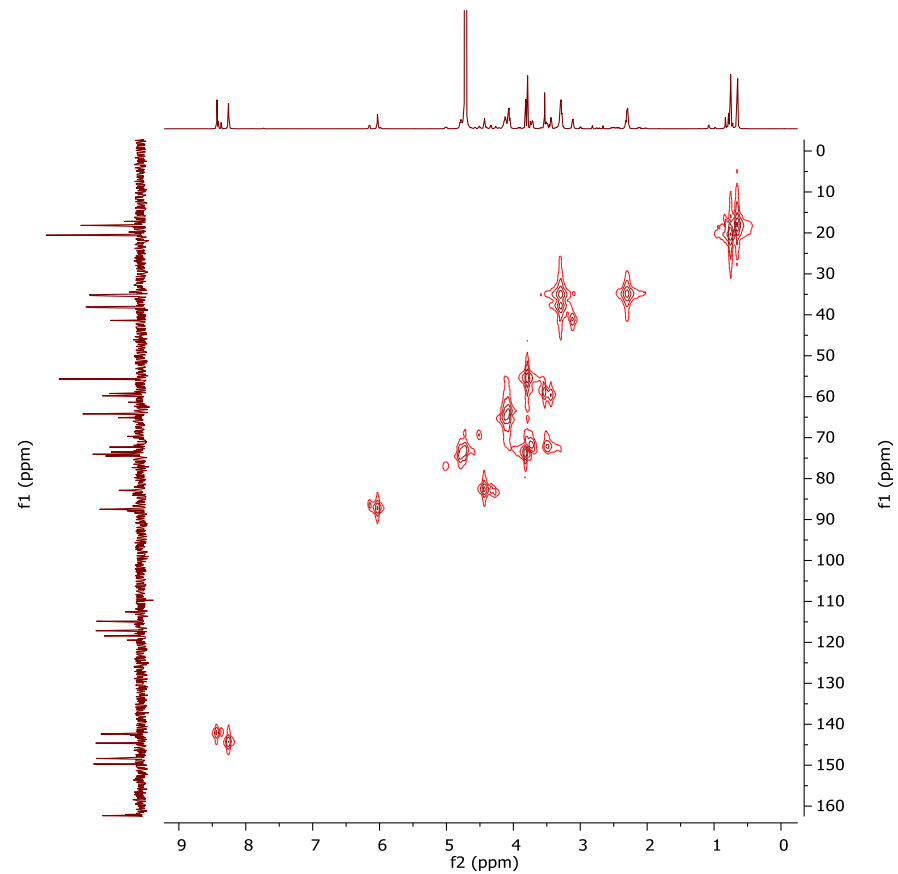
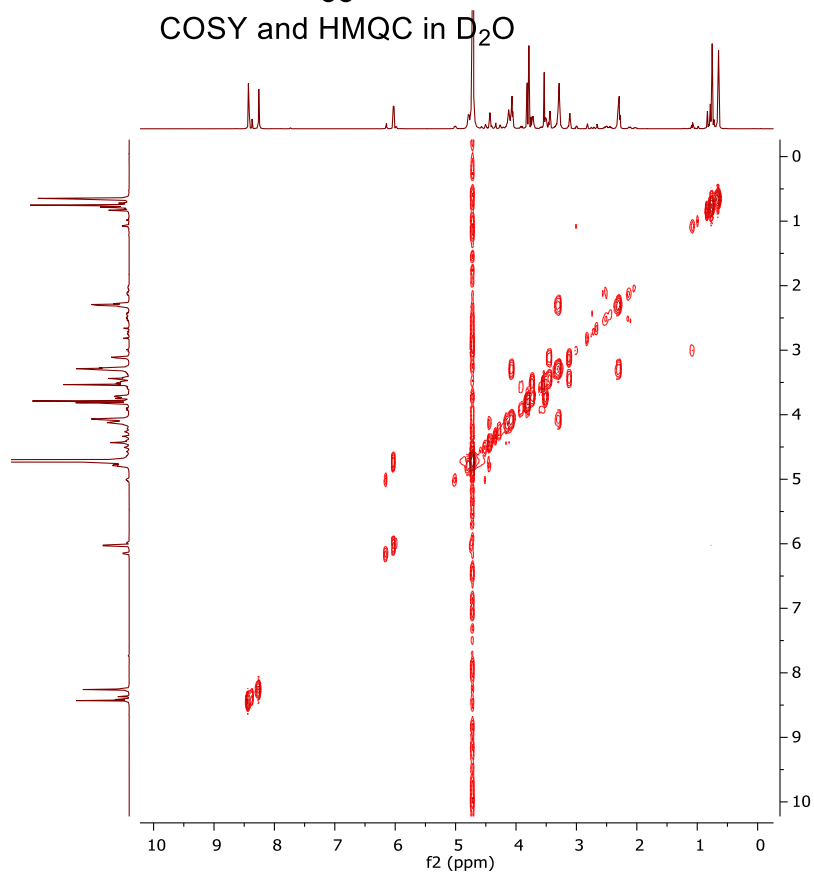
**38** ^{13}C in D_2O 

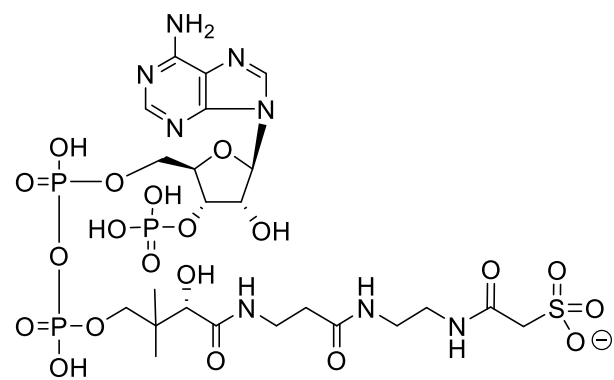
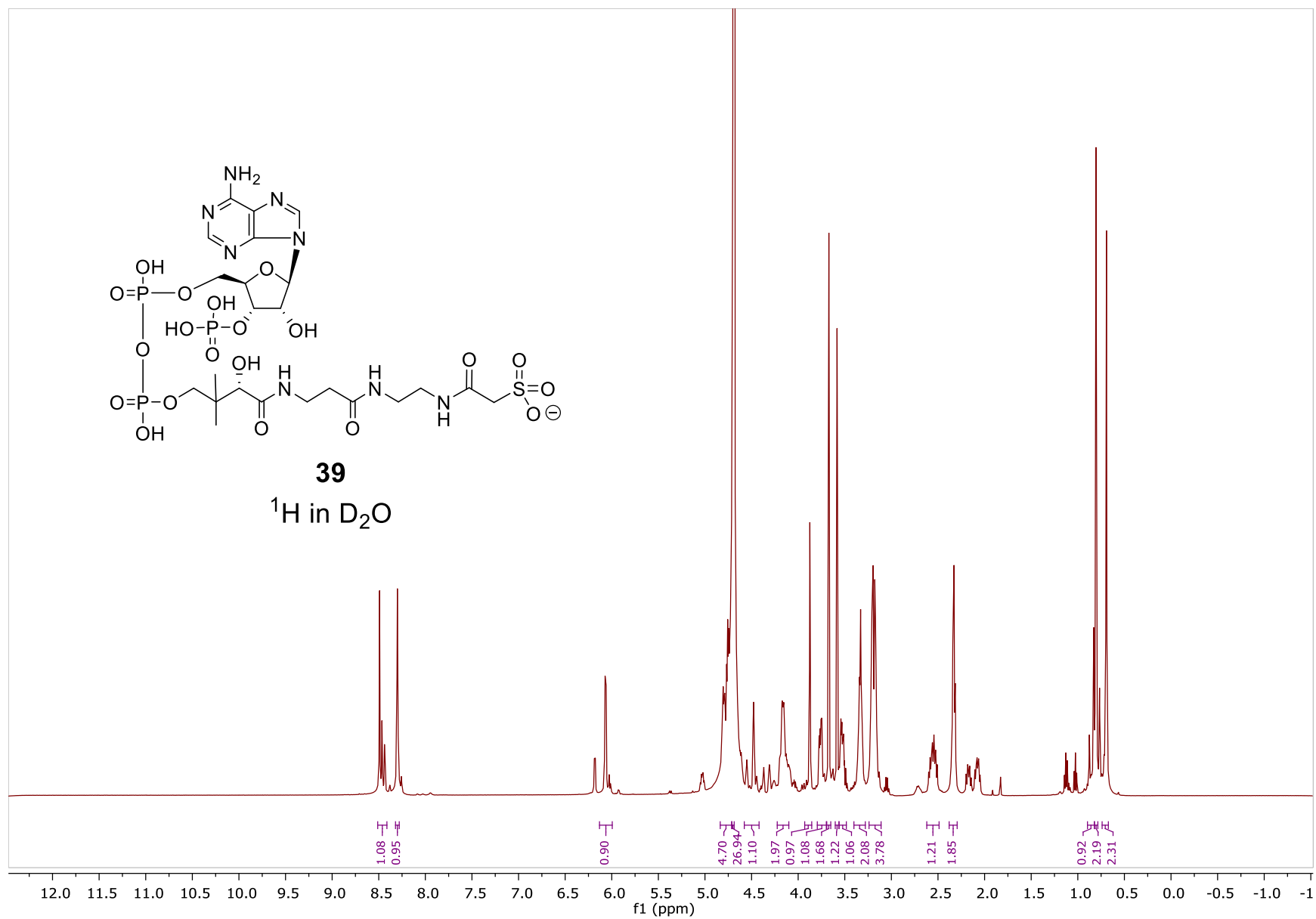


38

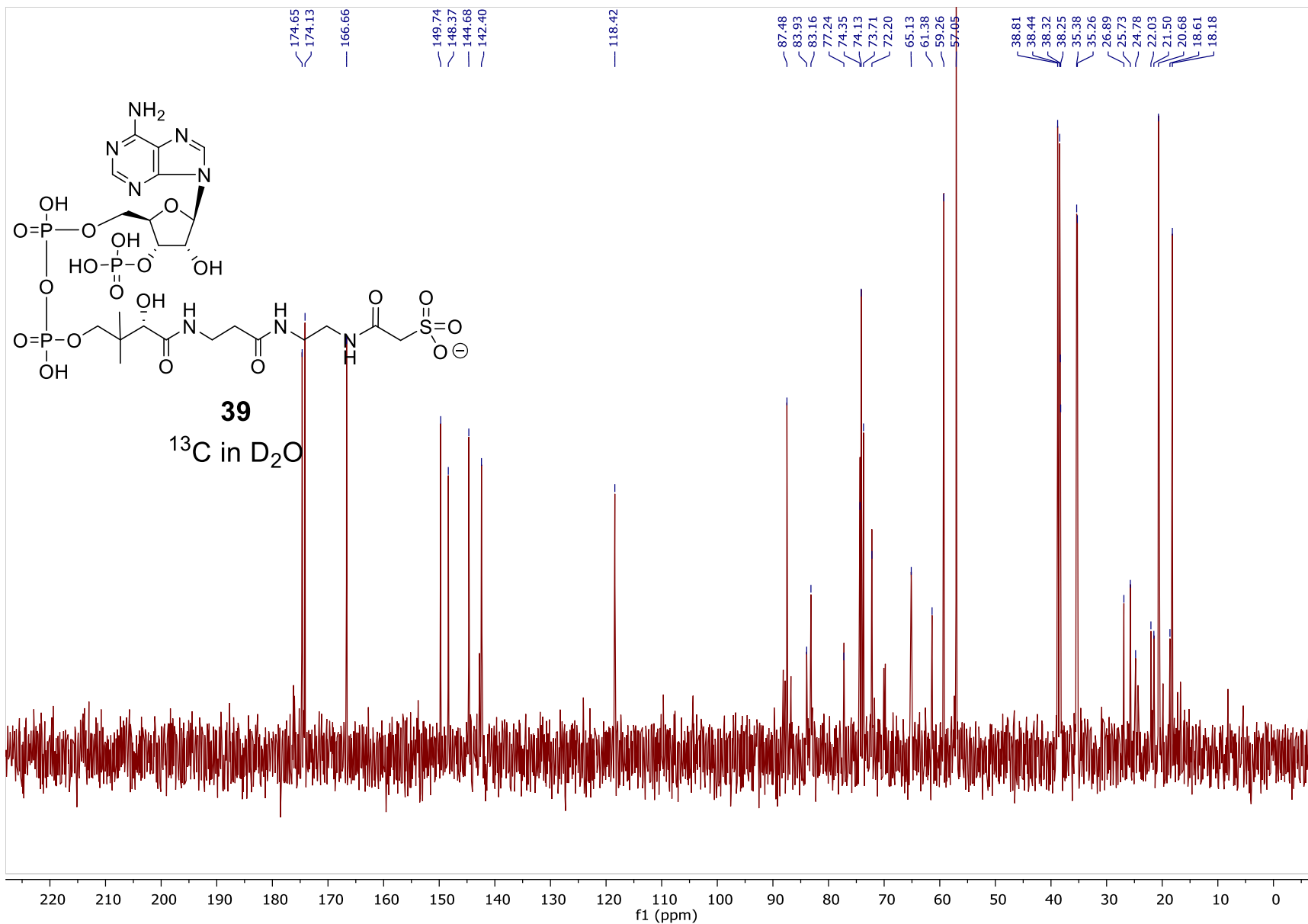
COSY and HMQC in D₂O

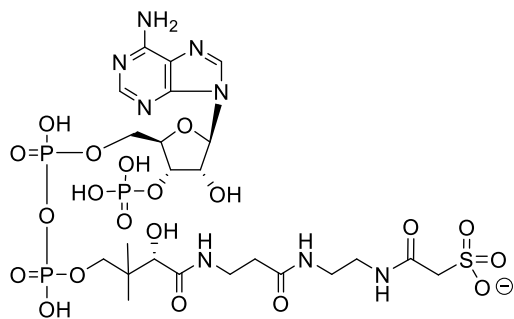
86



**39** ^1H in D_2O 

001

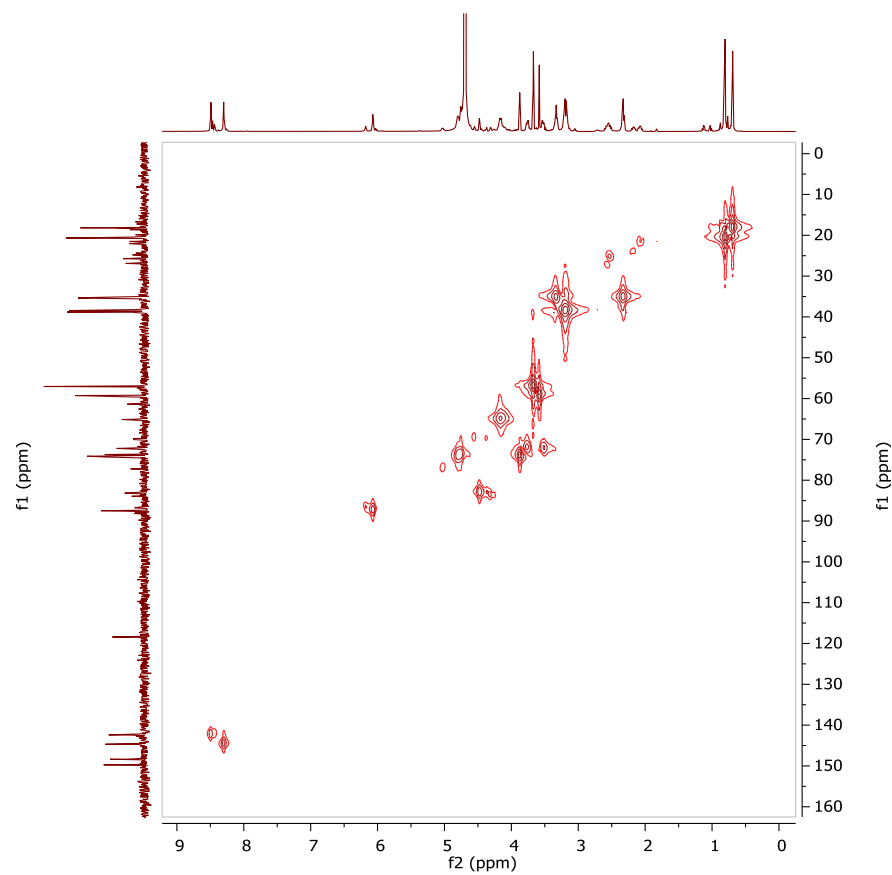
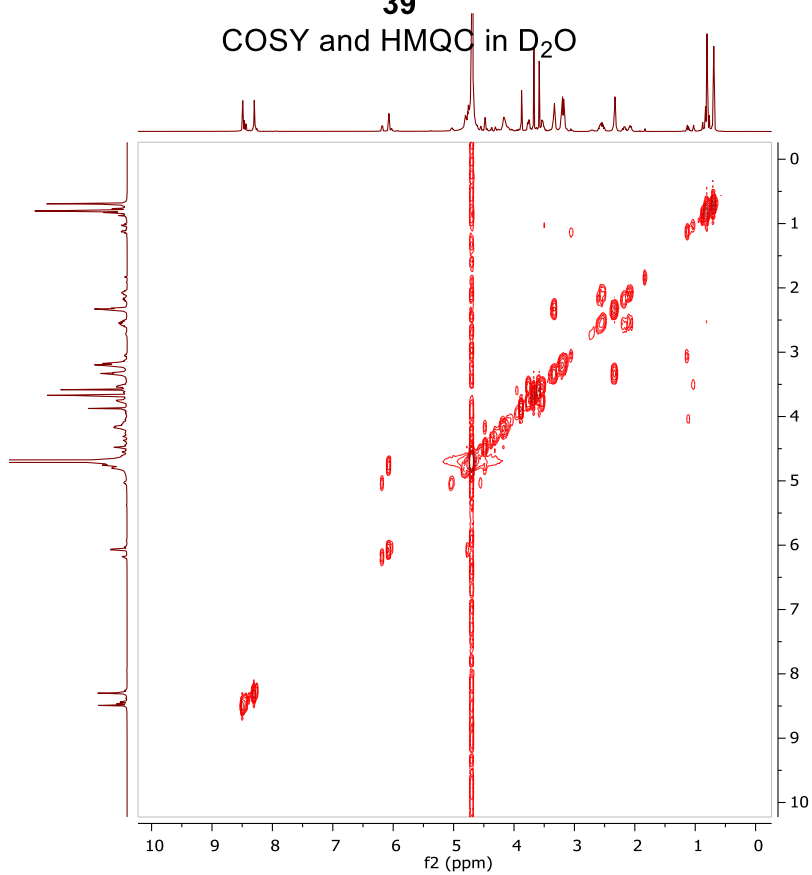


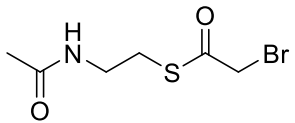


39

COSY and HMQC in D₂O

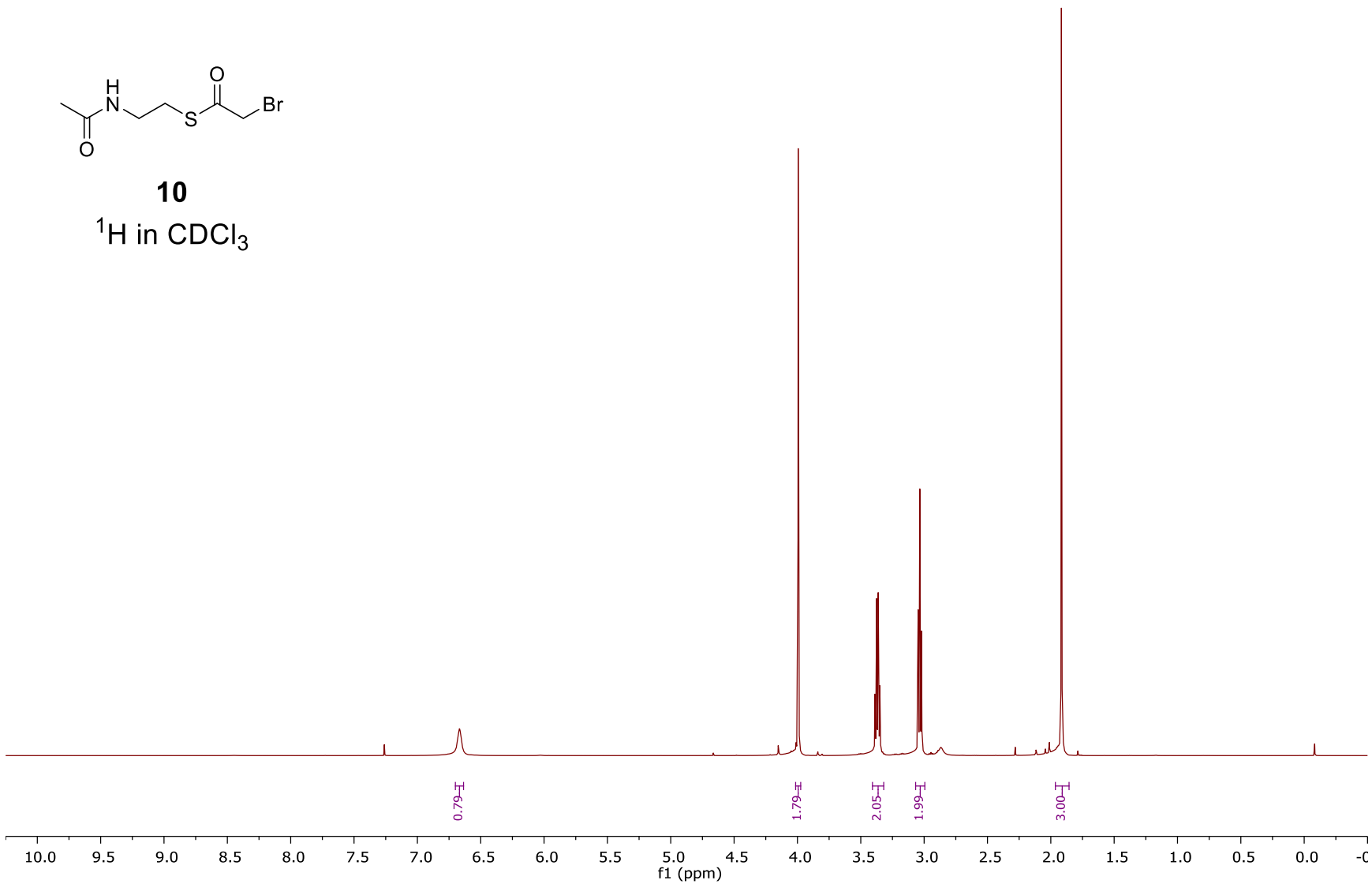
101

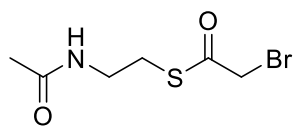




10

^1H in CDCl_3





10

¹³C in CDCl₃

192.90

170.85

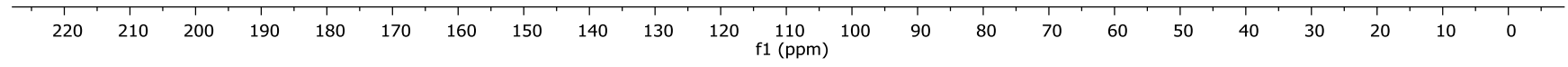
38.93

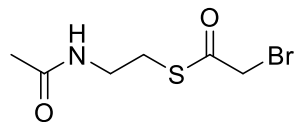
33.48

29.65

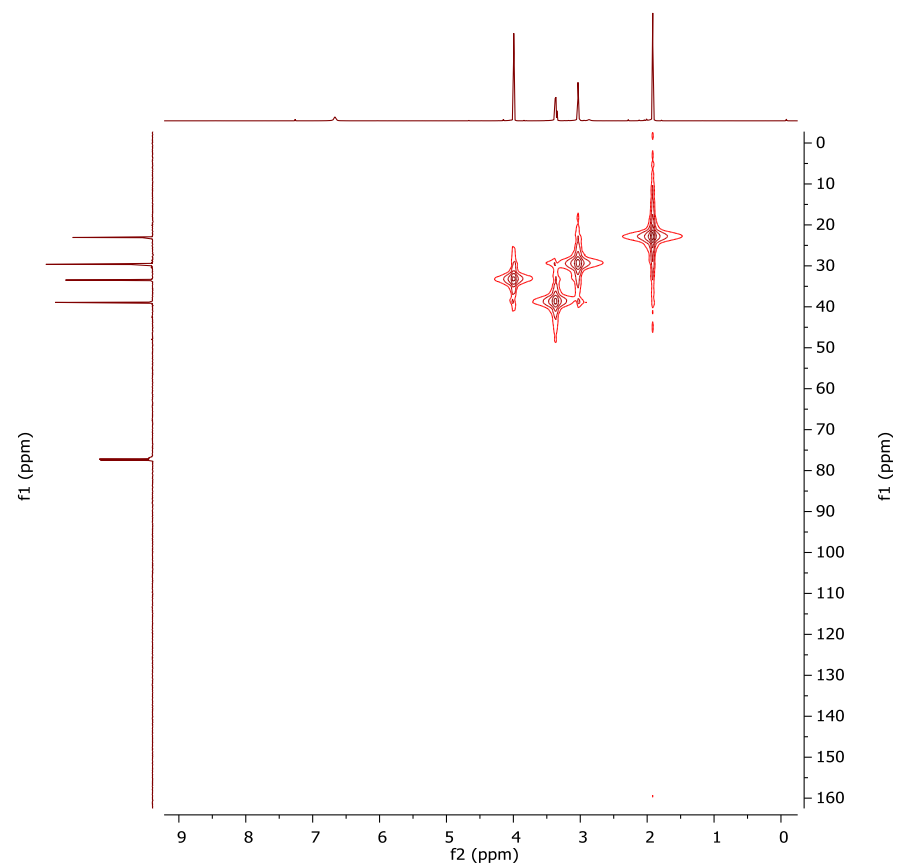
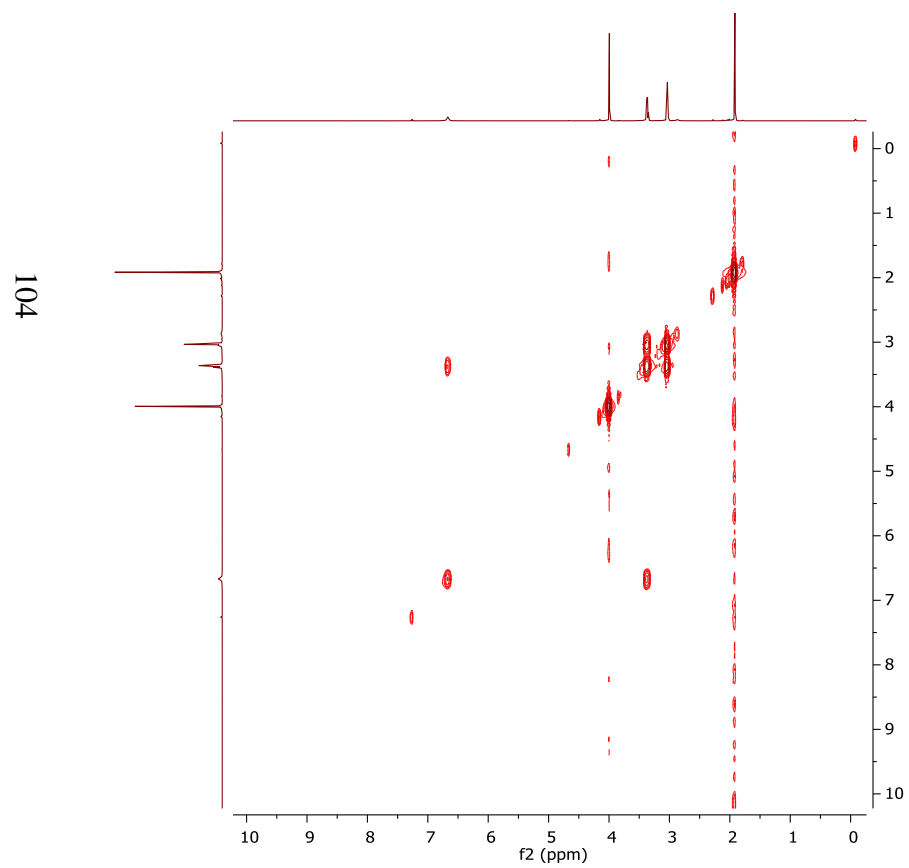
23.07

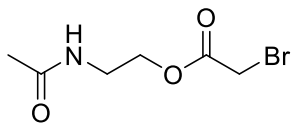
103





10
COSY and HMQC in CDCl₃

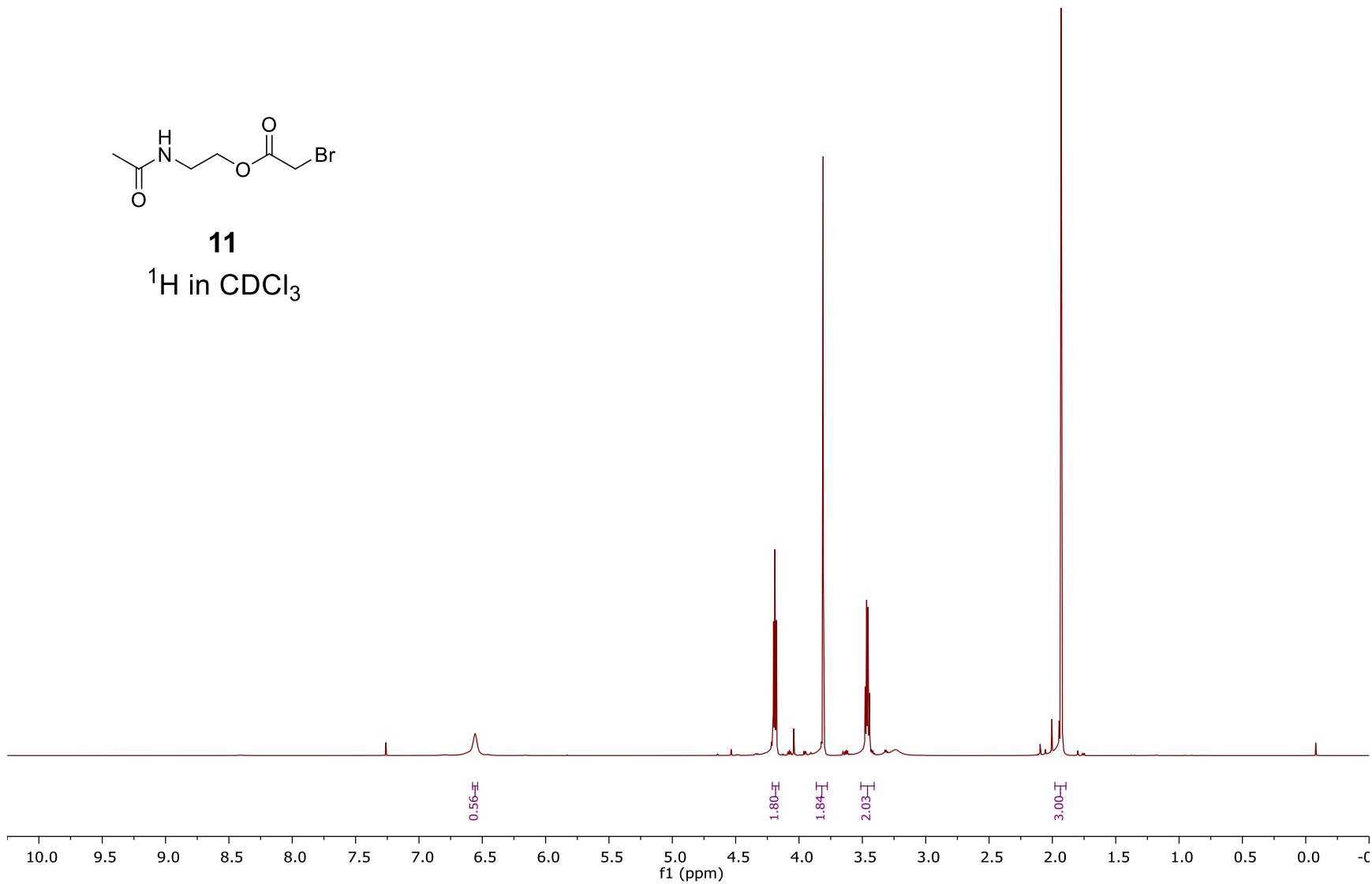


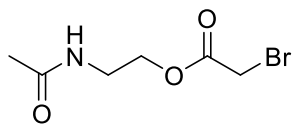


11

¹H in CDCl₃

105





11

¹³C in CDCl₃

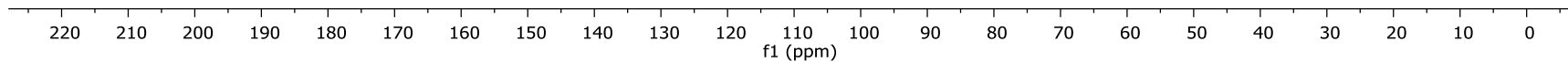
170.91
167.34

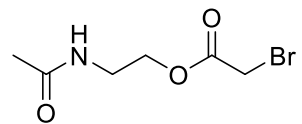
64.77

38.36

25.79
23.04

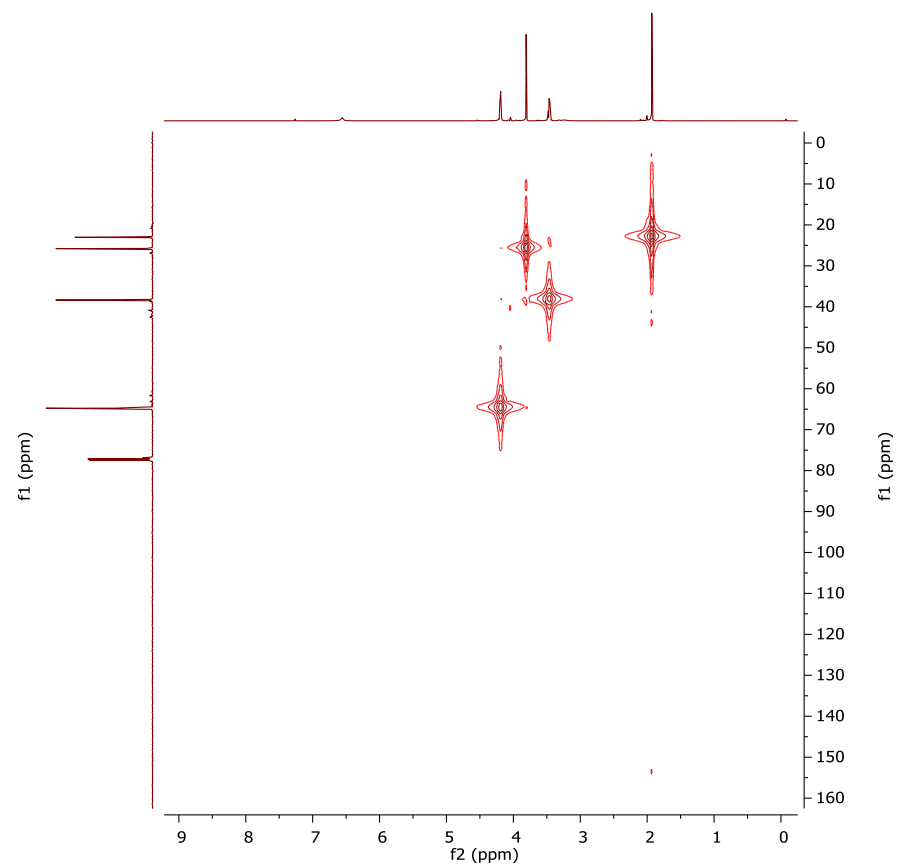
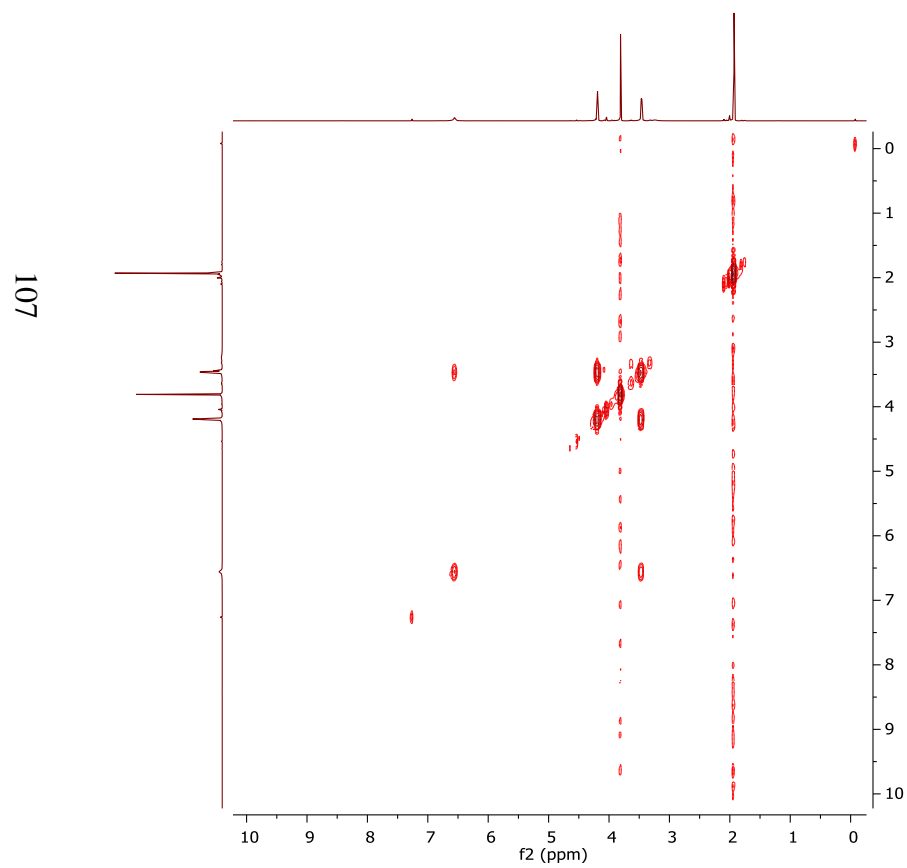
901





11

COSY and HMQC in CDCl₃



4.10 References

1. Kulkarni, R. A.; Worth, A. J.; Zengeya, T. T.; Shrimp, J. H.; Garlick, J. M.; Roberts, A. M.; Montgomery, D. C.; Sourbier, C.; Gibbs, B. K.; Mesaros, C.; Tsai, Y. C.; Das, S.; Chan, K. C.; Zhou, M.; Andresson, T.; Weissman, A. M.; Linehan, W. M.; Blair, I. A.; Snyder, N. W.; Meier, J. L., Discovering Targets of Non-enzymatic Acylation by Thioester Reactivity Profiling. *Cell Chemical Biology* **2017**, *24* (2), 231-242.
2. Ferrer, J. L.; Jez, J. M.; Bowman, M. E.; Dixon, R. A.; Noel, J. P., Structure of chalcone synthase and the molecular basis of plant polyketide biosynthesis. *Nature Structural & Molecular Biology* **1999**, *6* (8), 775-84.
3. Jez, J. M.; Ferrer, J. L.; Bowman, M. E.; Dixon, R. A.; Noel, J. P., Dissection of malonyl-coenzyme A decarboxylation from polyketide formation in the reaction mechanism of a plant polyketide synthase. *Biochemistry* **2000**, *39* (5), 890-902.
4. Rittner, A.; Paithankar, K. S.; Huu, K. V.; Grininger, M., Characterization of the Polyspecific Transferase of Murine Type I Fatty Acid Synthase (FAS) and Implications for Polyketide Synthase (PKS) Engineering. *ACS chemical biology* **2018**, *13* (3), 723-732.
5. Qiu, X.; Janson, C. A.; Smith, W. W.; Head, M.; Lonsdale, J.; Konstantinidis, A. K., Refined structures of beta-ketoacyl-acyl carrier protein synthase III. *Journal of molecular biology* **2001**, *307* (1), 341-56.
6. White, S. W.; Zheng, J.; Zhang, Y. M.; Rock, The structural biology of type II fatty acid biosynthesis. *Annual review of biochemistry* **2005**, *74*, 791-831.
7. Witkowski, A.; Joshi, A. K.; Lindqvist, Y.; Smith, S., Conversion of a beta-ketoacyl synthase to a malonyl decarboxylase by replacement of the active-site cysteine with glutamine. *Biochemistry* **1999**, *38* (36), 11643-50.
8. Benning, M. M.; Haller, T.; Gerlt, J. A.; Holden, H. M., New reactions in the crotonase superfamily: structure of methylmalonyl CoA decarboxylase from *Escherichia coli*. *Biochemistry* **2000**, *39* (16), 4630-9.
9. Ellis, B. D.; Milligan, J. C.; White, A. R.; Duong, V.; Altman, P. X.; Mohammed, L. Y.; Crump, M. P.; Crosby, J.; Luo, R.; Vanderwal, C. D.; Tsai, S. C., An Oxetane-Based Polyketide Surrogate To Probe Substrate Binding in a Polyketide Synthase. *Journal of the American Chemical Society* **2018**, *140* (15), 4961-4964.
10. Mancina, F.; Smith, G. A.; Evans, P. R., Crystal structure of substrate complexes of methylmalonyl-CoA mutase. *Biochemistry* **1999**, *38* (25), 7999-8005.
11. Stunkard, L. M.; Dixon, A. D.; Huth, T. J.; Lohman, J. R., Sulfonate/Nitro Bearing Methylmalonyl-Thioester Isosteres Applied to Methylmalonyl-CoA Decarboxylase Structure-Function Studies. *Journal of the American Chemical Society* **2019**, *141* (13), 5121-5124.
12. Lu, J.; Dong, Y.; Ng, E. C.; Siehl, D. L., Novel form of the Michaelis-Menten equation that enables accurate estimation of $(k_{cat}/K_M) \cdot KI$ with just two rate measurements; utility in directed evolution. *Protein engineering, design & selection : PEDS* **2017**, *30* (5), 395-399.

CHAPTER 5. CONCLUDING REMARKS

Note: Literature references are unique within this chapter.

5.1 Malonyl-thioester isosteres limit enzyme reactivity allowing for structure-function studies

The inherent reactivity of malonyl-CoA within enzymes has led to many unsuccessful substrate-bound structure-function studies. Therefore, we synthesized malonyl-thioester isosteres to limit enzyme reactivity for structure-function studies. We focused on altering the carboxylate to sulfonate or nitro isosteres to inhibit enzyme decarboxylation, acyl transfer, and hydrolysis. The methylmalonyl-thioesters proved to be easier to synthesize and purify, which is why we started with them. The nitro-bearing compounds formed a nitronate in solution, forming double bond character from the α -carbon to the nitrogen. Sulfonate-bearing compounds were synthesized and purified in a racemic mixture. Both the nitro- and sulfonate-bearing methylmalonyl-thioesters were synthesized through a similar scheme that proceeded through a 2-bromopropionyl-X-pantetheine intermediate. After synthesizing these methylmalonyl-thioester analogs, we performed structure-function studies focusing on the geometry of the bound substrate analogs to infer how enzymes orient malonyl-thioester substrates. In this chapter, I will describe and interpret some of the substrate bound geometries I observed in different enzyme structure-function studies.

5.2 Methylmalonyl-CoA analog studies with MMCD yield proposed decarboxylation mechanism

Co-crystallization of both of the sulfonate- and nitro-bearing analogs resulted in bound structures with MMCD. The nitro- and sulfonate-bearing isosteres was the first example of a β -keto decarboxylase with a substrate or substrate analog bound with the thioester, ester, or amide carbonyl position in the oxyanion hole. The electron density for both the sulfonate and nitro isosteres meant that they were both able to inhibit decarboxylase activity while being stable under crystallization conditions. The similar positioning of the sulfonate- and nitro-bearing analogs suggested that these isosteres were able to mimic the carboxylate of methylmalonyl-CoA.

The methylmalonyl-CoA isosteres are positioned with the thioester carbonyl in the oxyanion hole formed by the amide backbone of His66 and Gly110. Although MMCD decarboxylates (2R)-methylmalonyl-CoA to form propionyl-CoA *in vivo*, MMCD is able to decarboxylate both (2R)- and (2S)-methylmalonyl-CoA *in vitro*. I propose that MMCD is capable of decarboxylating both epimers of methylmalonyl-CoA because the oxyanion hole contains two amino acid interactions to stabilize the enolate intermediate. The combination of the oxyanion hole comprised of two interacting residues and the carboxylate situated in a hydrophobic cavity allows for either methylmalonyl-CoA epimer to turnover. The enolate carbonyl is situated in between the amide backbones of His66 and Gly110 suggesting that either substrate epimer would be able to form this intermediate. This phenomenon is different from the oxyanion hole seen in the stereospecific enzyme, LnmK, discussed below, which only has one interacting residue forming the oxyanion hole.

The nitro-bearing substrate analogs are bound within the active site of MMCD with a dihedral angle of 180° about the O-C_O-C _{α} -NO₂ compared to the sulfonate-bearing substrate analogs which have a dihedral angle of 90° about the O-C_O-C _{α} -SO₃. The natural substrate, methylmalonyl-CoA, likely is oriented with a dihedral angle of 90° about the O-C_O-C _{α} -CO₂ similar to the sulfonate-bearing analog. This dihedral angle is optimal for the carboxylate to get ejected in order to promote the formation of the enolate intermediate. The ease for the substrate to form the enolate intermediate as well as the produced carbon dioxide occupied in a hydrophobic cavity, promotes the carbon bond breakage. After formation of the enolate intermediate, the enzyme avoids C-C bond reversion through protonation of the enolate intermediate. The combination of stabilization and protonation of the enolate intermediate promotes decarboxylation over other possible enzyme reactions. When the positioning of the substrate is altered within the active site, similar to the alternative orientations of nitro-bearing thioester and ester analogs discussed in chapter 2, the preferred enzyme reactivity shifts to promote hydrolysis and decarboxylation. This can explain why the activity assays performed see low amounts of hydrolysis as well as decarboxylation.

5.3 Studies with LnmK reveal substrate geometry leading to proposed mechanism

The successful studies of our methylmalonyl-thioester analogs with MMCD motivated us to use them in structure-function studies with LnmK. LnmK is a bifunctional acyltransferase-

decarboxylase in the leinamycin biosynthetic pathway, as discussed in chapter 1¹⁻². Co-crystallization of LnmK with our nitro-bearing methylmalonyl-CoA analogs resulted in a bound orientation, Figure 5.1. The thioester carbonyl is situated within an oxyanion hole comprised of the amide backbone of Phe65. The nitro moiety interacts with the amide backbone of Phe223 and the side chain of Asn216, Figure 5.1.

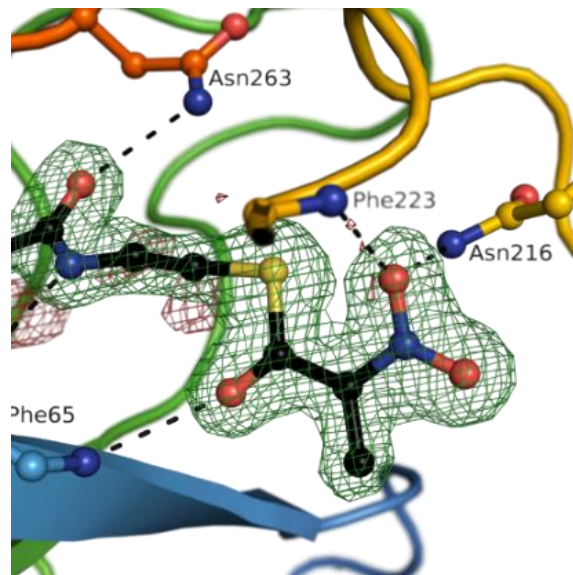


Figure 5.1 Nitro-bearing substrate analogs reveal substrate binding mode and active site amino acid residues Phe65, Phe223, and Asn216.

Since both the thioester and ester containing nitro-bearing analogs showed no signs of hydrolysis in the electron density, that suggests LnmK undergoes decarboxylation before self-acyl-transfer, Figure 5.2. If the substrate analog were oriented within an active site that promotes acyl transfer activity, it would be highly likely that hydrolysis would occur on a crystallization timeframe. Also, the geometry of the methylmalonyl analog thioester carbonyl in the oxyanion hole suggests that the enzyme stabilizes a planar enolate intermediate. This proposed planar enolate intermediate is further supported when comparing preliminarily determined K_D values of the thioester and amide containing nitro analogs, 47 ± 0.18 nM and 1.91 ± 0.16 μ M, respectively. The only difference between these substrate analogs is the sulfur and nitrogen atoms, but there is over a 40-fold difference in binding affinity.

The sulfonate-bearing analogs were also co-crystallized with LnmK, however two active site orientations were visible. The possibilities for there being two active site conformations are 1) the racemic mixture of the sulfonate compounds has each epimer bound in a different conformation; 2) the sp^3 hybridization of the α -carbon is not able to properly orient the thioester carbonyl in the oxyanion hole; or 3) the sulfonate isostere is too large of a mimic for a carboxylate that is proposed to interact with the amide backbone of Phe223 and the side chain of Asn216 based upon the nitro analog orientation. These multiple conformations remind us of the limitations of using substrate analogs where carboxylate isosteres might be useful in an enzyme specific manner.

Assuming methylmalonyl-CoA binds inside of the active site with an sp^3 hybridized $C\alpha$, the nitro-bearing analog does not directly promote the substrate binding mode. The carboxylate is

still likely stabilized by the amide backbone of Phe223 and the side chain of Asn216; however, it most likely will have a dihedral angle about the O-C₀-C_α-CO₂ of 90 degrees. The 90 degree dihedral angle will allow for the carboxylate to be ejected to form a planar enolate intermediate which is in the plane of the amide

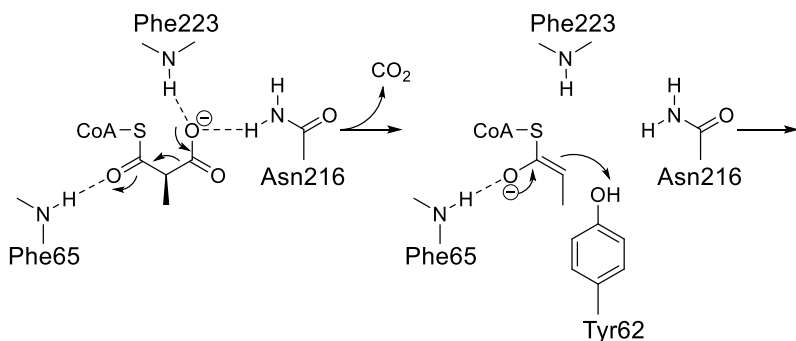


Figure 5.2 Model of LnmK decarboxylation: Phe223 amide stabilizes enolate, carboxylate interacts with Asn216 and Asn216. Tyr62 is the nucleophile for self-acyl-transfer.

backbone of Phe65. The presence of only one interacting residue within the oxyanion hole suggests how LnmK is stereospecific, as seen in chapter 3.

The nitro-bearing analogs in complex with LnmK provide information about amino acid residues involved in substrate binding and allow us to propose a decarboxylation mechanism. However, they do not provide any information about how the enzyme performs self and trans acyl transfer activity. The future goals of this project should focus on testing the nitro-bearing analog bound structures as well as performing structure-function studies focused on the self and trans acyl transfer activity of LnmK. I would suggest performing decarboxylation activity assays of LnmK with active site mutants to test the accuracy of predictions based on the nitro-bearing bound LnmK structure. These assays should be performed with *wild type*, Asn216Asp, Asn216Ala, Asn216His, and Asn216Leu to determine decarboxylation kinetics. An enolate intermediate analog can be synthesized and co-crystallized with LnmK to capture the self-acyltransferase activity conformation. The predicted nucleophile is Tyr62 which is normally pointed outside of the active site. Co-crystallization of an enolate analog may be able to capture the conformational change of Tyr62 flipped into the active site to act as the nucleophile. To test the trans-acyltransferase activity of LnmK, an unnatural amino acid mimicking the acylation of Tyr62 could be synthesized and incorporated into the enzyme. This mutated enzyme could then be co-crystallized with LnmL (ACP) to see how the propionyl group is transferred from Tyr62 of LnmK to the phosphopantetheine arm of LnmL. Both of the structure-function studies testing self- and trans-acyltransferase activity would need to have follow-up enzymology and mutagenesis experimentation to test the usefulness of these structures.

5.4 Expanding malonyl-thioester analog toolbox to study ketosynthases

Since we had previously shown that the sulfonate- and nitro-bearing analogs were suitable methylmalonyl-thioester isosteres for structure-function studies, we decided to expand on our analog toolbox to include malonyl-thioester analogs. Synthesis of nitro-bearing malonyl-thioester analogs was not possible through a similar synthetic scheme as our methylmalonyl-thioester analogs. Proceeding through a bromoacetyl intermediate yielded extremely low yields. We have been working on a different synthetic scheme by treating the (thioester, ester, and amide containing) pantetheine moiety with crotonyl chloride to give crotonyl-pantetheine acetonide. The crotonyl-pantetheine acetonide was treated with osmium tetroxide and sodium periodate to yield glyoxylate-pantetheine acetonide. This glyoxylate can be converted to an oxime using hydroxylamine. We are currently working on oxidizing the oxime with trifluoroacetic peroxide through a urea-hydrogen peroxide complex with trifluoroacetic anhydride to make the nitro.

Synthesis of sulfonate-bearing malonyl-thioester analogs was possible through a similar synthetic scheme to our previous studies. The thioester, ester, and amido containing pantetheine acetonide can be treated with bromoacetyl bromide and pyridine to form the corresponding bromoacetyl-pantetheine acetonide intermediates. These intermediates can be reacted with sodium dithionate and sodium bicarbonate in water to create the sulfonate-bearing malonyl-thioester analogs. The rest of the synthetic scheme before and after the bromoacetyl bromide treatment are the same from our previous study³. These sulfonate-bearing malonyl-thioester analogs were tested against ketosynthases KasIII (FabH) from *E. coli* and CHS II from *Medicago sativa*.

5.4.1 Malonyl-thioester analogs inhibit KasIII revealing potential structure-function applications

The potential for using sulfonate-bearing malonyl-thioester analogs in ketosynthases structure function studies is revealed by the compounds inhibition of KasIII, discussed in chapter 4. Keep in mind, the natural extender substrate of KasIII is malonyl-S-ACP. The CoA bearing a thioester had the best inhibition of any of our analogs suggesting that both the adenosine and thioester are important for binding. Therefore, the adenosine must have a specific mode of binding to the enzyme and upon this specific binding interaction, the geometry of the thioester bond orients the thioester carbonyl into the oxyanion hole. Altering the thioester to an ester or amide have

weaker, respectively, inhibition of KasIII when attached to CoA and theoretically binding to the same adenosine binding interaction. When the adenosine moiety is not present as is the case for our phosphopantetheine and pantetheine analogs, the overall inhibition of the thioester, ester, and amide containing compounds is weaker. However, the thioester, ester, and amide containing phosphopantetheine compounds appear to group in their inhibition constants as do the three pantetheine compounds (just slightly weaker than the phosphopantetheine compounds). This suggests that upon altering the compounds to not bind in an adenosine specific binding interaction, the flexibility is able to overcome the geometry differences between the thioester, ester, and amide bonds. All of these inhibition constants in the low micromolar range gives us confidence to proceed forward with analog-complex structure-function studies to understand the adenosine binding interaction compared to ACP and substrate positioning.

To this point we have attempted co-crystallization experiments with sulfonate-bearing (amido)dethia phosphopantetheine and pantetheine analogs in KasIII cysteine to glutamine mutants. The KasIII C \rightarrow Q mutant mimics an acyl-S-KS intermediate. These co-crystallization experiments have resulted in apo-structures. Overlaying these apo-structures with previous acyl-S-KS structures reveals a subtle geometry difference between an acyl-S-KS and the C \rightarrow Q mutant. It is possible that while the C \rightarrow Q mutant mimics an acyl-S-KS intermediate, that it effects binding of malonyl-thioesters. The binding of the *wild type* vs C \rightarrow Q mutant still needs to be tested. Co-crystallization experiments also can be attempted in capturing the acyl-S-KS intermediate or soaking in malonyl-thioester analogs.

5.4.2 Preliminary structure-function studies with CHS II from *Medicago sativa*

Once the sulfonate-bearing malonyl-thioester analogs were synthesized, we attempted structure-function studies with CHS II from *Medicago sativa* to determine how the enzyme orients malonyl-CoA and the acyl-S-CHS intermediate to perform a decarboxylative Claisen condensation. Co-crystallization of sulfonate-bearing malonyl-CoA analogs with CHS II have resulted in apo structures thus far. These co-crystallization experiments have been done with *wild type* cysteine nucleophile or a C \rightarrow S mutant. These enzyme conditions are set up to accept 4-coumaryl-S-CoA as a substrate instead of malonyl-CoA, which could be a reason for the apo-structures solved thus far. Attempts at expressing and purifying a CHS II C \rightarrow Q mutant have been unsuccessful thus far as well. Therefore, the focus for future experiments should be on obtaining

a 4-coumaryl-*S*-CHS intermediate or a cinnamoyl-*S*-CHS intermediate to perform co-crystallization experiments with the malonyl-CoA analogs. Another possible avenue for structure-function success would be to develop and optimize a method for expressing and purifying a CHS II C → Q mutant that could be co-crystallized with malonyl-CoA analogs.

While trying to perform structure-function studies of CHS II with the malonyl-CoA substrate analog and acyl-*S*-KS intermediate, I also attempted enolate intermediate analog co-crystallization. Co-crystallization of carboxy-carba(dethia)-CoA resulted in a bound analog structure with a Cys → Ser enzyme. The ketone carbonyl is positioned within the decarboxylation oxyanion hole between the His and Asn side chains. This structure by itself does not reveal much beyond a potential enolate position.

Overlaying this enolate bound CHS structure with an acyl-*S*-KS (PDB 1HNH) structure revealed the close proximity of the enolate analog and acyl-intermediate position, Figure 5.3. In the current orientation the enolate analog is pointed directly at the acyl-*S*-KS intermediate. If an enolate is formed after decarboxylation, the pi-orbitals are not in the correct position for Claisen condensation; however, if a carbanion is formed after decarboxylation, the carboxy-carba(dethia)-CoA molecule reveals a possible position for Claisen condensation to occur. The overlay of an enolate/carbanion bound CHS and acyl-*S*-

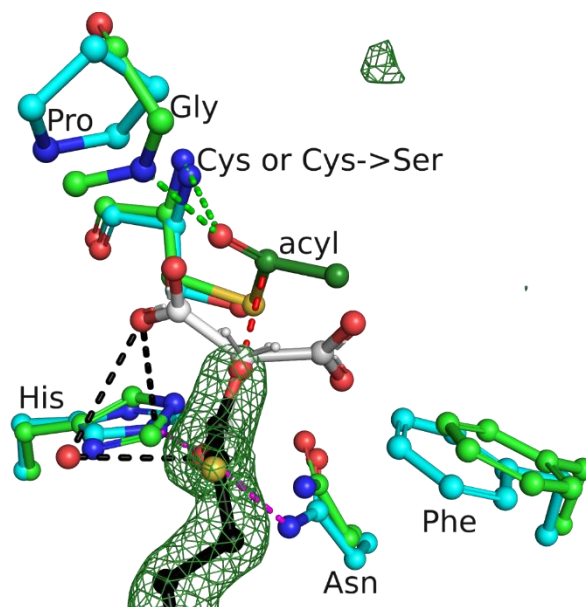


Figure 5.3 CHS II (cyan sticks) with carboxy-carba(dethia)-CoA bound (black sticks) overlaid with an acyl-*S*-KS (FabH, PDB 1HNH) intermediate to monitor a Claisen condensation-like conformation. The white sticks are theoretical carboxylate positions.

KS does not resolve where the carboxylate of the malonyl-thioester substrate is positioned. Modeling the carboxylate onto the enolate analog, Figure 5.3, reveals space on either side of the compound where it could be positioned. Future goals of studying CHS II are performing structure-function studies with both an acyl-*S*-CHS intermediate and malonyl-thioester analog bound to reveal where to substrate is positioned to undergo decarboxylation. Then structure-function studies

with an acyl-S-CHS intermediate and a bound enolate intermediate will help to more clearly visualize how Claisen condensation occurs within the active site.

5.4.3 Future goals for type I KS enzymes

A couple remaining questions in the ketosynthase field are what are the specific protein-protein interactions of KS-ACP as well as what are the mechanistically relevant amino acid residues in the active site of the KS and how do they function. Experimentation has not been started using our malonyl-thioester analogs for structure-function studies in type I KS enzymes; however, the future goal is to pursue a co-crystal structure with these analogs. In order to perform these structure-function studies, our malonyl-thioester analogs will need to be attached onto the phosphopantetheinyl arm of the ACP. Once malonyl-ACP analogs have been synthesized and purified, binding experiments could be performed with the KS. Inhibition assays could be performed to compare the malonyl-S-ACP, malonyl-CoA, malonyl-phosphopantetheine, and malonyl-pantetheine to determine the role of the ACP binding interaction. Also, the ACP-malonyl analogs could be co-crystallized, soaked, or tethered to the KS enzyme to capture a natural or natural-like ACP-KS interaction. This structure-function study would reveal protein-protein interactions as well as enzyme-substrate interacting amino acid residues in the active site of the KS. This structure-function study would reveal much needed information about any differences between the type I, II, and III KS mechanism, as well as the specific protein-protein interactions necessary for binding and catalysis. This type of structure-function study could open an avenue for studying KS-ACP, AT-ACP, and possible more di-domain interactions in different pathways to begin teasing out the different protein-protein interactions within different pathways. The information gained from these structure-function studies would assist in overcoming the protein engineering efforts in PKS systems.

5.5 Excitement of new malonyl-thioester analogs and their ability to perform structure function studies on enzymes not previously possible

My thesis work has focused on the synthesis of malonyl-thioester analogs for their use in structure-function studies. I have provided many examples of these malonyl-thioester analogs being used to perform structure-function studies for decarboxylase, bi-functional acyltransfer-decarboxylase, epimerase, and have preliminary data on ketosynthase enzymes. The possibility

to continue expanding the malonyl-thioester analog toolbox to study different enzyme chemistry is an exciting and fruitful possibility.

5.6 References

1. Lohman, J. R.; Bingman, C. A.; Phillips, G. N., Jr.; Shen, B., Structure of the bifunctional acyltransferase/decarboxylase LnmK from the leinamycin biosynthetic pathway revealing novel activity for a double-hot-dog fold. *Biochemistry* **2013**, *52* (5), 902-11.
2. Huang, S. X.; Yun, B. S.; Ma, M.; Basu, H. S.; Church, D. R.; Ingenhorst, G.; Huang, Y.; Yang, D.; Lohman, J. R.; Tang, G. L.; Ju, J.; Liu, T.; Wilding, G.; Shen, B., Leinamycin E1 acting as an anticancer prodrug activated by reactive oxygen species. *Proceedings of the National Academy of Sciences of the United States of America* **2015**, *112* (27), 8278-83.
3. Stunkard, L. M.; Dixon, A. D.; Huth, T. J.; Lohman, J. R., Sulfonate/Nitro Bearing Methylmalonyl-Thioester Isosteres Applied to Methylmalonyl-CoA Decarboxylase Structure-Function Studies. *Journal of the American Chemical Society* **2019**, *141* (13), 5121-5124.